

**CHARACTERIZATION OF GAS PHASE ADSORPTION CAPACITY OF UNTREATED
AND CHEMICALLY TREATED ACTIVATED CARBON CLOTHS**

BY

MARK P. CAL

B.S., University of Illinois at Urbana-Champaign, 1991

M.S., University of Illinois at Urbana-Champaign, 1993

THESIS

Submitted in partial fulfillment of the requirements
for the degree of Doctor of Philosophy in
Environmental Engineering in Civil Engineering
in the Graduate College of the
University of Illinois at Urbana-Champaign, 1995

Urbana, Illinois

UNIVERSITY OF ILLINOIS AT URBANA-CHAMPAIGN

THE GRADUATE COLLEGE

DECEMBER 1994

WE HEREBY RECOMMEND THAT THE THESIS BY

MARK P. CAL

ENTITLED CHARACTERIZATION OF GAS PHASE ADSORPTION CAPACITY OF

UNTREATED AND CHEMICALLY TREATED ACTIVATED CARBON CLOTHS

BE ACCEPTED IN PARTIAL FULFILLMENT OF THE REQUIREMENTS FOR

THE DEGREE OF DOCTOR OF PHILOSOPHY

Mark J. Nord

Susan M. Larson

Director of Thesis Research

David Beckwith

Head of Department

Committee on Final Examination†

Mark J. Nord

Chairperson

Susan M. Larson

James E. Economy

Mansour Postor-Alshali

† Required for doctor's degree but not for master's.

© Copyright by Mark P. Cal, 1995

Abstract

Granular activated carbon (GAC) and powdered activated carbon (PAC) have long been used to effectively treat drinking water, waste water, and industrial gas streams. Undesired contaminants are removed by adsorption onto activated carbon. While activated carbon has been used extensively in industrial applications, little research has been performed to evaluate using activated carbon to remove low concentrations of volatile organic compounds (VOCs) from indoor air environments. In this research, activated carbon cloth (ACC) is examined for its equilibrium adsorption capacity for several VOCs of relevance to indoor air quality. If the technology proves viable, filters made from ACC could be placed in new or existing air circulation systems of buildings and residences to effectively remove VOCs from indoor air.

Adsorption isotherms were measured for acetaldehyde, acetone, benzene, methyl-ethyl ketone, and water vapor and three ACC types. For the 10 to 1000 ppmv concentration range examined, benzene exhibited the highest adsorption capacity on ACC, followed by MEK, acetone, and acetaldehyde. Water vapor adsorption was not significant on ACC until relative humidities above about 50% ($P/P_o > 0.5$), when capillary condensation of $H_2O_{(g)}$ occurred within ACC pores.

Equilibrium adsorption experiments were not performed for VOCs in the sub-ppmv concentration range, due to the long times (estimated at weeks to months) to reach equilibrium and the high cost of compressed gases. The Freundlich and Dubinin-Radushkevich equations were used to model the adsorption capacities into the sub-ppmv range for the four adsorbates and three ACC types examined in this research. The sub-ppmv concentration range is a more realistic concentration range for VOCs present in indoor air environments.

It has been suggested that when using the DR equation to predict adsorption capacities of organic compounds using a reference adsorbate, reference adsorbates of similar polarity should be used. This hypothesis was examined by using acetone as a reference for polar compounds (e.g., acetaldehyde, MEK, and 1,1,1-trichloroethane). Using acetone as a reference adsorbate, predictions showed average errors of 9% for acetaldehyde and 5% for MEK (the improvement in prediction of adsorption capacity was not measured for non-polar compounds).

ACC-20 was chemically modified, producing oxidized, chlorinated, and nitrated samples. Adsorption capacities for VOCs in the 10 to 1000 ppmv concentration and water vapor from 0 to 95% RH were measured. Oxidized ACC-20 showed an enhanced physical adsorption for acetaldehyde, acetone, and water vapor, probably due to increased dipole-dipole interactions and hydrogen bonding. Oxidation of ACC-20 changed the shape of the water vapor adsorption isotherm, so that it no longer resembles a Brunauer type V. Benzene showed a decreased adsorption capacity on oxidized ACC-20, which may be due to an increase in hydrophilicity of ACC-20 or a change in pore size distribution.

Chlorination had little effect on VOC adsorption capacity, except in the case of acetone, where a decrease in adsorption capacity occurred. This may be due to pore blocking by chlorine molecules, or a decrease in hydrogen bonding between the ACC functional groups and acetone. Nitridation of ACC showed little effect on organic adsorption capacity, but increased the saturation adsorption capacity for water vapor on ACC-20 and increased the breadth of its hysteresis loop. These changes were the result of changes in the pore size distribution of the nitrated ACC-20. DR parameters were determined for VOC adsorption on ACC-20.

The effects of relative humidity (RH) on the adsorption of soluble (acetone) and insoluble (benzene) volatile organic compounds (VOCs) on activated carbon cloths (ACC) were measured. A gravimetric balance was used in conjunction with a gas chromatograph/mass spectrophotometer to determine the individual amounts of water and VOC adsorbed on an ACC sample. RH values from 0 to 90% and organic concentrations from 350 to 1000 ppmv were examined. The presence of water vapor in the gas-stream along with acetone (350 and 500 ppmv) had little effect on the adsorption capacity of acetone even at 90% RH. Water vapor in the gas-stream had little effect on the adsorption capacity of benzene (500 ppmv) until about 65% RH, when a rapid decrease in the adsorption capacity of benzene resulted with increasing RH. This RH was also about where capillary condensation of water vapor occurs within ACC pores. At this point water vapor condenses within the ACC pores, making them unavailable for benzene adsorption. Increasing benzene concentration, however, can have a significant effect on the amount of water vapor adsorbed. At 86% RH and 500 ppmv, 284 mg/g water was adsorbed, while at 86% RH and 1000 ppmv, only 165 mg/g water was adsorbed. Thus, water vapor was more inhibitory for benzene adsorption as benzene concentration in the gas stream decreased.

Acknowledgements

There are many people I would like to acknowledge during my graduate studies at the University of Illinois at Urbana-Champaign:

- First and foremost, my advisors and mentors: Dr. Mark J. Rood, Dr. Susan M. Larson, and Dr. Massoud Rostam-Abadi for their guidance and advice throughout my graduate studies.
- The Environmental Engineering and Science Program Lab Manager, Dan Ozier. Dan made life as a graduate student easier and more enjoyable.
- Many aspects of this research were performed in collaboration with the Materials Science and Engineering Department at the University of Illinois. Therefore, I would like to thank Dr. Kenneth Foster, Dr. Emmanuel Dimotakis, and Dr. James Economy for preparation of the ACC samples, their chemical characterization, and their insightful discussions of ACC.
- Dr. Tony Lizzio and Cuneyt Feizoulof of the Illinois State Geological Survey for performing the nitrogen and carbon dioxide surface area analysis on the ACC samples.
- My friends and colleagues with whom I've enjoyed stimulating conversation (and many beers) with over the years: Cuneyt Feizoulof, Dr. Eric Seagren, Dr. Lutgarde Raskin, Joe Debarr, Dr. Tony Lizzio, Dave Rapp, Mehrdad Lordgooei, Terry Kelly, Betsy Andrews, and Ann Dillner.
- And lastly, the Center for Indoor Air Research (CIAR) for funding this research.

Table of Contents

1. Introduction.....	1
1.1 Background.....	1
1.2 Indoor Air Quality	1
1.3 VOCs Present in Indoor Air	1
1.4 Activated Carbon Cloth	2
1.5 Objectives	3
1.6 References.....	4
2. Literature Review	5
2.1 Introduction.....	5
2.1.1 The Adsorption Isotherm.....	5
2.1.2 Adsorption Forces	6
2.1.3 Pore Size	6
2.2 Single Component VOC Adsorption	7
2.2.1 The Freundlich Equation	7
2.2.2 The Brunauer, Emmett, and Teller (BET) Model	8
2.2.3 The Theory of Volume Filling of Micropores.....	10
2.2.4 Dubinin-Astakhov (DA) Equation	11
2.2.5 Dubinin-Radushkevich (DR) Equation	12
2.2.6 Dubinin-Stoeckli (DS) Equation	13
2.2.7 The Affinity Coefficient	14
2.3 Pore Size Distributions for Microporous Materials.....	16
2.3.1 The Dubinin Method	16
2.3.2 The Horvath-Kawazoe (HK) Method.....	17
2.4 Water Vapor Adsorption on Activated Carbon	18
2.5 Multicomponent Organic Adsorption.....	19
2.5.1 Method of Bering et al.....	19
2.5.2 Grant and Manes Theory.....	20
2.5.3 Ideal Adsorbed Solution Theory (IAST).....	21
2.6 Adsorption of Organic Compounds from Humid Air Streams.....	24
2.7 Review of Previous Research on ACC.....	25
2.7.1 Research of Economy and Lin	25
2.7.2 Research of Foster	26
2.8 References.....	28
3. Characterization of ACC	31
3.1 Introduction.....	31
3.2 ACC Surface Areas, Pore Volumes, and Chemical Composition	31
3.3 Pore Size Distributions	33
3.4 References.....	35
4. Single Component Adsorption Measurements and Modeling.....	36
4.1 Introduction.....	36
4.2 Experimental Methods.....	36
4.2.1 Gas Generation System	37
4.2.2 Measurement of Mass Change of ACC.....	39

4.2.3 Experimental Procedure	39
4.3 Measurement of the Adsorption of Volatile Organic Compounds	39
4.4 Water Vapor adsorption with ACC	42
4.5 Single Component Adsorption Modeling	45
4.5.1 Freundlich Equation	45
4.5.2 Dubinin-Radushkevich (DR) Equation	45
4.5.3 Change of Affinity Coefficient in DR Equation for Adsorption Isotherm Prediction	50
4.6 Summary	55
4.7 References	56
5. Adsorption on Chemically Modified ACC	57
5.1 Introduction	57
5.2 Preparation of Chemically Modified ACC	59
5.2.1 Modification of ACC-20 with Ammonia	59
5.2.2 Modification of ACC-20 with Chlorine	59
5.2.3 Oxidation of ACC-20	60
5.3 X-Ray Photoelectron Spectroscopy (XPS) Measurements	60
5.4 VOC Adsorption on Chemically Modified ACC	60
5.4.1 Acetaldehyde Adsorption	61
5.4.2 Acetone Adsorption	62
5.4.3 Benzene Adsorption	63
5.4.4 Dubinin-Radushkevich (DR) Parameters for VOC Adsorption	64
5.5 Water Vapor Adsorption on Chemically Modified ACC	66
5.5.1 Water Vapor Adsorption on Oxidized and Nitridated ACC	66
5.5.2 Water Vapor Adsorption on Nitridated ACC	67
5.5.3 Adsorption of Water Vapor on Chlorinated ACC	68
5.6 Summary	69
5.7 References	69
6. Multicomponent Adsorption Measurements and Modeling	71
6.1 Introduction	71
6.2 Experimental Methods	71
6.3 Multicomponent Data Analysis	74
6.4 Multicomponent Adsorption Experimental Results	75
6.5 Modeling Adsorption of VOCs from Humid Air Streams	78
6.6 Modeling Multicomponent VOC Adsorption	81
6.7 Summary	84
6.8 References	84
7. Summary and Conclusions	86

Tables

Table 1.1. VOCs Present in Indoor Air Environments	2
Table 1.2. Chemical and Physical Properties of Organic Compounds	3
Table 2.1. Pore Classifications by Pore Width	7
Table 2.2. Cross-sectional Areas of Adsorbate Molecules	10
Table 2.3. Parachors and Affinity Coefficients of Adsorbates	15
Table 2.4. Parameters for calculation of affinity coefficient	16
Table 2.5. BET Surface Area and Elemental Composition of ACC Samples	26
Table 2.6. XPS Deconvolution of the Carbon 1s Peak Area	27
Table 2.7. Effective Pore Volume for Select VOCs	27
Table 2.8. Comparison of Carbon Oxygen Mass Ratios with XPS and Elemental Analysis	27
Table 3.1. BET Surface Areas and Total Pore Volumes for ACC Using N ₂ at 77 K.	32
Table 3.2. DR Surface Areas for ACC	32
Table 3.3. DS Parameters for ACC Using N ₂ at 77 K.....	33
Table 4.1. Dubinin Parameters for Equation 2.28 and ACC	45
Table 4.2. Freundlich Parameters for VOC Adsorbates and ACC	50
Table 4.3. DR Parameters for VOC Adsorbates and ACC	54
Table 5.1. Physical Characteristics and Elemental Composition of ACCs	58
Table 5.2. XPS Deconvolution of the Carbon 1s Peak Area for Chemically Modified ACC-20.....	61
Table 5.3. DR Parameters for VOC Adsorption on Chemically Modified ACC-20	65
Table 6.1. DR Parameters Used in IAST Modeling	81
Table 6.2. Calculated Activity Coefficients for Acetone-Benzene Mixture at a Total Pressure of 0.76 mm Hg	83

Figures

Figure 2.1. The Five Types of Adsorption Isotherms as Classified by Brunauer, Deming, Deming, and Teller (BDDT).....	6
Figure 3.1. Adsorption Isotherms for ACC and N ₂ at 77 K	32
Figure 3.2. Pore Size Distribution for ACC Using HK Method and N ₂ at 77 K.....	34
Figure 3.3. Pore Size Distributions for ACC Using DS Method and N ₂ at 77 K.....	34
Figure 4.1. Apparatus for Adsorption Measurements of VOCs in the ppmv Range	37
Figure 4.2. Apparatus for Measurement of Water Vapor Adsorption Isotherms	38
Figure 4.3. Adsorption Isotherms for Acetaldehyde and ACC.....	40
Figure 4.4. Adsorption Isotherms for Acetone and ACC	41
Figure 4.5. Adsorption Isotherms for Benzene and ACC.....	41
Figure 4.6. Adsorption Isotherms for Methyl Ethyl Ketone (MEK) and ACC	42
Figure 4.7. Adsorption Isotherms for Water Vapor and ACC.....	43
Figure 4.8. Measured and Modeled Adsorption Isotherms for Water Vapor and ACC-15.....	43
Figure 4.9. Measured and Modeled Adsorption Isotherms for Water Vapor and ACC-20.....	44
Figure 4.10. Measured and Modeled Adsorption Isotherms for Water Vapor and ACC-25.....	44
Figure 4.11. Experimental and Freundlich Modeled Adsorption Isotherms for Acetaldehyde and ACC.....	46
Figure 4.12. Experimental and Freundlich Modeled Adsorption Isotherms for Acetone and ACC	46
Figure 4.13. Experimental and Freundlich Modeled Adsorption Isotherms for Benzene and ACC.....	47
Figure 4.14. Experimental and Freundlich Modeled Adsorption Isotherms for MEK and ACC.....	47
Figure 4.15. Experimental and DR Modeled Adsorption Isotherms for Acetaldehyde and ACC.....	48
Figure 4.16. Experimental and DR Modeled Adsorption Isotherms for Acetone and ACC	48
Figure 4.17. Experimental and DR Modeled Adsorption Isotherms for Benzene and ACC.....	49
Figure 4.18. Experimental and DR Modeled Adsorption Isotherms for MEK and ACC.....	49
Figure 4.19. Predicted and Observed Adsorption Isotherms for ACC-15 Using N ₂ at 77K as a Reference Vapor in the DR Equation.....	51
Figure 4.20. Predicted and Observed Adsorption Isotherms for ACC-20 Using N ₂ at 77K as a Reference Vapor in the DR Equation.....	51
Figure 4.21. Predicted and Observed Adsorption Isotherms for ACC-25 Using N ₂ at 77K as a Reference Vapor in the DR Equation.....	52
Figure 4.22. Modeled Adsorption Isotherms for VOCs Using Benzene as a Reference Adsorbate in the DR Equation and ACC-15. Benzene Adsorption Capacity was Experimentally Measured.....	53
Figure 4.23. Modeled Adsorption Isotherms for VOCs Using Acetone as a Reference Adsorbate in the DR Equation and ACC-15. Experimental Plots for Acetaldehyde and MEK are Shown for Comparison to Modeled Curves. The Acetone Isotherm was Experimentally Determined	53
Figure 5.1. Chemical Treatment of ACC.....	57
Figure 5.2. Adsorption of Acetaldehyde on Chemically Modified ACC	62
Figure 5.3. Adsorption of Acetone on Chemically Modified ACC.....	63
Figure 5.4. Adsorption of Benzene on Chemically Modified ACC	64
Figure 5.5. Adsorption and Desorption of Water Vapor on Oxidized and Nitrated ACC-20	67
Figure 5.6. Adsorption and Desorption of Water Vapor on Chlorinated ACC-20.....	68

Figure 6.1. Experimental Apparatus for Measurement of VOC Adsorption in Humid Air Streams	72
Figure 6.2. Multi-ported Gravimetric Balance Hang-down Tube	73
Figure 6.3. Adsorption of 500 ppmv Benzene onto ACC-20 as a Function of Time	74
Figure 6.4. Influent and Effluent Benzene Concentrations as a Function of Time	75
Figure 6.5. Adsorption of 500 ppmv Benzene on ACC-20 at Several Relative Humidities	76
Figure 6.6. Adsorption Capacity Dependence on Relative Humidity of 500 ppmv Benzene on ACC-20	77
Figure 6.7. Adsorption Capacity Dependence on Relative Humidity of 1000 ppmv Benzene on ACC-20	77
Figure 6.8. Adsorption of 500 ppmv Acetone on ACC-20 at Several Relative Humidities	78
Figure 6.9. Adsorption Capacity dependence on Relative Humidity of 500 ppmv Acetone on ACC-20	79
Figure 6.10. Adsorption Potential for Acetone and Water Vapor	80
Figure 6.12. Measured and Modeled Results for Acetone Adsorption on ACC-20 at Various Relative Humidities	80
Figure 6.11. Measured and Modeled Results for Benzene Adsorption on ACC-20 at Various Relative Humidities	81
Figure 6.13. Reduced Spreading Pressure for Acetone and Benzene as a Function of Adsorbate Partial Pressure	82
Figure 6.14. Measured and Modeled Adsorption of Acetone and Benzene on ACC-20 at 1000 ppmv (0.76 mm Hg) Total Concentration	83

Chapter 1

Introduction

1.1 Background

Granular activated carbon (GAC) and powdered activated carbon (PAC) have long been used to effectively treat drinking water, waste water, and industrial gas streams. Undesired contaminants are removed by adsorption onto activated carbon. While activated carbon has been used extensively in industrial applications, little research has been performed to evaluate using activated carbon to remove low concentrations of volatile organic compounds (VOCs) from indoor air environments. In this research, activated carbon cloth (ACC) is examined for its equilibrium adsorption capacity for selected VOCs of relevance to indoor air quality. If the technology proves viable, filters made from ACC could be placed in new or existing air circulation systems of buildings and residences to effectively remove VOCs from indoor air.

1.2 Indoor Air Quality

A large amount of research has been devoted to assessment of indoor air quality during the past few decades. During the early 1970's there was a push to make buildings more energy efficient, because of the high cost of petroleum derived fuels. Increasing the heating and cooling efficiency of buildings meant decreasing indoor-outdoor air exchange rates and sealing windows. This facilitated the build-up of organic contaminants present in indoor environments from sources such as, building materials, paints, adhesives, and tobacco smoke. This increase in concentration of organic contaminants causes concern, because health risks may be increased due to long exposure times to low concentrations of organic contaminants (Tancrede, 1987). Many of the organic compounds present in indoor air are known to be carcinogenic or mutagenic.

1.3 VOCs Present in Indoor Air

Sources of VOCs in indoor environments are varied, as are the contaminants. According to Ramanathan (1988), more than 250 VOCs have been measured in indoor air environments at concentrations greater than 1 ppbv[†]. By reviewing the literature over the period of 1979 through 1990, Samfield (1992) compiled a list of

[†]. ppbv = part per billion by volume; similarly, ppmv = part per million by volume.

220 compounds present in indoor air environments ranging in molecular weight from 30 to 446, and from 1 to 31 carbon atoms. The following compounds were the most frequently reported (but were not necessarily present in the largest quantity): formaldehyde, tetrachloroethylene, 1,1,1-trichloroethane, trichloroethylene, benzene, p-dichlorobenzene, toluene, ethylbenzene, xylenes, decane, and undecane. About 50% of the compounds reported had fewer than 9 carbon atoms, and about 90% had fewer than 23 carbon atoms. A list of organic compounds used in this research, their mean indoor air concentrations, and sources is presented in Table 1.1 (Samfield, 1992) Chemical and physical properties for the same organic compounds are presented in. Table 1.2.

Table 1.1. VOCs Present in Indoor Air Environments (Samfield, 1992).

Organic Compound	Molecular Formula	Molecular Weight	Mean (Max) Concentration [ppbv] [†]	Some Substantiated (and Possible) Sources [‡]
Acetaldehyde	C ₂ H ₄ O	44.05	9.5 (27)	auto exhaust (perfumes, tobacco smoke)
Acetone	C ₃ H ₆ O	58.08	17 (66)	lacquer solvent (tobacco smoke)
Benzene	C ₆ H ₆	78.11	5 (2000)	tobacco smoke, adhesives, wood stain
Ethylbenzene	C ₈ H ₁₀	106.17	5 (185)	insulation foam, fiberboard, adhesives
2-Butanone (MEK)	C ₄ H ₈ O	72.11	3 (13)	particle board, floor/wall covering
Toluene	C ₇ H ₈	92.14	12 (600)	adhesives, paint, sealing cmpd.
1,1,1-Trichloroethane	C ₂ H ₃ Cl ₃	133.41	5.5 (180)	dry cleaning, cleaning fluid
p-Xylene	C ₈ H ₁₀	106.17	5 (280)	adhesives, wallpaper, caulking cmpd.

†. Samfield (1992) reported concentrations in $\mu\text{g}/\text{m}^3$. The author (M.P. Cal) changed the concentrations to ppbv to facilitate comparison with results presented later in this dissertation.

‡. The list of sources for most of the organic compounds in the table was extensive, so only some sources are given.

1.4 Activated Carbon Cloth

The ACC samples used in this study (ACC-5092) were obtained from American Kynol, Inc. (New York, NY). The starting material for the manufacture of ACC are cross-linked phenol-aldehyde fibers (novoloid fibers). These fibers are infusible and insoluble and have very high resistance to chemical attack (Hayes, 1985). ACC are used in solvent recovery systems, wound dressings, filters, and as electrodes in high-capacity rechargeable batteries (Hayes, 1985).

Novoloid fibers are carbonized and activated in a one step process to produce ACC. As the fibers are activated for longer times, the surface area of the ACC, the pore volume, and the mean pore size all increase (Hayes, 1985). This makes it possible to tailor the level of activation of the fibers for the optimal adsorption of a particular compound.

Table 1.2. Chemical and Physical Properties of Organic Compounds.

Organic Compound	Boiling Point [°C]	Saturation Vapor Pressure [mm Hg]	Density @ 20 °C [g/cm ³]	Surface Tension @ 20 °C [dyne/cm]	Dipole Moment [debyes]
Acetaldehyde	21	1000	0.783	21.2	2.71
Acetone	56.5	229	0.790	23.0	2.77
Benzene	80.1	94.5	0.877	28.9	0
Ethylbenzene	136.2	9.43	0.867	29.0	0.37
2-Butanone (MEK)	79.6	89.5	0.805	24.6	3.2
Toluene	110.6	28.34	0.866	28.5	0.45
1,1,1-Trichloroethane	74.1	133	1.34	25.7	1.79
p-Xylene	138.4	8.68	0.861	28.3	0

ACC are produced by gradually heating the novoloid fibers to 900 °C in an atmosphere of steam and/or carbon dioxide. This may be either a batch or continuous process. Specific surface areas as high as 2500 m²/g may be obtained, but due to increased costs and diminishing yields, ACC with specific surface areas of 1500 or 2000 m²/g are usually the practical limit for most purposes (Hayes, 1985). ACC have nearly all of their pores in the micropore range (pore diameter < 2 nm). These micropores exist on the fiber surface, permitting rapid adsorption of gases (Hayes, 1985).

1.5 Objectives

This research attempts to examine ACC in detail for use in gas-phase organic contaminant removal. While kinetic (adsorption bed) tests are important in the design of a filtering system, this research only attempts to characterize ACC in terms of equilibrium adsorption capacities. Knowledge gained in this research is useful for designing adsorption bed systems and to test designs. This dissertation addresses six main objectives:

- 1) Measure adsorption isotherms for several VOC adsorbates (acetaldehyde, acetone, benzene, and methyl ethyl ketone [MEK]) and ACC in the 10 to 1000 ppmv concentration range; use adsorption models to model adsorption capacities in the sub-ppmv concentration range, which is more relevant for indoor air quality studies.
- 2) Characterize ACC in terms of micropore size distribution and surface area.
- 3) Measure adsorption isotherms for water vapor and ACC; determine competitive adsorption effect when polar and nonpolar VOCs are present in humid gas streams.
- 4) Use the Dubinin-Radushkevich (DR) model to predict the adsorption capacity of other adsorbates of

Chapter 1: Introduction

interest to indoor air quality, but not measured in this study.

- 5) Evaluate the effect of chemical modification of ACC on the adsorption capacity of VOCs and water vapor.
- 6) Measure and model multicomponent VOC adsorption on ACC.

1.6 References

Hayes, J.S., "Novoloid Nonwovens," *Nonwoven Symposium*, TAPPI Press, pp. 257-263, April, 1985.

Ramanathan, K., Debler, V., Kosusko, M., and Sparks, L., "Evaluation of Control Strategies for Volatile Organic Compounds in Indoor Air," *Environmental Progress*, **7**(4), 1998.

Samfield, M.M., "Indoor Air Quality Data Base for Organic Compounds," *United States Environmental Protection Agency*, EPA-600-R-92-025, 1992.

Tancrede, M., Wilson, R., Zeise, L., Crouch, E.A., "The Carcinogenic Risk of Some Organic Vapors Indoors: A Theoretical Study," *Atmospheric Environment*, **21**(1):2187-2205, 1987.

Chapter 2

Literature Review

2.1 Introduction

This chapter details the theory and numerical methods used to characterize microporous adsorbents. This includes modeling of single and multicomponent adsorption isotherms, determination of adsorbent surface area and pore volume, and the determination of micropore size distributions.

2.1.1 The Adsorption Isotherm

When a solid (adsorbent) is exposed to a gas or vapor (adsorbate), the solid begins to adsorb the gas onto its surface and into its pores, if the solid is porous. Adsorption occurs because of forces acting between the solid and the gas molecules. Two kinds of forces give rise to adsorption: physical (van der Waals) and chemical. These types of adsorption are termed physical adsorption and chemisorption, respectively.

In a closed system, the adsorption of a gas onto a solid can be measured by monitoring the decrease in adsorbate pressure within a known volume or by measuring the mass gain of the adsorbent due to the adsorbing gas molecules. Both methods are commonly used and give accurate results.

The amount of a gas adsorbed in moles per gram solid, is a function of partial pressure (concentration) of the adsorbate, temperature of the system, the adsorbate, and the adsorbent. Measuring the amount of a compound adsorbed on an adsorbent versus concentration or pressure at a constant temperature results in an adsorption isotherm. Adsorption isotherms are useful for characterizing adsorbents with respect to different adsorbates.

The adsorption literature has reported tens of thousands of adsorption isotherms, measured for many different adsorbents. The majority of these isotherms fall into five types, as classified by Brunauer, Deming, Deming and Teller (BDDT)[†], and are presented in Figure 2.1 (Gregg and Sing, 1982; Brunauer, et al., 1940). Type I is observed by the physical adsorption of gases onto microporous solids. Type II results from the physical adsorption of gases by nonporous solids. Type IV is from the physical adsorption of gases by mesoporous solids. Types III and V may originate from the adsorption of either polar or nonpolar molecules, provided that the adsorbate-adsorbent force is relatively weak. It should also be noted that a type V isotherm

[†]. Also sometimes referred to as the Brunauer, Emmett, and Teller (BET), or just Brunauer classification, e.g., Brunauer type I isotherm.

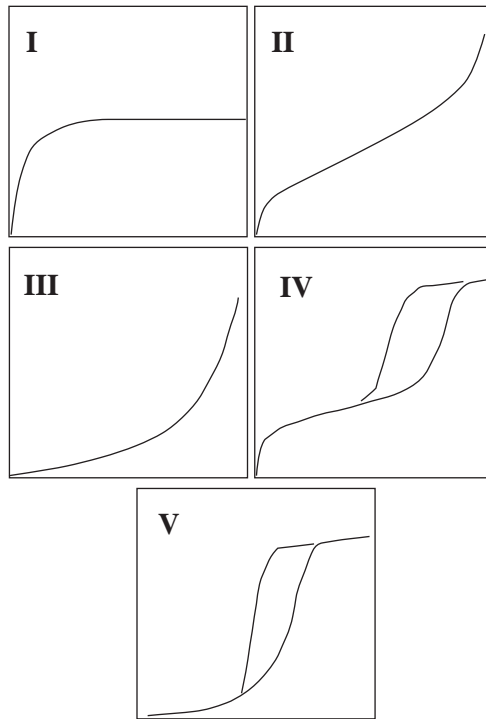


Figure 2.1. The Five Types of Adsorption Isotherms as Classified by Brunauer, Deming, Deming, and Teller (BDDT).

possesses a hysteresis loop. Water vapor adsorption on microporous activated carbon is an example of a type V isotherm.

2.1.2 Adsorption Forces

Adsorption of a gas onto a solid is the result of the attraction forces between adsorbate and adsorbent molecules. Currently, adsorption models are idealized and it is not possible to calculate an adsorption isotherm based upon independently determined parameters of gas and solid (Gregg and Sing, 1982). Adsorption forces include dispersion forces (attractive), short-range repulsive forces, and electrostatic (coulombic) forces if either the solid or the gas is polar. Dispersion forces (also called London or van der Waals forces) arise from the rapid fluctuation in electron density within each atom. This induces an electrical dipole moment in neighboring atoms, leading to an attraction between the atoms.

2.1.3 Pore Size

The size of individual pores can vary greatly in size and shape for different adsorbents and even within the same adsorbent. Pores are usually characterized in terms of their width, meaning the diameter of a cylindrical pore or the distance between two sides of a slit-shaped pore. Dubinin (1960) proposed a

classification of pores presented in Table 2.1 which was later adopted by the International Union of Pure and Applied Chemistry (IUPAC, 1972).

Table 2.1. Pore Classifications by Pore Width.

Pore Classification	Pore Width
Micropores	less than ~20 Å (2 nm)
Mesopores	between ~20 and ~500 Å (2 and 50 nm)
Macropores	more than ~500 Å (50 nm)

The basis for the pore classifications presented in Table 2.1 is that each size range corresponds to different adsorption effects, as observed in an adsorption isotherm. The interaction potential in micropores is much greater than that in larger pores due to the closeness of the pore walls, resulting in an enhanced adsorption potential. An adsorbate molecule within a micropore is held there by adsorption forces originating from approximately the ten nearest surface atoms. The forces on adsorbate molecules are a function of distance between adsorbate and adsorbent atoms (pore size) and polarity (permanent or induced) of the adsorbate and adsorbent atoms (Marsh, 1987). Capillary condensation takes place within mesopores, resulting in a hysteresis loop in the adsorption isotherm. The pores are so wide in the macropore range that it is nearly impossible to map out the isotherm in detail because the relative pressures of the adsorbate (P/P_0) would be so close to unity. Mercury is typically used to examine macropore structure, due to its low vapor pressure.

2.2 Single Component VOC Adsorption

2.2.1 The Freundlich Equation

The Freundlich equation is an empirical expression used to describe adsorption isotherms where there is a linear response for adsorption capacity as a function of adsorbate concentration (or partial pressure) when this function is plotted on log-log scales. The valid concentration range for the Freundlich equation varies according to the adsorbate-adsorbent combination. The Freundlich equation is represented as:

$$\frac{x}{m} = k C^{1/n} \tag{2.1}$$

where x is the mass of solute adsorbed; m is the mass of adsorbent; k and n are empirical constants and C is the equilibrium concentration of the adsorbate in the bulk gas phase. The constants k and n in equation 2.1 are determined by plotting $\log(C)$ on the abscissa and $\log(x/m)$ on the ordinate (the line determined from the plot has a slope of $1/n$ and an intercept of $\log(k)$). The Freundlich equation is useful in cases where the

actual identity of the adsorbate is not known (Treybal, 1980). The disadvantages of using the Freundlich equation is that it is only useful for limited adsorbate concentration ranges and it has no predictive ability with regard to adsorption isotherms for similar adsorbates. A new Freundlich plot must be produced for each adsorbate-adsorbent combination.

2.2.2 The Brunauer, Emmett, and Teller (BET) Model

BET theory (Brunauer et al., 1938) is based on a kinetic model of adsorption proposed by Langmuir in 1916 and portrays a solid surface as an array of adsorption sites. Equilibrium occurs when the rate at which molecules arriving from the gas phase and condensing or adsorbing onto unoccupied adsorption sites is equal to the rate at which molecules evaporate or desorb from occupied sites.

For the case of monolayer adsorption, the Langmuir equilibrium adsorption equation results (Langmuir, 1916):

$$\frac{n}{n_m} = \frac{B P}{1 + B P} \quad (2.2)$$

where n is the amount in moles adsorbed on 1 g of adsorbent; n_m is the monolayer capacity (the adsorption of one molecular layer of the adsorbate on the adsorbent); B is an empirical constant; and P is the partial pressure of the adsorbate. Assuming multiple adsorptive layers[†], the BET equilibrium adsorption equation is produced:

$$\frac{n}{n_m} = \frac{c (P/P_o)}{(1 - P/P_o)(1 + (c - 1)(P/P_o))} \quad (2.3)$$

where

$$c = \exp\left(\frac{(q_1 - q_L)}{RT}\right) \quad (2.4)$$

P_o is the saturation vapor pressure of the adsorbate; $(q_1 - q_L)$ is the net heat of adsorption; R is the ideal gas law constant and T is the temperature in Kelvin (Gregg and Sing, 1982).

Because adsorption experiments frequently measure volume adsorbed, rather than moles adsorbed, it is convenient to represent equation 2.3 as equation 2.5, where V is the volume adsorbed per gram of adsorbent and V_m is the monolayer adsorption capacity in terms of volume.

[†]. The reader is asked to consult Brunauer, Emmett and Teller (1938), or Gregg and Sing (1982) for the assumptions made and the resulting derivation for equation 2.3.

$$\frac{V}{V_m} = \frac{c(P/P_o)}{(1 - P/P_o)(1 + (c - 1)(P/P_o))} \quad (2.5)$$

Plotting P/P_o versus $(P/P_o)/V(1 - P/P_o)$ over the range of $0.05 < P/P_o < 0.35$, the parameters V_m and c can be determined using equations 2.6 and 2.7.

$$V_m = \frac{1}{\text{slope} + \text{intercept}} \quad (2.6)$$

$$c = \frac{\text{slope}}{\text{intercept}} + 1 \quad (2.7)$$

The surface area of adsorbent can then be determined using equation 2.8, where S is the surface area of the adsorbent [m^2/g], σ is the area of an adsorbate molecule, N_A is Avagadro's number (6.022×10^{23} number/mole), ρ is the adsorbate liquid density, and MW is the molecular weight of the adsorbate molecule.

$$S = \frac{V_m \sigma N_A \rho}{MW} \quad (2.8)$$

Many sorption analyzers measure the amount of gas adsorbed and convert it to volume of gas adsorbed at standard temperature and pressure (STP) (273 K and 1 atm). If adsorption data are determined in that manner, the volume of gas adsorbed can be converted to a liquid volume adsorbed using the ratio of the adsorbed phase (liquid) and gas densities and using equation 2.8 to calculate the surface area. One could also use equation 2.9 presented below:

$$S = \frac{V_m N_A \sigma}{V_i} \quad (2.9)$$

where V_i is the molar volume of the gas (22.4 L/mol at STP) and V_m is in units of [cm^3 gas/g adsorbent].

Several adsorbates are commonly used to determine surface area of an adsorbent, with the most common being nitrogen at 77 K. Other common adsorbates are benzene at 293 K and carbon dioxide at 195, 273, or 293 K. The equations described above can be used for any adsorbate, but molecular packing and pore sieving effects should be considered when choosing an adsorbate molecule for surface area determination. An adsorbate with a relatively large saturation pressure should also be chosen for surface area determination, so that a wide range of relative pressures can be covered at the chosen adsorption temperature. McClellan and Harnsberger (1967) compiled a list of adsorbate molecular areas, some of which are presented in Table 2.2.

Table 2.2. Cross-sectional Areas of Adsorbate Molecules.

Adsorbate Molecule	Cross-sectional Area (σ) [†] [Å ²]	Molecular Dimension (Lennard-Jones) [‡] [Å]
Water (H ₂ O)	12.5	2.64
Nitrogen (N ₂)	16.2	3.80
Acetone (C ₃ H ₆ O)	16.7	4.60
Carbon Dioxide (CO ₂)	22.0	3.94
Benzene (C ₆ H ₆)	43.0	5.35 (3.7 Å x 7.0Å)

†. McClellan and Harnsberger, 1967.

‡. Determined from viscosity data. Reference: Reid, R.C., Prausnitz, J.M., and Poling, B.E., *Properties of Gases and Liquids, Fourth Edition*, McGraw-Hill, pp. 733-734, 1987.

A criticism of BET theory is the assumption that all adsorption sites on the solid surface are energetically homogeneous. In reality, most adsorption surfaces are energetically heterogeneous, not homogeneous as BET theory proposes. Another criticism is that the model neglects adsorbate-adsorbate interactions, which are not negligible when an adsorption layer is near completion and the average separation of the molecules is small in relation to their size (Gregg and Sing, 1982).

2.2.3 The Theory of Volume Filling of Micropores

One of the most widely used theories to describe physical adsorption of gases and vapors onto microporous adsorbents was developed by M. M. Dubinin and co-workers and is generally referred to as the theory of volume filling of micropores (TVFM) (Dubinin, 1975). Several equations have been proposed based upon this theory, e.g., Dubinin-Astakhov, Dubinin-Radushkevich, and Dubinin-Stoeckli equations.

All physical adsorption theories existing previous to the work done by Dubinin used the same physical image for describing adsorption onto both porous and nonporous adsorbents. This physical image is that of formation of one or more successive adsorption layers onto a surface. In contrast, Dubinin conceived micropores as space volumes in a porous material where the molecules that successively adsorbed do not form adsorption layers, but rather adsorption is characterized by volume filling within the adsorption space. The adsorbed substance is present in the form of a liquid in a highly compressed state in the adsorption field.

The micropores within a substantially microporous adsorbent are thought to be slit-shaped (Dubinin, 1991). The width of these slits can be varied with activation. Longer activation times can produce wider slits. The slits or pores with smaller widths are characterized as having the greatest adsorption energy due to the superposition of the adsorption potentials of opposite pore walls (Carrott et al., 1991; Everett and Powl, 1976). This observation is important for the adsorption of low concentrations of gases onto microporous

adsorbents; it suggests that highly microporous materials are best suited for removal of low concentrations of VOCs (Dubinin, 1960; Dubinin, 1991; Carrott et al., 1991; Foster et al., 1992; Cal et al., 1994).

2.2.4 Dubinin-Astakhov (DA) Equation

The fundamental basis for the Dubinin et al. equations is Polanyi's potential theory of adsorption (Polanyi, 1932). At a given temperature, T , and an equilibrium partial pressure of the adsorbate, P , the maximum differential molar work, A , needed to transport one mole of the adsorbate from the liquid or gas phase to a surface of an infinitely large amount of adsorbent is expressed as

$$A = -\Delta G = RT \ln \frac{P_0}{P} \quad (2.10)$$

where ΔG is the Gibbs free energy, R is the ideal gas law constant and P_0 is the saturation vapor pressure of the adsorbate.

TVFM can be expressed in a general form, usually denoted as the Dubinin-Astakhov (DA) equation (Dubinin, 1975):

$$W = W_0 \exp \left[- \left(\frac{A}{\beta E_0} \right)^n \right] \quad (2.11)$$

where W represents the volume of the adsorbate condensed within the micropores at temperature T and relative pressure P/P_0 (P is the partial pressure of the adsorbate, and P_0 is the saturation vapor pressure of the adsorbate); W_0 is the total volume of the micropores accessible to the given adsorbate (units of $[\text{cm}^3/\text{g}]$ or $[\text{mmol}/\text{g}]$, but consistent with W); A is as presented in equation 2.10; E_0 is the characteristic adsorption energy; β and the exponent n are parameters specific to the adsorbate. β is the affinity coefficient and is the ratio of adsorption potentials of the adsorbate to a reference adsorbate. β for benzene is usually taken to be one by convention. Methods for calculating β will be discussed in section 2.2.7. The parameter, n , can be calculated by rearranging equation 2.11:

$$n = \frac{\log [2.30 \log (W_0/W)]}{\log (A/\beta E_0)} \quad (2.12)$$

At values of W close to W_0 , $\log (W_0/W)$ approaches zero, making the determination of n unreliable. Unreliable estimates of n are also found at isotherm points close to the characteristic point when $\log (A/E_0)$ in the denominator approaches zero (Dubinin, 1975).

Experiments have shown that n varies from 1.5 to 3 for microporous activated carbons, increasing as the microporous structure of the activated carbons become more homogeneous, i.e., the breadth of the micropore distribution about some mean pore size decreases (Dubinin and Stoeckli, 1980; Finger and

Bulow, 1979). A value of $n = 2$ has been chosen for the derivation of the Dubinin-Radushkevich equation and appears to be a good assumption when representing the adsorption of vapors by average activated carbons over a limited range of vapor pressures ($10^{-5} < P/P_0 < 0.4$ to 0.5) (Stoeckli et al., 1989).

2.2.5 Dubinin-Radushkevich (DR) Equation

The Dubinin-Radushkevich (DR) equation was developed to describe physical adsorption onto microporous carbons. The DR equation was developed by setting the exponent n in the DA equation (equation 2.11) equal to 2, resulting in the relationship

$$W = W_0 \exp \left[- \left(\frac{A}{\beta E_0} \right)^2 \right] \quad (2.13)$$

The value of $n = 2$ was chosen after examining experimental data on the adsorption of vapors of various substances onto activated carbons with different microporous structures (Dubinin, 1975).

Plotting equation 2.13 with $\ln(W)$ on the ordinate and A^2 on the abscissa yields a straight line called the characteristic adsorption equation. The characteristic adsorption equation has the form

$$\ln W = \ln W_0 - \left(\frac{1}{\beta E_0} \right)^2 A^2 \quad (2.14)$$

The parameters E_0 (or βE_0 , if β is not equal to one) and W_0 in equation 2.14 can now be determined from the slope and the intercept, respectively, of the straight line presented in equation 2.14 because all other parameters (W , β , and A) are known or measured.

Dubinin introduced a useful method of characterizing microporous carbons by introducing a relationship for the slit-shaped micropore half-width, x_0 ,

$$k = x_0 E_0 \quad (2.15)$$

where k is the energy characteristic constant, which was estimated using small-angle x-ray scattering and benzene adsorption data on various activated carbons and assuming that the micropores of the adsorbent are slit-shaped (Dubinin, 1989a); x_0 is the pore half-width and E_0 is the characteristic adsorption energy. Equation 2.15 is only valid for benzene adsorption. If other adsorbates are used, then $x_0\beta$ represents the pore half-width. This will be discussed in more detail in a later section. Using equation 2.15, the DR equation can be represented by

$$W = W_0 \exp \left[- \left(\frac{A x_0}{\beta k} \right)^2 \right] \quad (2.16)$$

or

$$W = W_o \exp(-m x_o^2 A^2) \quad (2.17)$$

where

$$m = \left(\frac{1}{\beta k}\right)^2 \quad (2.18)$$

with A as defined in equation 2.10. Dubinin suggests a value of 12.0 kJ-nm/kg-mol for k when using benzene adsorption on microporous activated carbons (Dubinin, 1985).

2.2.6 Dubinin-Stoeckli (DS) Equation

The Dubinin-Stoeckli (DS) equation incorporates a Gaussian distribution of pore half-widths in its description of adsorption of vapors and gases onto heterogeneous microporous adsorbents (Dubinin, 1989a). If a Gaussian distribution is used to describe the micropores' size distribution, then equation 2.19 can be used to describe the adsorption of gases and vapors onto heterogeneous microporous adsorbents with slit-shaped pores, where x is the normal half-width distribution of micropore volumes (W_o) for the slit-pore model. Defining W_o^o as the total of the volume of micropores and supermicropores[†], the normal distribution equation is obtained:

$$\frac{d(W_o)}{d(x)} = \frac{W_o^o}{\delta\sqrt{2\pi}} \exp\left(-\frac{(x_o - x)^2}{2\delta^2}\right) \quad (2.19)$$

where x_o is the modal micropore half-width for the distribution and δ is the variance of the pore half-width.

Using equation 2.17 for adsorbents with a homogeneous structure and equation 2.19 for the micropore volume distribution, a TVFM adsorption equation can be derived for adsorbents with heterogeneous microporous structure. Differentiating equation 2.17 and substituting $d(W_o)$ into equation 2.19, the adsorption equation in integral form is obtained:

$$W = \frac{W_o^o}{\delta\sqrt{2\pi}} \int_0^\infty \exp\left(-\frac{(x_o - x)^2}{2\delta^2}\right) \exp(-m x_o^2 A^2) dx \quad (2.20)$$

Integrating equation 2.20 yields the DS adsorption equation for adsorbents with heterogeneous microporous structure (Dubinin, 1989a):

[†]. According to Dubinin, the micropore range includes slit-shaped pores with $x < 0.6-0.7$ nm, and the supermicropore range includes larger sized pores with $0.6-0.7 < x < 1.5-1.6$ nm, where x is the micropore half-width for the slit-pore model (Dubinin, 1989b).

$$W = \frac{W_o^o}{2\sqrt{1 + 2m\delta^2A^2}} \exp\left[-\frac{mx_o^2A^2}{\sqrt{1 + 2m\delta^2A^2}}\right] \left[1 + \operatorname{erf}\left(\frac{x_o}{\delta\sqrt{2}\sqrt{1 + 2m\delta^2A^2}}\right)\right] \quad (2.21)$$

By noting that the probability integral $\operatorname{erf}(\infty) = 1$, the DS equation 2.21 becomes the DR equation 2.17 for adsorbents with homogeneous microporous structure, i.e., for $\delta = 0$.

2.2.7 The Affinity Coefficient

For different vapors, the attractive forces of the molecules to the surface of the adsorbent are not the same. According to the theory of dispersion interaction (Muller, 1936), the adsorption spaces filled by two different substances is proportional to the ratio of the polarizabilities (α) of the two vapors. For identical adsorption capacities, W , or volume fillings of the adsorption space, the adsorption potentials, E , have a constant ratio (Dubinin, 1975):

$$\beta = \frac{E}{E_o} = \frac{\alpha}{\alpha_o} \quad (2.22)$$

Two methods are commonly used to calculate β . The somewhat simpler method for the calculation of β , shown in equation 2.23, is to approximate β with the ratio of the parachor ($[P]$) of the adsorbate of interest to the parachor of the reference adsorbate ($[P]_o$), which is usually taken to be benzene.

$$\beta = \frac{[P]}{[P]_o} \quad (2.23)$$

A parachor is a secondary derived function dependent on the primary properties of surface tension, density, and molecular weight of the adsorbate, and can be represented as (Quayle, 1953):

$$[P] = \gamma^{1/4} \frac{M}{(D - d)} \quad (2.24)$$

where $\gamma = C(D - d)^4$

and D and d are the densities of a liquid and its vapor, respectively, γ is the surface tension, C is a constant characteristic of the liquid, and M is the molecular weight of the compound. The parachor of a substance is equal to its molar volume in liquid form when its surface tension (in units of dynes/cm) is close to unity. At this condition, the intermolecular forces of attraction between adsorbate molecules produce identical compression of the liquid compound, and the proportionality between its molar volume and the volume of molecules hold more precisely (Dubinin, 1960).

Table 2.3 shows parachors for select adsorbates of interest in indoor air quality and the affinity coefficients calculated using equation 2.23 with nitrogen, benzene and acetone as the reference adsorbates. The parachor values in Table 2.3 are mean values calculated by the author (M.P. Cal) from data provided by

Chapter 2: Literature Review

Quayle (1953), with the exception of the parachor for acetaldehyde which was calculated by treating the parachor as an additive function (Quayle, 1953). In this method, each chemical functional group of a molecule is given a reduced parachor value. These reduced parachors are then summed to give the parachor for the molecule. A thorough discussion of this method is presented by Quayle (1953).

Table 2.3. Parachors and Affinity Coefficients of Adsorbates.

Adsorbate	Parachor, [P]	β (wrt [†] nitrogen)	β (wrt benzene)	β (wrt acetone)
Acetaldehyde	134.5	1.98	0.653	0.83
Acetone	161.2	2.37	0.782	1.00
Benzene	206.1	3.03	1.00	1.28
Ethylbenzene	284.3	4.18	1.38	1.76
Methyl Ethyl Ketone (MEK) (2-Butanone)	245.9	2.92	0.96	1.23
Nitrogen	68.0	1.00	0.33	0.42
Toluene	246.0	3.62	1.19	1.53
1,1,1 Trichloroethane	224.8	3.31	1.09	1.39
p-Xylene	285.0	4.19	1.38	1.77

†. wrt = with respect to.

The second method used to calculate the affinity coefficient is based upon dispersion interaction theory according to Kirkwood and Muller (Muller, 1936) using the equation

$$\beta = \frac{\alpha}{\alpha_o} \left(\frac{\alpha_o/\chi_o + \alpha_s/\chi_s}{\alpha/\chi + \alpha_s/\chi_s} \right) \quad (2.25)$$

where α and α_o are polarizabilities of the test and reference vapor, respectively; and χ and χ_o are diamagnetic susceptibilities of the test and reference vapor, respectively. The variables α_s and χ_s denote the corresponding values for the adsorbent material (e.g., activated carbon) (Dubinin, 1991). The polarizabilities and diamagnetic susceptibilities of several compounds of interest are presented in Table 2.4 along with β , which was calculated using equation 2.25 (Lide, 1990).

Table 2.4. Parameters for calculation of affinity coefficient.

Adsorbate	α [cm ³]	χ	β (wrt nitrogen)	β (wrt benzene)	β (wrt acetone)
Acetaldehyde	4.59 E - 24	- 22.7 E - 6	2.33	0.432	0.704
Acetone	6.33 E - 24	- 33.7 E - 6	3.31	0.614	1.00
Benzene	10.32 E - 24	- 54.8 E - 6	5.40	1.00	1.63
Ethylbenzene	14.2 E - 24	- 77.3 E - 6	7.50	1.39	2.26
Methyl Ethyl Ketone (2-Butanone)	8.13 E - 24	- 45.6 E - 6	4.34	0.805	1.31
Nitrogen	1.74 E - 24	- 12.0 E - 6	1.00	0.185	0.302
Toluene	12.3 E - 24	- 65.9 E - 6	6.46	1.20	1.95
p-Xylene	14.1 E - 24	- 76.8 E - 6	7.45	1.38	2.25
Carbon (adsorbent)	1.76 E - 24	- 6.0 E - 6	N/A [‡]	N/A	N/A

†. wrt = with respect to.

‡. N/A = not applicable.

Both equations 2.23 and 2.25 have been used in the adsorption literature. Thus far, it is not clear which equation gives a better estimate of β , but it is clear from Tables 2.3 and 2.4 that both methods, while presenting similar values for β , do differ.

2.3 Pore Size Distributions for Microporous Materials

Currently, there is no standard for determining a pore size distribution of a microporous adsorbent (Gregg and Sing, 1982). Several models have been proposed, however, and will be described in sections 2.3.1 and 2.3.2. All of the models rely on using adsorption isotherm data of a single adsorbate and then converting that adsorption data into a pore size distribution. It is very likely that none of the methods described here give a true representation of the pore size distribution of a microporous adsorbent, because of the assumptions made in their derivations. The data obtained using the various pore size distribution methods are probably best used to compare similar adsorbents with varying degrees or types of activation. While the pore size distribution data may not be accurate, they may give useful information on how the pore structure changes with different activation times or methods. Currently, the best method for determining a pore size distribution is to use molecular probes of different sizes. Molecular probes produce a discrete distribution based upon the sizes of the molecules used. This method tends to be time consuming and is rarely warranted for the characterization of particular adsorbent. Additionally, molecular probes should be used which rely solely on physical adsorption and not on chemical adsorption or hydrogen-bonding, as this will distort the pore size distribution.

2.3.1 The Dubinin Method

The Dubinin-Stoeckli (DS) equation (equation 2.21) can be used to represent a pore size distribution for a microporous adsorbent (Dubinin, 1989a). As previously mentioned, the DS equation assumes a Gaussian distribution of pores about some slit-pore half-width (x_0). It is unlikely that a pore size distribution assumes a Gaussian shape for any microporous adsorbent, no matter the extent of the homogeneity of the adsorbent starting material before activation, because on a microscopic scale carbon surfaces tend to be heterogeneous. A Gaussian distribution was chosen by Dubinin because it was assumed that activation is a random process and therefore may follow a Gaussian distribution. It was also used simply because of mathematical convenience. Nevertheless, the DS method and variations of it have been used extensively in the literature. Since the DS equation requires the simultaneous solution of three parameters (W_0 , x_0 , and δ), non-linear regression techniques must be used. This means that enough data points over a sufficiently large enough pressure range must be available so that DS parameters converge to their proper values. A P/P_0 range of about 10^{-6} or 10^{-5} up to about 0.4 to 0.5 is recommended when trying to fit adsorption data to the DS equation (Dubinin, 1989a).

The Dubinin-Radushkevich (DR) equation (equation 2.13) may also be used along with equation 2.15 to obtain some information about the pore size of a particular microporous adsorbent. Fitting adsorption isotherm data to the DR equation to obtain E_0 and then solving for x_0 using equation 2.15 gives a measurement of the mean micropore half-width. Using the DR equation gives a single value for micropore half-width, rather than a distribution, as obtained with the DS equation. For the calculation of x_0 to be valid, adsorption isotherm data for benzene at 293 K must be used. This is because the relationship between x_0 and E_0 was experimentally determined for benzene. If other adsorbates are used, x_0 must be corrected by multiplying by the affinity coefficient, β . Therefore, other adsorbates may be used to calculate x_0 , but the results may differ from that obtained using benzene adsorption, because of the accuracy in determining β , the interaction of the adsorbate with the adsorbent (e.g., due to polarity), and molecular sieving effects.

2.3.2 The Horvath-Kawazoe (HK) Method

Horvath and Kawazoe (1983) developed a method for determining effective pore size distributions from adsorption isotherms on molecular-sieve activated carbon. They claim that the HK method is more exact theoretically and more practical than previously developed methods (e.g., t-plot and α_s -plot). While the HK model outlined is for slit-shaped pores using N_2 isotherms at 77 K, it can be extended to other pore shapes (e.g., cylindrical) and other adsorbates, using slight modifications to the model. The HK model assumes an average potential function between two parallel layers of carbon and then adds the interaction effects of adsorbate molecules within these layers or slit-shaped pores. Integration of the resulting adsorption potential gives the following:

$$R T \ln\left(\frac{P}{P_0}\right) = K \frac{N_a A_a + N_A A_A}{\sigma^4 (1-d)} \left[\frac{\sigma^4}{3 (1-d/2)^3} - \frac{\sigma^{10}}{9 (1-d/2)^9} - \frac{\sigma^4}{9 (d/2)^3} + \frac{\sigma^{10}}{9 (d/2)^9} \right] \quad (2.26)$$

where K is Avagadro's number, N_a is the number of atoms per unit area of adsorbent [atom/cm²], N_A is the number of molecules per unit area of adsorbate [molec/cm²], A_a and A_A are Lennard-Jones potentials constants [J/molec], σ is the distance between a gas atom and the nuclei of the surface at zero interaction energy [nm], l is the distance between nuclei of two layers (pore width), and d is the diameter of an adsorbent atom plus the diameter of an adsorbate molecule. Substituting the values for carbon and nitrogen atoms into equation 2.26 results in

$$\ln\left(\frac{P}{P_0}\right) = \frac{62.38}{(1-0.64)} \left[\frac{1.895 \times 10^{-3}}{(1-0.32)^3} - \frac{2.7087 \times 10^{-7}}{(1-0.32)^9} - 0.05014 \right] \quad (2.27)$$

where l is in nm.

Equation 2.27 is solved for l as a function of P/P_0 using any root-finding numerical technique. The volume adsorbed at a particular P/P_0 value can then be related to the l calculated for that P/P_0 . This is done for every adsorption isotherm point, providing a distribution of l values. The HK model is valid for $(1-d)$ of about 1.5 nm. For effective pore sizes greater than that, other pore size distribution models should be used.

2.4 Water Vapor Adsorption on Activated Carbon

Water vapor adsorption on granulated activated carbon follows a characteristic s-shaped curve (Dubinin, 1980) and is dependent on relative humidity (RH)[†]. This has also been shown to be true for water vapor adsorption onto ACC. At RHs < 50%, the amount of water vapor adsorption is directly proportional to the number of oxygen groups on the surface of the carbon adsorbent (Dietz, 1991; Dubinin, 1980). This is believed to be due to the hydrogen bonding between the water molecule and the oxygen atoms present on the activated carbon surface. At RHs above about 50%, the main volume of the carbon micropores fills due to capillary condensation of the water within the pores. The main causes of water adsorption are primary adsorption centers (i.e. oxygen surface complexes). They are capable of enhancing physical adsorption of water molecules due to hydrogen bonding. Each adsorbed water molecule is a secondary adsorption center, which is also capable of forming hydrogen bonds with other water molecules.

One other feature of water vapor adsorption on microporous carbons is the development of a hysteresis loop, meaning that water vapor is not desorbed from activated carbon in the same manner as it is adsorbed. The most widely accepted explanation for the observed hysteresis is the "ink bottle" theory. It is assumed that in the desorption process small pores constrict the openings to larger pores such that adsorbed water in

[†]. For water vapor, RH = (P/P₀)*100.

the larger pores is not desorbed until the relative pressure corresponds to the adsorption capacity of the smaller pore size (Mahle and Friday, 1989).

No models have been able to adequately describe both the adsorption and desorption isotherms of water onto activated carbon. Since condensation of water vapor is due to the formation of hydrogen bonds between its molecules, concepts of water adsorption as a result of the hydrogen bonding have been developed by Dubinin (1980). Dubinin has proposed an adsorption isotherm equation which fits the water vapor adsorption isotherm curve in the range of about 5 to 50% RH (Dubinin, 1980):

$$W = W_o \frac{c h}{(1 - c h)} \quad (2.28)$$

where W is the mass $H_2O_{(g)}$ adsorbed per unit mass carbon [mg/g], W_o is the primary number of adsorption centers per unit mass carbon [mg/g], $h = P/P_o = RH/100$, and c is a constant. Equation 2.28 describes the initial and some of the sharp rise of the isotherm up to $h < 1/c$. The equation parameters W_o and c are determined from the linearized form of equation 2.28:

$$\frac{h}{W} = \frac{1}{W_o c} - \frac{h}{W_o} \quad (2.29)$$

2.5 Multicomponent Organic Adsorption

Most adsorption systems contain multiple compounds. If the systems of interest contain one strongly adsorbed compound and one or more weakly adsorbed compounds, e.g. a VOC in air, a single component adsorption isotherm model can be used to model the adsorption of the strongly adsorbed compound. If more than one strongly adsorbed compounds are present, other multicomponent adsorption models must be used to predict the adsorption of the compounds present in the system. Indoor air represents an extreme example of multicomponent adsorption, because several hundred organic compounds may be present. This section examines some of the models available for modeling the adsorption in multicomponent systems.

2.5.1 Method of Bering et al.

Bering et al. (1963) modified the potential theory for the prediction of binary gas-mixture adsorption equilibria by assuming that the potential curves of the pure adsorbates follow the form of equation 2.30 proposed by Dubinin (1960):

$$V_a = V_{ao} \exp\left(-B \frac{A^2}{\beta^2}\right) \quad (2.30)$$

Chapter 2: Literature Review

where V_a is the volume adsorbate adsorbed per unit mass of the adsorbent, V_{ao} is the limiting volume of the adsorption space per unit mass of the adsorbent, B is a parameter reflecting the distribution of the volumes of the pores according to their sizes, A is the adsorption potential, and β is the affinity coefficient. Bering generalized equation 2.30 for each component in the mixture resulting in equation 2.31:

$$N_{am} V_{sm} = V_{ao} \exp \left(-B \left(\frac{RT}{\beta_m} \sum_{n=1}^2 x_i \ln \left(\frac{P_{si}}{P_i} \right) \right)^2 \right) \quad (2.31)$$

$$N_{am} = N_{a1} + N_{a2} \quad (2.32)$$

$$\beta_m = x_1 \beta_1 + x_2 \beta_2 \quad (2.33)$$

$$V_{sm} = x_1 V_{s1} + x_2 V_{s2} \quad (2.34)$$

$$x_1 + x_2 = 1 \quad (2.35)$$

where subscript i indicates the i 'th component, N_{am} is the total moles adsorbed per unit mass of adsorbent (N_{a1} and N_{a2} are the individual amounts adsorbed of each component), V_{sm} is the partial molar volume of the mixture, R is the ideal gas constant, T is the gas temperature, β_m is the affinity coefficient of the mixture (β_1 and β_2 are the affinity coefficient of the individual components), x_i is the mole fraction of the i 'th component, P_i is partial pressure of component i , and P_{si} is the saturation vapor pressure of component i .

Bering et al. found good agreement between their predictions and experimental data for the adsorption systems of diethyl ether-ethyl chloride and diethyl ether-chloroform on activated carbon. The average prediction errors for x_1 and N_{am} were on the order of a few percent.

2.5.2 Grant and Manes Theory

Grant and Manes (1966) extended their previous potential theory of adsorption (Grant and Manes, 1964) to predict the adsorption equilibria of gas mixtures. Grant and Manes, as did Bering et al. (1963), assumed properties of pure components could be used to predict the adsorption of mixtures. Grant and Manes proposed the following equations for the adsorption of gas mixtures:

$$\frac{RT}{V_{b1}^{\circ}} \ln \left(\frac{x_1 f_{s1}^{\circ}}{f_1} \right) = \frac{RT}{V_{b2}^{\circ}} \ln \left(\frac{x_2 f_{s2}^{\circ}}{f_2} \right) \quad (2.36)$$

$$x_1 + x_2 = 1 \quad (2.37)$$

where f_{si} is the saturation fugacity of the pure component i at the adsorption temperature, the x 's are the gas-phase mole fractions of the adsorbates, and the f 's are the fugacities of the adsorbates. Adsorbate partial pressures can be substituted for fugacities at low total pressures ($P_{\text{total}} < \sim 5 \text{ atm}$), because the gases behave essentially in an ideal manner.

It can be noticed that equation does not contain a variable for total pressure and that the gas temperature, T , is present on both sides of the equation and therefore cancels out. The method of Grant and Manes therefore implies that the adsorption phase diagram for a binary system is independent of the adsorption pressure and temperature. This is not in agreement with experimental data. Experiments have shown that adsorption capacity is insensitive to relatively small changes in temperature and pressure (those exhibited under typical ambient conditions), but it is sensitive to large changes in temperature (tens of degrees C) and pressure (several atmospheres; when the gases start to behave non-ideally). One other criticism of Grant and Manes theory is the assumption that adsorption isotherms can be predicted without knowledge of pure-component isotherms, or properties of the adsorbent, as these variables do not appear in equation. Much experimental evidence has shown that this is not true. In fact, for gas adsorption the amount of micropores present in the adsorbent can greatly affect adsorption capacity.

Grant and Manes tested their theory for the adsorption of various hydrocarbon mixtures methane, ethane, propane, and n-butane and found agreement within about 10% of the experimental adsorption values at atmospheric pressure.

2.5.3 Ideal Adsorbed Solution Theory (IAST)

Myers and Prausnitz (1965) took a somewhat different approach to the prediction of the adsorption of gas mixtures than those taken by Bering et al. (1963) and Grant and Manes (1966). They proposed using thermodynamic equations to describe the adsorbed phase on an adsorbent, and their treatment of adsorption is termed ideal adsorbed solution theory (IAST). The validity of using thermodynamic equations relies on three assumptions:

1. The adsorbent is assumed to be thermodynamically inert, meaning that a change in a thermodynamic property, such as internal energy, during an adsorption process at constant temperature is assumed to be negligible compared with the change in the same property for the adsorbing gas.
2. The adsorbent possesses a temperature-invariant area which is the same for all adsorbates. This assumption is not valid for a molecular sieve adsorbent, because the area available for adsorption depends upon the size of the adsorbate molecule.
3. The Gibbs definition of adsorption applies. In most cases, this definition corresponds to the usual methods in which volumetric or gravimetric adsorption experimental results are obtained.

Chapter 2: Literature Review

In IAST, the following basic equations are used to predict multicomponent adsorption isotherms from single-component adsorption isotherms:

$$Py_i = P_i^o x_i \gamma_i \quad \{i = 1, 2, \dots, N\} \quad (2.38)$$

$$\psi_1^o(P_1^o) = \psi_2^o(P_2^o) = \dots = \psi_N^o(P_N^o) \quad (2.39)$$

$$\psi = \frac{\Pi A}{RT} = \int_0^P \frac{n}{P} dP \quad (2.40)$$

$$\sum_{i=1}^N x_i = 1 \quad (2.41)$$

After the above equations are solved, the total amount of x adsorbed, n_t , is found from:

$$\frac{1}{n_t} = \sum_{i=1}^N \frac{x_i}{n_i^o} \quad (2.42)$$

The amount of the i 'th component adsorbed is given by:

$$n_i = n_t x_i \quad (2.43)$$

where P is pressure [Pa], P_i^o is partial vapor pressure of adsorbate in standard state [Pa], y_i is mole fraction of component i in gas phase, x_i is mole fraction i in adsorbed phase, γ_i is the adsorbed phase activity coefficient and is used to describe the non-ideality of the mixture components, n is the specific amount adsorbed [mol/kg], n_i^o is the specific amount of i adsorbed at P_i^o [mol/kg], n_i is the amount of i adsorbed [mol/kg], ψ_i^o is $(\Pi A/RT)$ of i at standard state [mol/kg], Π is the spreading pressure of the adsorbed phase [N/m], A is the specific surface area [m²/kg], R is the gas constant [8.3145 J/(mol-K)], T is temperature [K], and N is the number of components. The spreading pressure, Π , corresponds to the difference in surface tension between a clean surface and an adsorbate covered surface, and can be expressed as:

$$\Pi = -\left(\frac{\partial U}{\partial A}\right)_{S, V, n} \quad (2.44)$$

where U is the internal energy of n moles adsorbed, A is the surface area occupied by n moles of adsorbate, S is entropy, and V is volume.

Crittenden et al. (1985) made a useful modification by incorporating the Freundlich equation 2.45 with IAST to obtain equation 2.46:

$$n = C P^{1/t} \quad (2.45)$$

$$P y_i = \left(\frac{n_i}{\sum_{j=1}^{\infty} n_j} \right) \left(\frac{\sum_{j=1}^{\infty} n_j t_j}{C_i t_i} \right)^{t_i} \quad (2.46)$$

where n is the number of moles adsorbed, y_i is the gas-phase mole fraction of component i , P is the total pressure, and C and t are constants. Incorporating the Freundlich equation into IAST produces one serious flaw: it does not reduce to Henry's law at low adsorbate coverage. In general, the Freundlich equation does not fit pure-component isotherms well at low adsorption coverages. Therefore Crittenden's modifications to IAST will not work well when trying to predict an entire adsorption isotherm. Nevertheless, the simplifications introduced to the IAST equations by Crittenden's modifications have proved useful in modeling multicomponent adsorption over regions where the Freundlich equation is valid for the adsorbates modeled.

As with the Freundlich equation, the DR equation can also be substituted into IAST for the calculation of spreading pressure, yielding the following equation:

$$\psi_i = \frac{\Pi_i A}{RT} = \frac{n_{m,i} \pi^{1/2}}{2 \left(\frac{RT}{\beta E_o} \right)_i} \operatorname{erfc} \left[\left(\frac{RT}{\beta E_o} \right)_i \ln (P_{o,i} / P_i) \right] \quad (2.47)$$

where $n_{m,i}$ is the micropore volume of component i in mmol/g. Equation 2.47 fails at very low pressure, but its accuracy improves with increasing pressure. It is probably within experimental error in the moderate and high adsorbate coverage regions of interest (Richter et al., 1989).

Making modifications to the original IAST equations by substituting adsorption isotherm equations, such as the Freundlich equation or the DR equation, makes the equations easier to use, but generally introduces some problems. The success of the calculations depends greatly upon the ability of the equation to fit the single-component adsorption data accurately. Small errors in fitting the experimental data, particularly at low surface coverages, may generate large errors in the calculated adsorption capacities. Other sources of error are neglect of surface heterogeneity and adsorbate-adsorbate interactions, both of which can cause the mixture equilibria to exhibit non-ideal behavior. IAST generally tends to be accurate when the amount adsorbed is less than half of the saturation capacity of the adsorbent (Myers, 1988). At higher surface coverages, negative deviations from Raoult's law have been observed for some systems, due to the aforementioned reasons.

Myers (1968) compiled several comparison between binary experimental data and IAST predictions. The mixtures examined included organic mixtures adsorbed on activated carbon and silica gel and mixtures of elementary atoms and molecules, such as, Ne, H₂, and O₂. The greatest deviation observed between IAST predicted and experimental data was about 20% for mixtures at high surface coverage (multilayer adsorption). For low surface coverages (less than a monolayer), the IAST predictions closely matched the experimental measurements, making the calculation of activity coefficients unnecessary. A benzene-cyclohexane mixture on activated charcoal at 30°C was shown to be ideal (Myers et al., 1982), as was a mixture of ethyl chloride and diethyl ether at 50°C on activated carbon (Bering et al., 1972).

Several researchers investigated the adsorption of non-ideal mixtures on activated carbon and compared experimental results with IAST predictions. Costa et al. (1981) examined binary adsorption for hydrocarbon mixtures on activated carbon at 20°C and a total pressure of 75 mm Hg and found that the activity coefficients ranging from 0.5 to 1.0. Hoppe et al. (1978) examined benzene-toluene adsorption on activated carbon at 30°C and found that IAST predictions deviated from experimental measurements by 24%. Hoppe and Worch (1982) showed that a mixture of benzene and isopropyl alcohol adsorbed on activated carbon at 30°C was non-ideal with activity coefficients of the components ranging from about 1 to 2.

2.6 Adsorption of Organic Compounds from Humid Air Streams

Water vapor is ubiquitous in indoor environments, and since it can competitively adsorb onto ACC or even alter the adsorption capacity of a regenerated activated carbon, it is important to understand ACC water vapor adsorption and its effects on ACC for the design and operation of carbon adsorption processes.

Competitive adsorption between water vapor and organics can be considered a special case of multicomponent adsorption, because water vapor is nearly always present in gas streams and as discussed earlier water vapor exhibits much different adsorption characteristics on active carbon than do organics.

Manes (1983) developed a method to predict simultaneous adsorption of water vapor and organics based on Polanyi (1932) potential adsorption theory by assuming adsorbed water reduces adsorbent pore volume available for the adsorption of organic compounds on a one-to-one volume basis. Manes also assumed that the adsorption of an organic vapor at 100% RH (or $P/P_o = 1$) was equivalent to its adsorption from a bulk aqueous solution.

At 100% relative humidity, the net adsorption potential for an organic adsorbate is its calculated potential without interference from water vapor (A_i) diminished by the adsorption potential of an equal volume of water (A_w) which the organic must displace from the activated carbon pores.

$$\frac{A'_i}{V_i} = \frac{A_i}{V_i} - \frac{A_w}{V_w} \quad (2.48)$$

where A_i' = corrected adsorption potential of component i considering interference with water vapor and V_w = molar volume of water ($18 \text{ cm}^3/\text{gmol}$).

Equation 2.48 applies to any immiscible organic assuming that the adsorbed organic volume is less than the volume of the adsorbed water (Manes, 1983). If the organic volume is greater than the volume of water, the model assumes no interference from the presence of water. If the relative humidity is less than 100%, an additional term is required to describe the effect of water vapor on organic adsorption, as shown in equation 2.49:

$$\frac{A_i'}{V_i} = \frac{A_i}{V_i} - \frac{A_w}{V_w} - R T \ln \frac{h}{V_w} \quad (2.49)$$

where h is the fractional relative humidity (P/P_0).

2.7 Review of Previous Research on ACC

Much collaborative research has been performed on the characterization and application of ACC[†] in the Department of Civil Engineering and Department of Materials Science and Engineering at the University of Illinois at Urbana-Champaign. The research performed at the Department of Materials Science and Engineering has mainly centered around the fundamental characterization of ACC, while the research in the Department of Civil Engineering has examined applied uses of ACC, e.g. to remove VOCs from indoor air. This section highlights some of the previous research performed using ACC.

2.7.1 Research of Economy and Lin

Lin and Economy (1973) developed the activated carbon cloth (ACC) used in this research while working at the Carborundum Company. The starting material is a highly cross-linked phenolic precursor (Kynol) whose surface area and pore size distribution can be tailored using controlled pyrolysis and steam activation. The phenolic fiber can be carbonized very rapidly with a carbon yield as high as 60%. Surface areas of up to $3000 \text{ m}^2/\text{g}$ were observed for the steam activated fiber. The diameter of the individual fibers composing the ACC is 10 to $33 \mu\text{m}$, and their specific gravity is 1.27 (Andreopoulos and Economy, 1991).

Lin and Economy (1973) suggested that using a highly cross-linked fiber as a carbon fiber precursor has three basic advantages: (1) high carbon yield in excess of 55%; (2) fast carbonization rate without serious

†. In many of the publications referenced in this section, the term activated carbon fiber (ACF) is used instead of ACC. While the same samples were used in all the research mentioned, the author prefers the use of the term ACC, because it is a more accurate description of the physical form of the material. When reviewing publications, the author has changed the ACF notation to ACC, so that it is consistent with the terminology presented in this manuscript.

loss in mechanical properties; and (3) controllable degrees of activation to produce ACC with different surface areas and pore size distributions.

Economy and Lin (1976) examined the adsorption capacities in a carbon bed for butane in N₂ and phenol in water for BPL activated carbon granules (1200 m²/g) and ACC (1200 m²/g). The ACC showed a higher adsorption capacity (longer time to breakthrough) for both the butane and the phenol. They also showed that ACC could be electrically regenerated by passing 2 to 3 amps through the ACC for 5 to 25 min with little change in surface area or phenol adsorption capacity. Electrical regeneration provides a effective and economical solution for reusing ACC.

2.7.2 Research of Foster

Ken Foster of the Department of Materials Science and Engineering performed some fundamental research on ACC for his doctoral dissertation, entitled "The Role of Micropore Size and Chemical Nature of the Pore Surface on the Adsorption Properties of Activated Carbon Fibers" (Foster, 1993). Some of the results important to this research will be highlighted here.

Foster (1992) characterized the ACC samples with the BET method (for surface area), X-ray photoelectron spectroscopy (XPS), elemental analysis, and saturated gas adsorption of several organic adsorbates to determine the pore volume of ACCs.

The surface areas of the ACC samples were determined with a Micromeritics ASAP 2400 using liquid nitrogen at 77 K and then fitting the BET equation for $0.01 < P/P_0 < 0.25$ (Table 2.5). Elemental analysis was used to determine the amount of carbon, hydrogen, nitrogen, and oxygen. Carbon, hydrogen, and nitrogen were determined using a combustion technique and a Model 240XA elemental analyzer (Control Equipment Corp.). Oxygen content was determined by mass difference, assuming that the ACC consisted only of carbon, hydrogen, nitrogen, and oxygen (Table 2.5). XPS analysis was performed using a PHI 5400 (Perkin-Elmer Corp., PE Div., Eden Prairie, MN) to determine the oxygen functional groups on the ACC surface (Table 2.6). Pore volumes were measured using saturated gas streams of several adsorbates (Table 2.7) (Foster, 1992).

Table 2.5. BET Surface Area and Elemental Composition of ACC Samples (Foster, 1992).

ACC Sample	BET Surface Area [m ² /g]	C [wt%]	H [wt%]	O [wt%]	N [wt%]
ACC-15	900	92.8	1.04	6.12	< 0.05
ACC-20	1610	95.4	0.68	3.92	< 0.05
ACC-25	2420	95.4	0.59	3.97	< 0.05

Chapter 2: Literature Review

Comparing the XPS and elemental analyses for oxygen showed that the oxygen was present throughout the ACC samples and not just on the surface. XPS analyzes a surface to a depth of about 30 to 100 Å, while the combustion technique is a bulk technique. Comparing the C/O ratios of the two methods shows good agreement, suggesting that oxygen is present throughout ACC (Table 2.8).

Table 2.6. XPS Deconvolution of the Carbon 1s Peak Area (Foster, 1992).

ACC Sample	Carbon (graphite)	Hydroxyl (C-OH)	Quinone (C=O)	Carboxylic (C=OOH)
ACC-15	46.0	33.5	10.3	4.1
ACC-20	50.9	27.9	9.3	5.6
ACC-25	54.7	24.4	8.4	5.7

Table 2.7. Effective Pore Volume for Select VOCs (Foster, 1992).

Adsorbate	ACC-15 [cm ³ /g]	ACC-20 [cm ³ /g]	ACC-25 [cm ³ /g]
Acetone	0.326	0.613	0.859
Cyclohexane	0.314	0.638	0.805
Benzene	0.323	0.653	0.849
Toluene	0.345	0.632	0.877
1,1,1-Trichloroethane	0.319	0.643	0.834
Mean Pore Volume	0.325	0.636	0.845
Std. Dev.	0.012	0.015	0.027

Table 2.8. Comparison of Carbon Oxygen Mass Ratios with XPS and Elemental Analysis (Foster, 1992).

ACC Sample	C/O (XPS)	C/O (Elemental)
ACC-15	19.0	15.2
ACC-20	23.8	24.3
ACC-25	27.3	24.0

Chapter 2: Literature Review

2.8 References

- Andreopoulos, A.G, and Economy, J., "Thermally Activated Phenolic Fibers," *Chemistry of Materials*, **3**(4):594-597, 1991.
- Bering, B. P., Serpinskii, V. V. and Surinova, S. I., "Calculation of adsorption equilibrium parameter for adsorbent-binary gas mixture systems," *Doklady Physical Chemistry*, **153**, 949-952, 1963.
- Bering, B. P., Serpinskii, V. V. and Surinova, S. I., *Acad. Sci. USSR Bull., Div. Chem. Sci.*, (2):381, 1972.
- Brunauer, S., Emmett, P.H., and Teller, E., "Adsorption of Gases in Multimolecular Layers," *J. Amer. Chem. Soc.*, **60**:309, 1938.
- Brunauer, S. Deming, L.S., Deming, W.S., and Teller, E., *J. Amer. Chem. Soc.*, **62**:1723, 1940.
- Cal, M.P., Larson, S.M., Rood, M.J., "Experimental and Modeled Results Describing the Adsorption of Acetone and Benzene onto Activated Carbon Fibers," *Environmental Progress*, **13**(1):26-30, 1994.
- Carrott, P.J.M., Carrott, M.M.L, and Roberts, R.A., "Physical Adsorption of Gases by Microporous Carbons," *Colloids and Surfaces*, **58**:385-400, 1991.
- Costa, E., Sotelo, J.L., Calleja, G., and Marron, C., *AIChE J.*, **27**(1):5, 1981.
- Crittenden, J. C., Luft, P., Hand, D. W., Oravitz, J. L., Loper, S. W. and Ari, M., "Prediction of multicomponent adsorption equilibria using ideal adsorbed solution theory," *Environ. Sci. Technol.*, **19**(11): 1037-1043, 1985.
- Dietz, V.R., "The rates of adsorption and desorption of water vapor from air flows through activated carbons," *Carbon*, **29**, 569-573, 1991.
- Dubinin, M.M., "The potential theory of adsorption of gases and vapors for adsorbents with energetically nonuniform surfaces." *Chem. Rev.*, **60**, 235-241, 1960.
- Dubinin, M. M., "Physical adsorption of gases and vapors in micropores," In D. A. Cadenhead, J. F. Danielli, & M. D. Rosenberg (Eds.), *Progress in Surface and Membrane Science*, Academic Press, 1-70, 1975.
- Dubinin, M.M., Stoeckli, H.F., "Homogeneous and Heterogeneous Micropore Structures in Carbonaceous Adsorbents," *Journal of Colloid and Interface Science*, **75**(1):34-42, 1980.
- Dubinin, M.M., "Water vapor adsorption and the microporous structures of carbonaceous adsorbents," *Carbon*, **18**, 355-364 (1980).
- Dubinin, M.M., "Generalization of the Theory of Volume Filling of Micropores to Nonhomogeneous Microporous Structures," *Carbon*, **23**(4):373-380, 1985.
- Dubinin, M. M., "Fundamentals of the theory of adsorption in micropores of carbon adsorbents: characteristics of their adsorption properties and microporous structures," *Carbon*, **27**(3):457-467, 1989a.
- Dubinin, M.M., "Fundamentals of the Theory of Adsorption in Micropores of Carbon Adsorbents: Characteristics of Their Adsorption Properties and Microporous Structures," *Pure and Appl. Chem.*,
-

Chapter 2: Literature Review

61(1):1841-1843, 1989b.

Dubinin, M. M., Polyakov, N. S. and Kataeva, L. I., "Basic properties of equations for physical vapor adsorption in micropores of carbon adsorbents assuming a normal micropore distribution," *Carbon*, **29**(4/5), 481-488 (1991).

Lin, R.Y., and Economy, J., "The Preparation and Properties of Activated Carbon Fibers Derived From Phenolic Precursor," *Applied Polymer Symposium No. 21*, 143-152, 1973.

Economy, J. and Lin, R.Y., "Adsorption Characteristics of Activated Carbon Fibers," *Applied Polymer Symposium No. 29*, 199-211, 1976.

Everett, D.H., and Powl, J.C., *J. Chem. Soc., Faraday Trans. I*, **72**:619, 1976.

Finger G.; Bulow, M. *Carbon*, **1979**, 17, 87-91.

Foster, K.L., Fuerman, R.G., Economy, J., et al., "Adsorption of volatile organic compounds in gas streams onto activated carbon fiber," *Chemistry of Materials*, **4**:1068-1073, 1992.

Foster, K.L., "The Role of Micropore Size and Chemical Nature of the Pore Surface on the Adsorption Properties of Activated Carbon Fibers," Doctoral Dissertation, Department of Materials Science and Engineering, University of Illinois at Urbana-Champaign, 1993.

Grant, R. J. and Manes, M., "Correlation of some gas adsorption data extending to low pressures and supercritical temperatures," *Ind. Eng. Chem. Fundam.*, **3**(3):221-224, 1964.

Grant, R. J. and Manes, M., "Adsorption of binary hydrocarbon gas mixtures on activated carbon," *Ind. Eng. Chem Fundam.*, **5**(5):491-498, 1966.

Gregg, S.J.; Sing, K.S.W. *Adsorption, Surface Area and Porosity*, 2nd ed.; Academic: London, 1982.

Hall, C. Richard, and Holmes, Richard J., "Chemically modified carbons for gas separation," presented at the Summer National Meeting of the American Institute of Chemical Engineers, Seattle, WA, 1993.

Hayes, J.S., "Novoloid Nonwovens," *Nonwoven Symposium*, TAPPI Press, April, 257-263, 1985.

Hoppe, H., Winkler, F., and Worch, E., *Z. Chem.*, **18**(4):154, 1978.

Hoppe, H., and Worch, E., *Z. Phys. Chem., Leipzig*, **263**(6): 1169, 1982.

Horvath, G. and Kawazoe, K., "Method for the calculation of effective pore size distribution in molecular sieve carbon," *Journal of Chemical Engineering of Japan*, **16**(6):470-475, 1983.

IUPAC Manual of Symbols and Terminology, Appendix 2, Pt. 1, Colloid and Surface Chemistry, *Pure Appl. Chem.*, **31**:578, 1972.

Langmuir, I. *J. Amer. Chem. Soc.*, **38**:2221, 1916.

Lide, D.R., Ed., *Handbook of Chemistry and Physics*, 71st Ed., CRC Press, Boca Raton, 1990.

Mahle, J.J., and Friday, D.K., "Water Adsorption Equilibria on Microporous Carbons Correlated Using a Modification to the Sircar Isotherm," *Carbon*, **27**(6):835-843, 1989.

Chapter 2: Literature Review

- Manes, M., "Estimation of the effects of humidity on the adsorption onto activated carbon of the vapors of water-immiscible organic liquids," *Fundamentals of Adsorption Proceedings of the Engineering Foundation Conference*, A. L. Myers and G. Belfort, Eds., Bavaria, West Germany, 335-344, 1983.
- Myers, A. L. and Prausnitz, J. M., "Thermodynamics of mixed-gas adsorption," *AIChE Journal*, **11**(1):121-127, 1965.
- Myers, A.L., *Ind. Eng. Chem.*, **60**(5):45, 1968.
- Myers, A.L., Minka, C., Ou, D.Y., *AIChE J.*, **28**(1):97, 1982.
- Myers, A.L., "Theories of Adsorption in Micropores," *Adsorption: Science and Technology*, ed. by Alirio E. Rodrigues, M. Douglas Levan, and Daniel Tondeour, NATO ASI Series, Kluwer Academic Publishers, pp. 15-36, 1988.
- Marsh, H., "Adsorption Methods to Study Microporosity in Coals and Carbons--A Critique," *Carbon*, **25**(1):49-58, 1987.
- McClellan, A.L., and Harnsberger, H.F., "Cross-sectional Areas of Molecules Adsorbed on Solid Surfaces," *Journal of Colloid and Interface Science*, **23**:577-599, 1967.
- Muller, A. *Proc. Roy. Soc. (London)*, **A154**:682, 1936.
- Polanyi, M., "Section III.-Theories of the adsorption of gases. A general survey and some additional remarks," *Transactions of the Faraday Society*, **28**:316-333, 1932.
- Quayle, O.R., "The Parachors of Organic Compounds: An Interpretation and Catalogue," *Chem Rev.*, **53**:439-589, 1953.
- Richter, E., Schutz, W., and Myers, A.L., "Effect of Adsorption Equation on Prediction of Multicomponent Adsorption Equilibria by the Ideal Adsorbed Solution Theory," *Chemical Engineering Science*, **44**(8):1609-1616, 1989.
- Stoeckli, H.F., Kraehenbuehl, F., Ballerini, L., De Bernardini, S., "Recent Developments in the Dubinin Equation," *Carbon*, **27**(1):125-128, 1989.
- Treybal, R.E., *Mass-Transfer Operations*, 3rd ed., McGraw-Hill, New York, 581-582, 1980.
- Zukal, A. and Kadlec, O., *Coll. Czech. Chem. Comm.*, **37**(6):1952, 1972.

Chapter 3

Characterization of ACC

3.1 Introduction

The chapter presents pore size distributions, surface areas using different adsorbates, pore volumes, and chemical composition of three ACC samples used in this research.

3.2 ACC Surface Areas, Pore Volumes, and Chemical Composition

N₂ at 77 K (liquid nitrogen temperature) adsorption isotherms were performed for ACC-15, ACC-20, and ACC-25 using a Quantachrome sorption analyzer (Quantachrome Corporation, Boca Raton, FL)[†]. The isotherms are Brunauer type I when plotted on a linear-linear scale, but are presented on a log-linear scale so that the entire adsorption isotherm can be viewed (Figure 3.1). It can be seen in Figure 3.1 that ACC-15 is nearly saturated with N₂ at very low P/P₀, this is probably due to its relatively homogeneous pore distribution and lower pore volume compared to the other ACC samples. ACC-25 had the highest adsorption capacity for N₂ at saturation (P/P₀ = 1), followed by ACC-20, and ACC-15.

BET and DR surface areas were determined using N₂ at 77 K, CO₂ at 273 K[†], benzene at 298 K, and acetone at 298 K. The isotherm data used for the surface area calculations were obtained using a Quantachrome sorption analyzer for N₂ and CO₂, and using a Cahn gravimetric balance for benzene and acetone. The Quantachrome instrument measures volume of gas adsorbed, while the Cahn gravimetric balance measures mass adsorbed which was then converted to liquid adsorbed using the respective liquid densities for surface area calculations. BET surface areas and total pore volumes taken at P/P₀ = 0.99 for ACC using N₂ at 77 K are presented in Table 3.1. Differences between the data reported in Table 3.1 and those reported by Foster (1992) in Tables 2.5 and 2.7 may be due to differences in the ACC lot used or experimental error. DR surface areas for ACC and N₂, CO₂, benzene and acetone are presented in Table 3.2. Molecular cross-sectional areas presented in Table 2.2 along with equation 2.8 were used for surface area calculations.

[†]. Experiments performed by A. Lizzio and/or C. Feizoulof at the Illinois State Geological Survey.

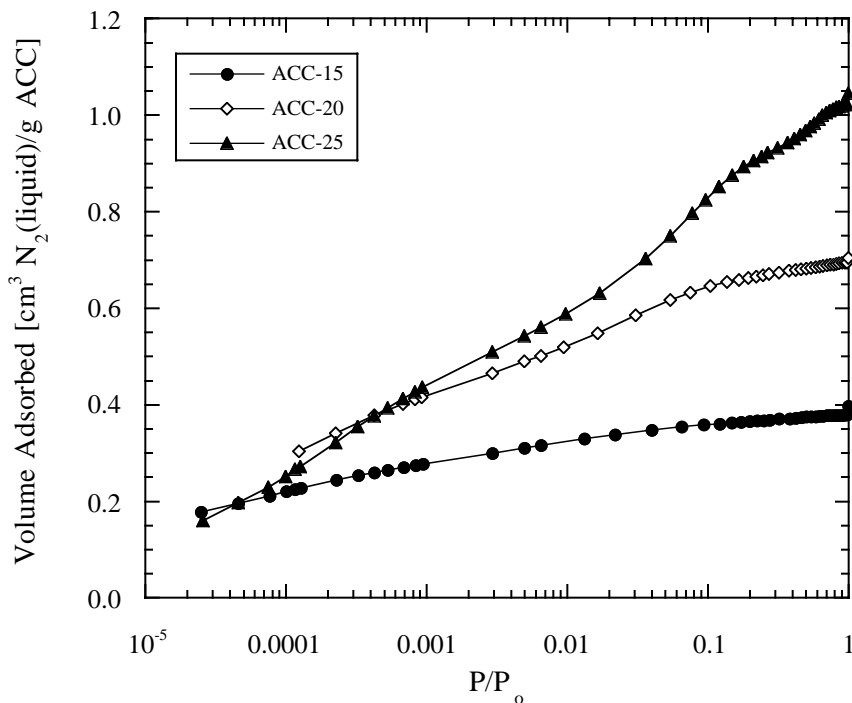


Figure 3.1. Adsorption Isotherms for ACC and N₂ at 77 K.

Table 3.1. BET Surface Areas and Total Pore Volumes for ACC Using N₂ at 77 K.

ACC Sample	BET Surface Area [m ² /g]	Total Pore Volume [cm ³ /g]
ACC-15	730	0.379
ACC-20	1330	0.694
ACC-25	1860	1.023

Table 3.2. DR Surface Areas for ACC.

Adsorbate	P/P ₀ Range	DR Surface Area		
		ACC-15	ACC-20	ACC-25
N ₂ (77 K)	10 ⁻⁵ to 0.4	1040	1870	2510
CO ₂ (273 K)	0.010 to 0.029	1310	1640	1710
Benzene (298 K)	8×10 ⁻⁵ to 8×10 ⁻³	1320	2060	1630
Acetone (298 K)	3×10 ⁻⁵ to 3×10 ⁻³	1080	1130	850

The reason for the low DR surface areas using acetone compared with the other adsorbates is probably due to the low adsorption capacity acetone has on ACC at the relative pressures (P/P_0) examined. This tends to make the surfaces areas appear lower than they actually are. The other possibility for the DR surface areas could be due to molecular sieving effects, but that appears unlikely due to acetone's relatively small molecular area and the fact that the ACC samples with the largest pore sizes had the largest surface area discrepancy.

Surface areas for ACC observed using CO_2 at 273 K are lower than those observed using N_2 at 77 K or benzene at 298 K, because N_2 measures the total micropore volume (including supermicropores). CO_2 , because of the higher temperature and much lower relative pressure range covered, only measures microporosity (Garrido et al., 1987). There is some question as to the pore filling mechanism observed with CO_2 at 273 K. Unlike N_2 (at 77 K) and benzene (at 298 K) which fill micropores in a liquid-like fashion at very low relative pressures ($P/P_0 < 0.01$), CO_2 (at 273 K) is believed to form a monolayer on pore walls (Garrido, et al., 1987; Marsh, 1987).

3.3 Pore Size Distributions

The Horvath-Kawazoe (HK) (equation 2.27) and Dubinin-Stoeckli (DS) (equation 2.21) methods were used to obtain an estimate of the pore size distributions of ACC. N_2 at 77K was used as the adsorbate for both methods, because N_2 adsorption data were available over a large pressure range ($1 \times 10^{-5} < P/P_0 < 1.00$) for the ACC samples. Since the ACC samples are almost entirely microporous, adsorption data were needed for nearly the entire P/P_0 range (from 0 to 1) to obtain a good estimate of the pore size distribution.

The pore size distributions using the HK method are presented in Figure 3.2. The pore size distribution using the DS method are presented in Figure 3.3. Parameters used for these calculations are in Table 3.3. The

Table 3.3. DS Parameters for ACC Using N_2 at 77 K.

ACC Sample	W_0 [cm^3/g]	E_0 [kJ/mol]	x_0 [nm]	δ [nm]	β
ACC-15	0.372	24.3	0.494	0.014	0.33
ACC-20	0.839	26.5	0.453	0.500	0.33
ACC-25	1.137	17.9	0.670	0.663	0.33

parameters for the HK method were solved using a root-finding algorithm in *HiQ*®, and the DS parameters were obtained using a nonlinear parameter estimation algorithm in *HiQ*® (National Instruments

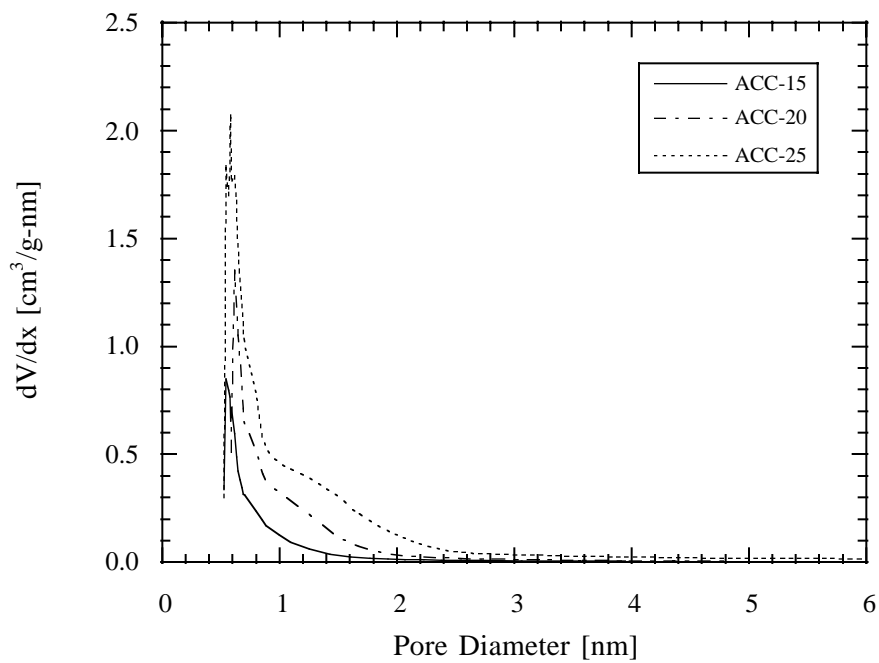


Figure 3.2. Pore Size Distribution for ACC Using HK Method and N₂ at 77 K.

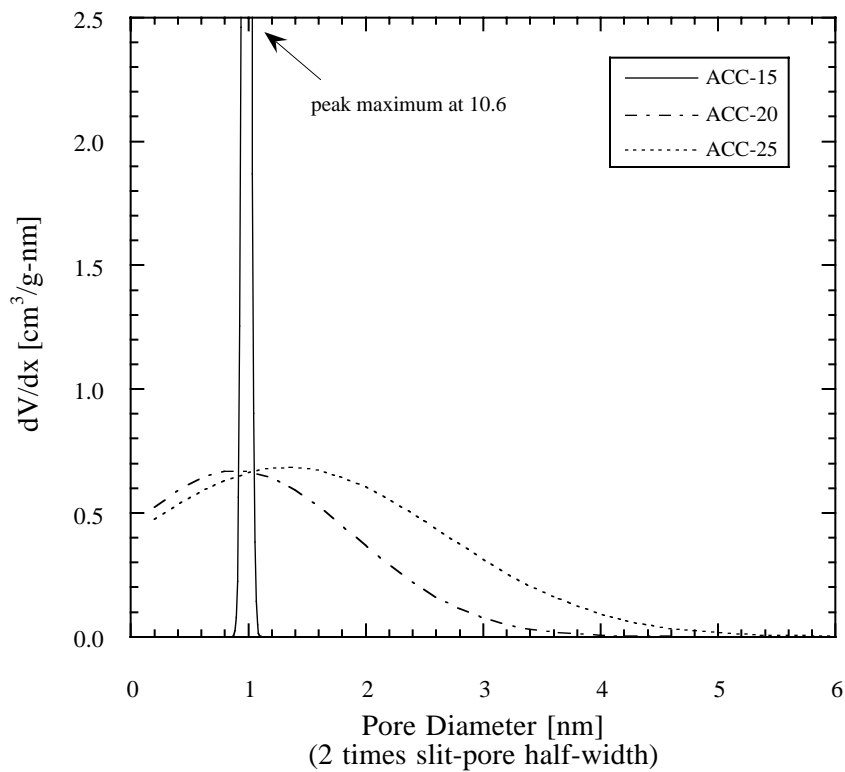


Figure 3.3. Pore Size Distributions for ACC Using DS Method and N₂ at 77 K.

Corporation, 1994). Since the DS method contains three variables in a nonlinear equation, multiple solutions are possible. The most reasonable estimates obtained for the DS parameters are reported in Table 3.3 i.e., unusually large or small values for the DS parameters were not used.

While the HK and DS plots show different results for the pore size distributions for ACC, there are similarities. Both methods show a broadening of the pore size distribution with increasingly activated (higher surface area) ACC. The modal pore size is also centered around the same point for the two methods. Using either method shows that all of the pores for ACC-15 lie in the micropore region ($d < 2$ nm). This suggest that ACC-15 would be the best adsorbent for removing low concentrations of VOCs, as are present in indoor air environments. This fact is also confirmed by VOC adsorption experiments presented in Chapter 4.

3.4 References

Garrido, J., Linares-Solano, A., Martin-Martinez, J.M., Molina-Sabio, M., Rodriguez-Reinoso, F., and Torregrosa, R., "Use of N₂ vs. CO₂ in the Characterization of Activated Carbons," *Langmuir*, **3**:76-81, 1987.

Foster, K.L., Fuerman, R.G., Economy, J., et al., "Adsorption of volatile organic compounds in gas streams onto activated carbon fiber," *Chemistry of Materials*, **4**:1068-1073, 1992.

Marsh, H., "Adsorption Methods to Study Microporosity in Coals and Carbons--A Critique," *Carbon*, **25**(1):49-58, 1987.

National Instruments Corporation, *HiQ® Software for the Power Macintosh Version 2.1*, Austin, TX, 1994.

Chapter 4

Single Component Adsorption Measurements and Modeling

4.1 Introduction

The focus of the experimental research in this section was to measure adsorption isotherms using ACC for adsorbates of interest to indoor air quality. Adsorbates examined were acetaldehyde, acetone, benzene, methyl ethyl ketone (MEK), and water vapor. Adsorption isotherms were measured for VOC adsorbate concentrations in the 10 to 1000 ppmv range and water vapor from 0 to 95% RH. Single VOC adsorbate concentrations were higher than the sub-ppmv concentrations observed in indoor air environments. This was due to the long times (estimated at several weeks to months, depending on the VOC concentration) involved in the experimental determination of the adsorption capacities of VOC adsorbates at sub-ppmv concentrations. The Freundlich and Dubinin-Radushkevich equations were used to extend adsorption capacity characterization for the VOC adsorbates into the sub-ppmv range using the experimental data obtained in the 10 to 1000 ppmv concentration range.

4.2 Experimental Methods

The experimental apparatus used to measure adsorption isotherms for contaminant concentrations in the ppmv range consists of a gas generation system and a Cahn gravimetric balance (Cahn Model C-2000) (Figure 4.1). The gravimetric balance is used to observe the mass of an ACC sample that is exposed to a gas stream containing a known concentration of a select organic contaminant in a carrier gas of ultra-zero air. The compressed ultra-zero air has a certified maximum hydrocarbon concentration of less than 0.1 ppmv and a water vapor concentration of less than 3 ppmv. The oxygen content is between 19.5 and 23.5 percent by volume. The adsorption isotherms are measured at room temperature ($25^{\circ}\text{C} \pm 1^{\circ}\text{C}$).

Certified compressed gas cylinders are used to generate gas streams containing organic contaminants at ppmv concentrations mixed with ultra-zero air. The certified gas cylinders are specially made, and their concentrations are certified by the manufacturer. Mass flow controllers (Tylan Model No. FC-280) regulate the amount of contaminant gas entering the gas generation system, and dilution air is added as needed to obtain the final desired contaminant concentration. Once the gas stream is generated, it is then passed through the gravimetric balance containing the ACC sample. The ACC sample then adsorbs the gaseous organic contaminant until equilibrium is reached. Adsorption equilibrium is assumed to occur when the

change in mass of the sample with respect to time approaches zero (i.e., no mass change is observed over a several hour period). The gain in sample mass is recorded, and the mass ratio of adsorbed material to ACC is determined. For contaminant concentrations in the 10 to 50 ppmv range, the time required to reach equilibrium is typically between 2 to 7 days for ACC masses of 10 to 30 mg and total gas flow rates of 100 cm³/min. The experimental system also provides for thermal regeneration of the ACC to desorb any volatile materials that may have adsorbed onto the ACC sample during its manufacture, storage, and handling.

4.2.1 Gas Generation System

The gas generation system uses certified calibration gas mixtures (Matheson) containing known concentrations of hydrocarbons (e.g., benzene or acetone), ultra-zero air and mass flow controllers to generate gas streams in the ppmv concentration range of hydrocarbons. Gas cylinders with contaminant

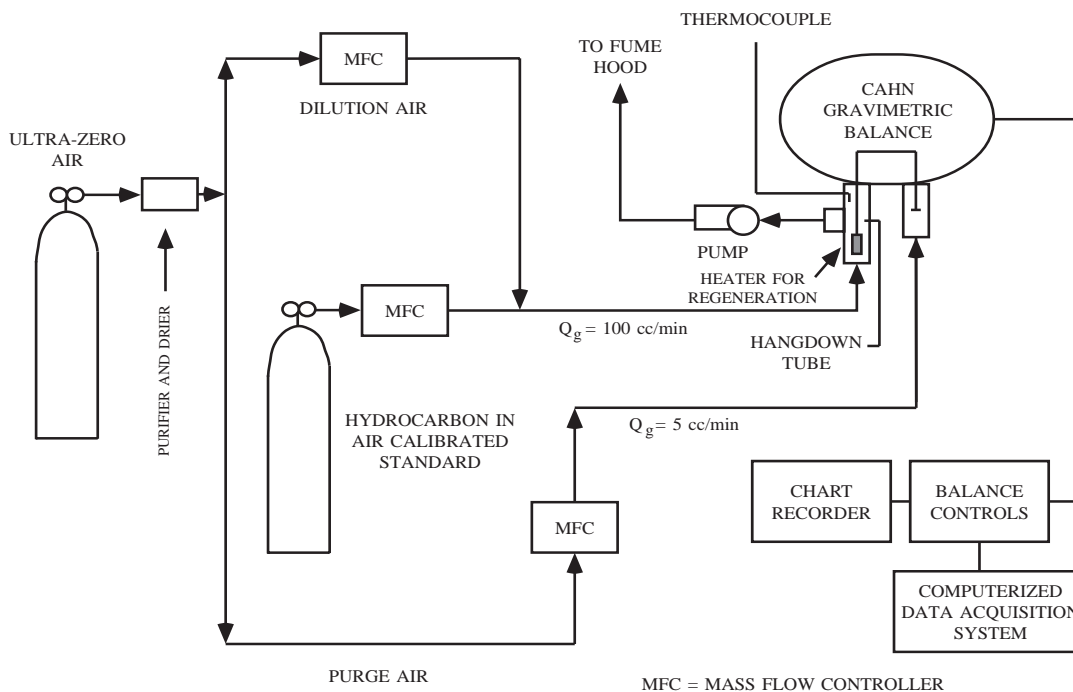


Figure 4.1. Apparatus for Adsorption Measurements of VOCs in the ppmv Range.

concentrations of 1000 ppmv were diluted with ultra-zero air for use in adsorption capacity measurements for contaminants in the 10 to 1000 ppmv range. An ultra-zero air dilution gas is used for generating different gas concentrations from the calibrated compressed gas cylinders. Additionally, the ultra-zero air passes through a gas purifier and drier (Drierite Model No. L68GP). The Drierite cylinder uses silica gel to remove

Chapter 4: Single Component Adsorption Measurements and Modeling

water vapor to a terminal dryness of 0.005 mg/L or -37.7°C dewpoint and 5 Å molecular sieves to remove dilute concentrations of hydrocarbons. The total gas flow rate through the gravimetric balance was $100\text{ cm}^3/\text{min}$.

The measurement of the water vapor adsorption isotherms was performed using a similar system as presented in Figure 4.1 with a few modifications and is presented in Figure 4.2. Measurement of the water

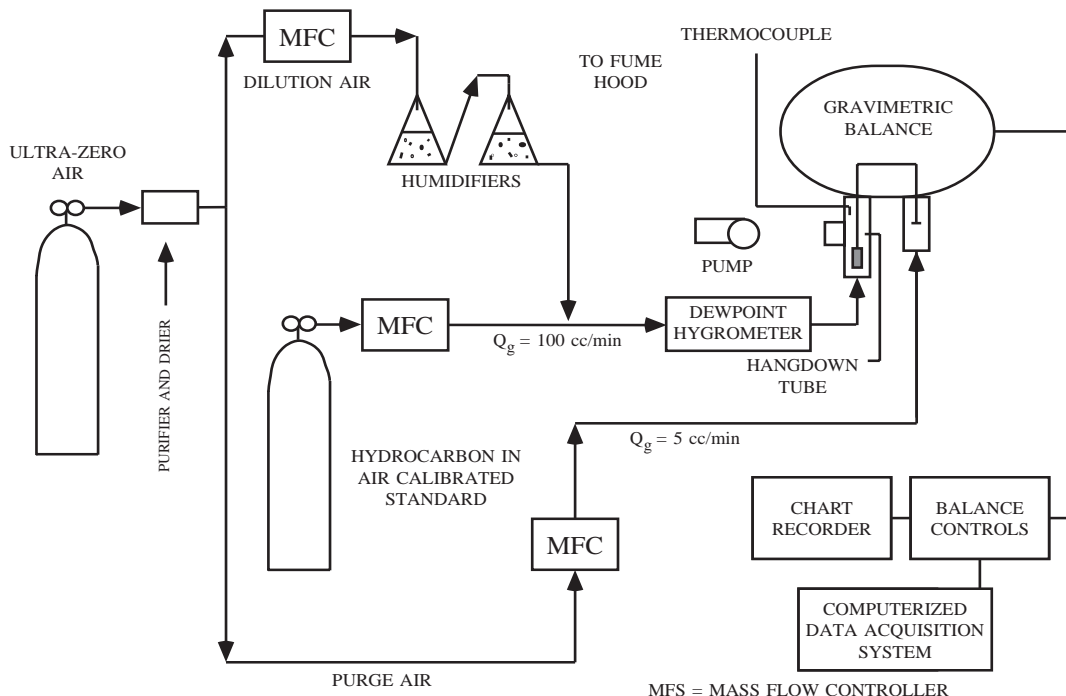


Figure 4.2. Apparatus for Measurement of Water Vapor Adsorption Isotherms.

vapor adsorption isotherms for the ACC samples was performed gravimetrically using a Cahn microbalance (model C-2000). The humidified gas stream was generated by passing a hydrocarbon-free air stream through two Erlenmeyer flasks in series containing water and gas dispersion tubes (see Figure 4.2). The humidified gas stream was then diluted with hydrocarbon-free air using mass flow controllers (Tylan model FC-280) to obtain the desired relative humidities. The adsorption isotherms were measured at 25°C and a total pressure of 1 atm. ACC sample masses were between 10 and 20 mg, and the total gas flow rate through the gravimetric balance was $150\text{ cm}^3/\text{min}$.

4.2.2 Measurement of Mass Change of ACC

The mass change of ACC during adsorption is recorded on a strip chart recorder (Linseis, Model No. L6514) and is also recorded using *Labtech Notebook* and an IBM PC computer. As previously mentioned, adsorption equilibrium is assumed to occur when the change in mass of the ACC sample with respect to time approaches zero. At this time, a voltmeter (Omega, Model No. 881C) is used to obtain a precise mass reading at equilibrium, and this value is recorded on the strip chart containing the adsorption data. The concentration of contaminant in the gas stream is then increased, and the sample is allowed to reach equilibrium with this new bulk gas phase concentration. These measurements are repeated until an entire adsorption isotherm is obtained for the sample. The adsorption capacity for each equilibrium concentration is normalized to the ACC sample mass by dividing by the initial adsorbent sample weight as determined in the experimental procedure discussed below.

4.2.3 Experimental Procedure

The 10 to 30 mg ACC sample is weighed 10 times using an analytical balance (Satorius Analytic, Model No. A200S), and an average of these measurements is used to determine an initial mass of the sample. The ACC sample is then placed in the gravimetric balance. Ultra-zero air is flowed over the sample while the air surrounding the ACC sample is heated to 140°C for 30 minutes with heating tape placed around the balance hang-down tube to desorb any water vapor and other contaminants adsorbed onto the sample. The amount of mass lost by desorption is subtracted from the initial sample mass to give the actual sample mass used in the normalization procedure discussed above. The sample is then allowed to cool to room temperature (25°C ± 1°C). Once the sample has cooled to room temperature, a contaminant gas stream is passed through the balance. Duplicate measurements were made for most adsorbate-adsorbent combinations and agreed within about 10%.

4.3 Measurement of the Adsorption of Volatile Organic Compounds

The adsorption capacities for acetaldehyde were only measured up to 250 or 500 ppmv, depending on the ACC sample, because acetaldehyde converts to acetic acid in the presence of oxygen when the concentration is high enough (Venugopal, 1967; Matheson Gas, 1993). In the case of acetaldehyde (Figure 4.3), ACC-15 had the greatest adsorption capacity. ACC-25 had a higher adsorption capacity than ACC-20 until about 100 ppmv, then ACC-20 started to exhibit the highest adsorption capacity. The adsorption capacities for acetaldehyde and ACC were far less than the adsorption capacities for any of the other VOC adsorbates, mainly due to the low boiling point and high vapor pressure (1000 torr) of acetaldehyde at 25°C.

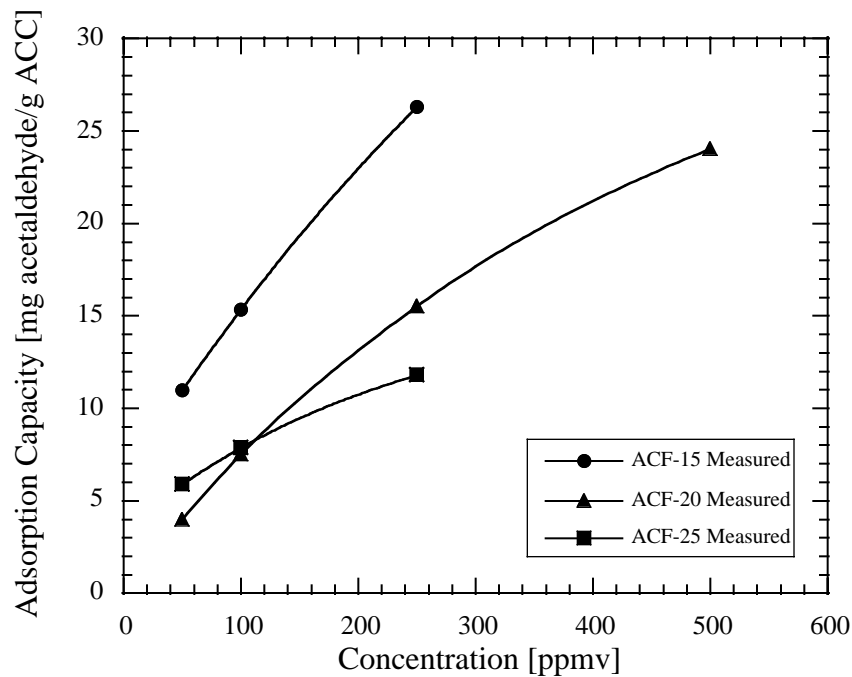


Figure 4.3. Adsorption Isotherms for Acetaldehyde and ACC.

In the case of acetone (Figure 4.4), there was a trend of lower specific surface area having the higher adsorption capacity, i.e., ACC-15 adsorbed more acetone at a given concentration than ACC-20, which adsorbed more than ACC-25 for concentrations between 10 and 1000 ppmv.

It can be seen from the experimental results that benzene had a higher adsorption capacity than either for acetone, acetaldehyde or methyl ethyl ketone (MEK) for the three ACC samples. ACC-15 had a higher adsorption capacity for benzene (Figure 4.5) than ACC-20 at low concentrations (less than 100 to 200 ppmv), but at higher concentrations ACC-20 exhibited higher adsorption capacity than ACC-15. ACC-25 had a lower adsorption capacity than ACC-20 for benzene in the 10 to approximately the 1000 ppmv range.

The adsorption capacities for MEK on ACC (Figure 4.6) were nearly as great as those observed for benzene over the 10 to 1000 ppmv concentration range. ACC-15 had the highest adsorption capacity (235 mg/g) for MEK up to about 200 ppmv until it was exceeded by ACC-20. Likewise, the adsorption capacity of MEK on ACC-25 (260 mg/g) exceeded that of ACC-15 at around 650 ppmv.

As expected, all of the VOC adsorbates exhibited a type I isotherm by Brunauer's classification. It can be stated for all three adsorbates that as the concentration in the gas stream increases, ACC-25 will eventually have a greater adsorption capacity than ACC-20, and ACC-20 will have a greater adsorption capacity than ACC-15, due to the differences in micropore volume of the ACC samples.

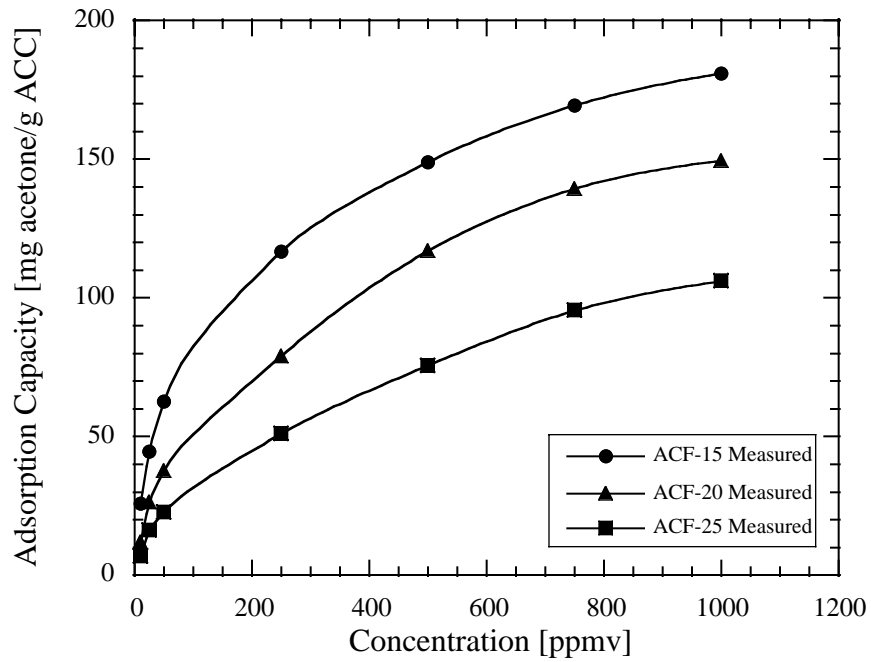


Figure 4.4. Adsorption Isotherms for Acetone and ACC.

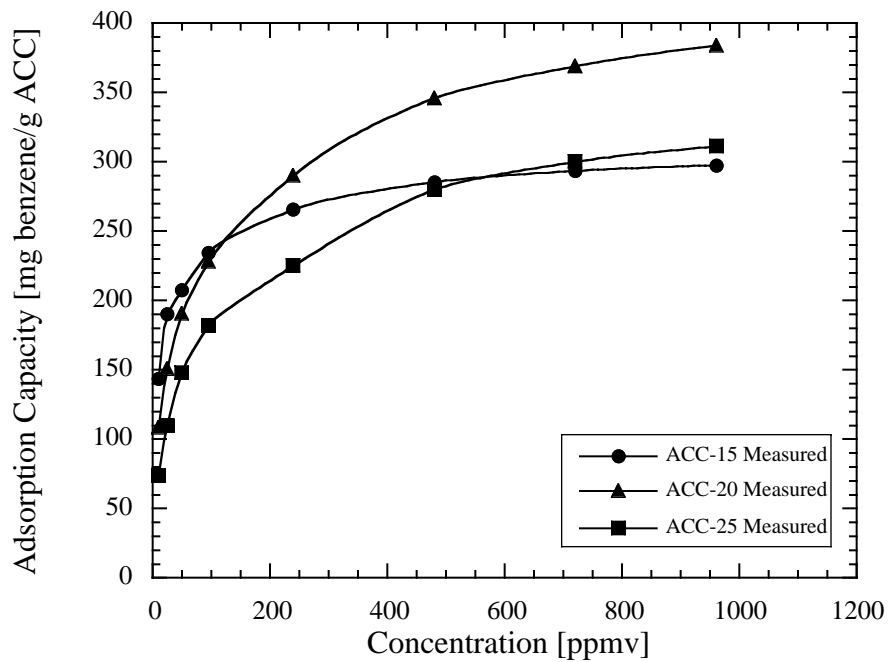


Figure 4.5. Adsorption Isotherms for Benzene and ACC.

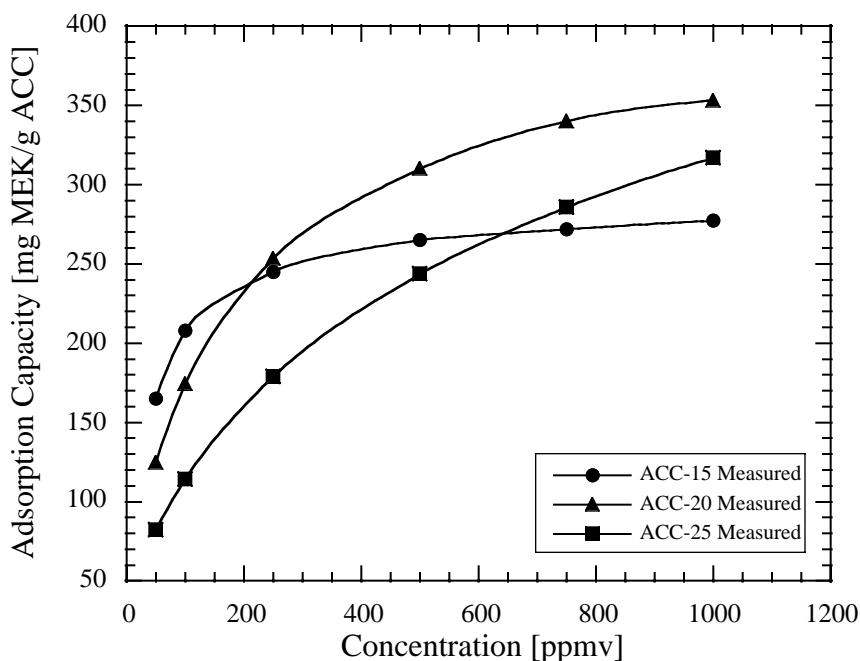


Figure 4.6. Adsorption Isotherms for Methyl Ethyl Ketone (MEK) and ACC.

4.4 Water Vapor adsorption with ACC

Adsorption and desorption isotherms were measured for water vapor from 0 to 95% RH. In most cases, duplicate measurements were made for each isotherm data point, and the values were within 10% of each other.

Adsorption and desorption isotherms for water vapor at RH values between 0 and about 90% and ACC-15, ACC-20 and ACC-25 are presented in Figure 4.7. Significant water vapor adsorption did not occur until about 30% RH for ACC-15, about 45% RH for ACC-20 and about 50% RH for ACC-25. These results indicate that water vapor adsorption may interfere with hydrocarbon adsorption at RH values greater than about 30%.

It can be seen in Figure 4.7 from the differences in the measurements for water vapor adsorption and desorption that water vapor adsorption onto ACC exhibits hysteresis. The spread or width of the hysteresis loop increased, as did the total amount adsorbed at saturation, with increased BET surface area. The most widely accepted explanation for the observed hysteresis is that in the desorption process small pores constrict the openings to larger pores such that adsorbed water in the larger pores is not desorbed until the relative pressure corresponds to that of the smaller pore size (Mahle and Friday, 1989).

Equation 2.28 (Dubinin, 1980) was used to model the adsorption of water vapor onto ACC over the RH range of about 5 to 50% or P/P_0 of 0.05 to 0.5 (Figures 4.8 to 4.10). The parameters used for equation 2.28

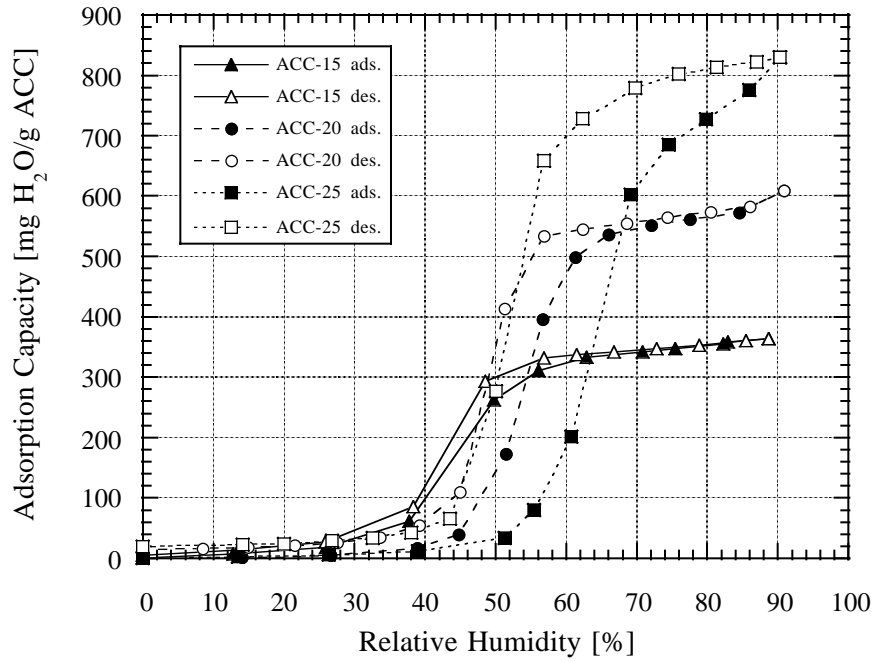


Figure 4.7. Adsorption Isotherms for Water Vapor and ACC.

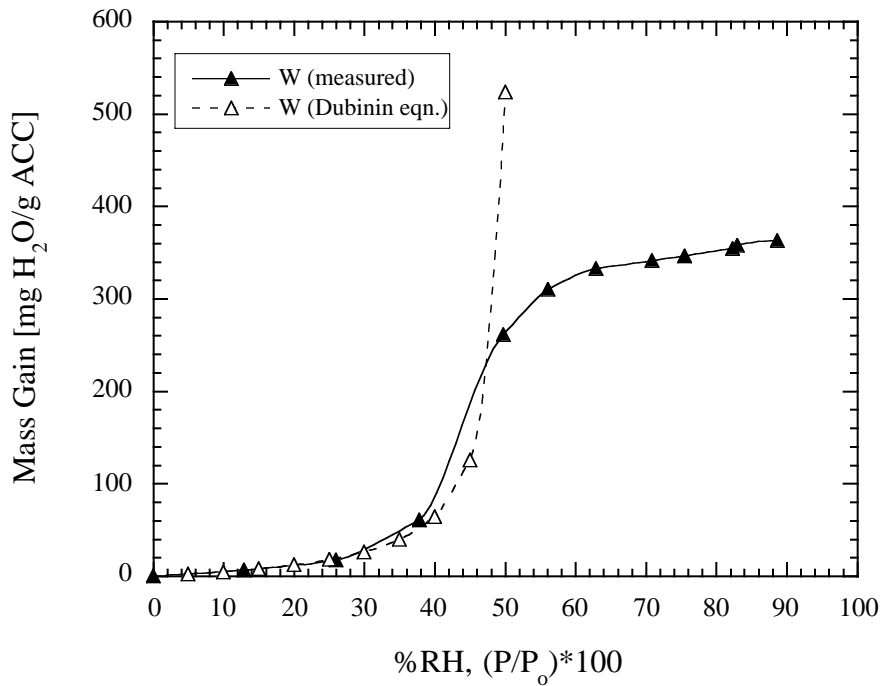


Figure 4.8. Measured and Modeled Adsorption Isotherms for Water Vapor and ACC-15.

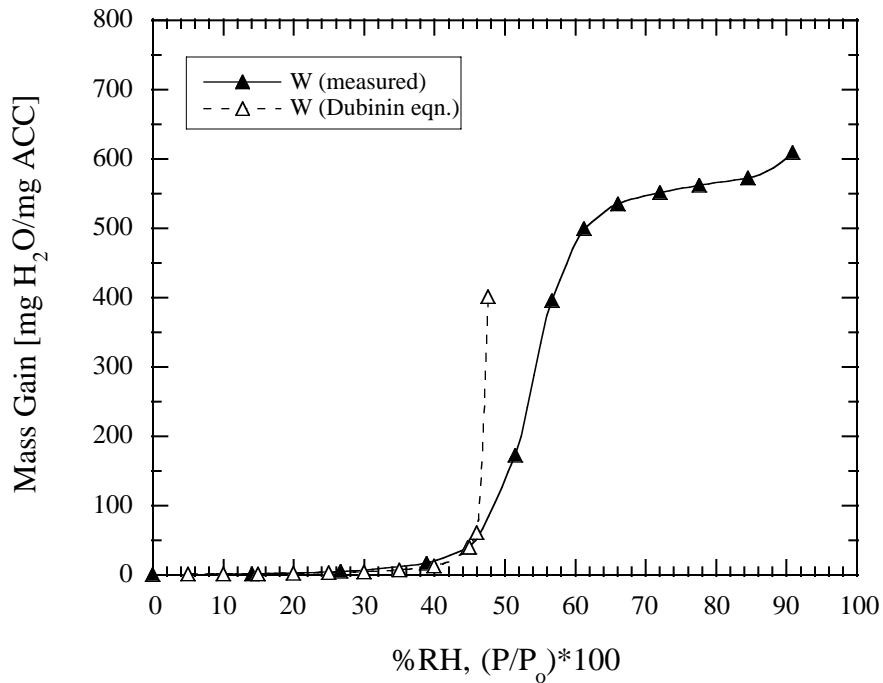


Figure 4.9. Measured and Modeled Adsorption Isotherms for Water Vapor and ACC-20.

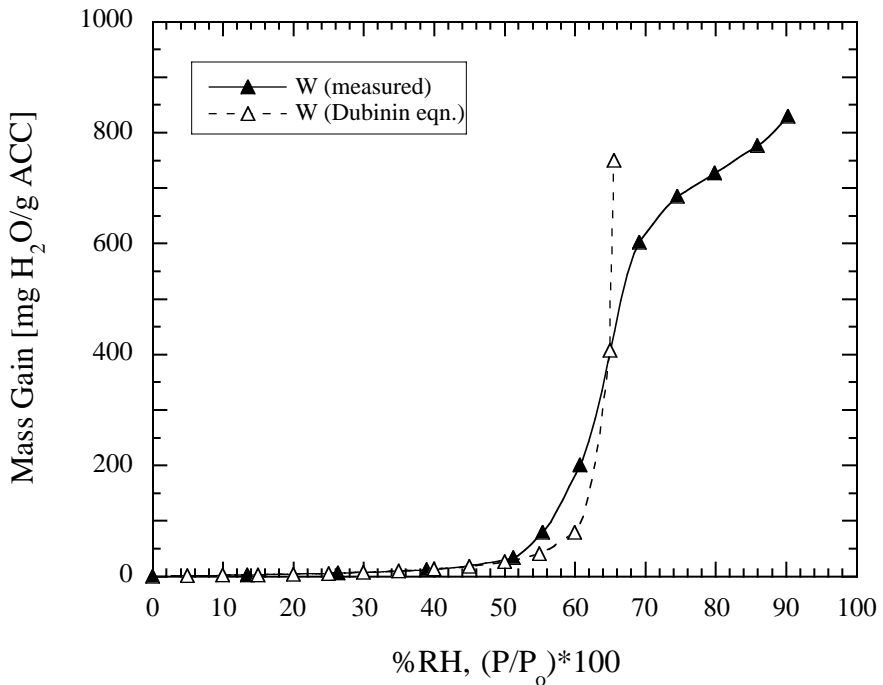


Figure 4.10. Measured and Modeled Adsorption Isotherms for Water Vapor and ACC-25.

and three ACC samples are presented in Table 4.1. It can be seen in Figures 4.8 to 4.10 that equation 2.28

Table 4.1. Dubinin Parameters for Equation 2.28 and ACC.

Adsorbent	W_o [mg/g]	c
ACC-15	19.0	1.93
ACC-20	2.51	2.09
ACC-25	8.31	1.51

provides a good fit of the water vapor adsorption curve until about the inflection point ($45\% < RH < 65\%$). Equation 2.28 is not able to model the entire water vapor adsorption isotherm or any portion of the water vapor desorption isotherm.

4.5 Single Component Adsorption Modeling

The VOC adsorption isotherms were modeled using the Freundlich and Dubinin-Radushkevich (DR) equations. The parameters for the Freundlich and DR equations are presented below along with plots adsorption capacity using the equations for the concentration range of 0.1 to 10000 ppmv. Since VOC concentrations in air are usually in the sub-ppmv range, the Freundlich and DR models were used to extrapolate the adsorption capacities at low concentrations, using the experimental adsorption capacity data obtained in the 10 to 1000 ppmv range.

4.5.1 Freundlich Equation

The Freundlich parameters for the adsorption of acetaldehyde, acetone, benzene, and MEK on ACC are presented in Table 4.2. Plots of the adsorption isotherms for each of the adsorbates and the three ACC samples are presented in Figures 4.11 through 4.14. The use of the Freundlich equation over such a wide range of concentrations (six orders of magnitude), almost certainly guarantees that the adsorbate concentrations at the high and low end are incorrectly estimated. This is not to say that the data are useless for this concentration range, on the contrary, for many applications this may give a reasonable estimate of the adsorption capacity for VOC adsorbates. If more accurate estimates are sought, use of the DR equation as described in section 4.5.2 is recommended.

4.5.2 Dubinin-Radushkevich (DR) Equation

Plots of the adsorption isotherms for each of the adsorbates and the three ACC samples are presented in Figures 4.15 through 4.18. The DR parameters (equation 2.13) for the adsorption of acetaldehyde, acetone,

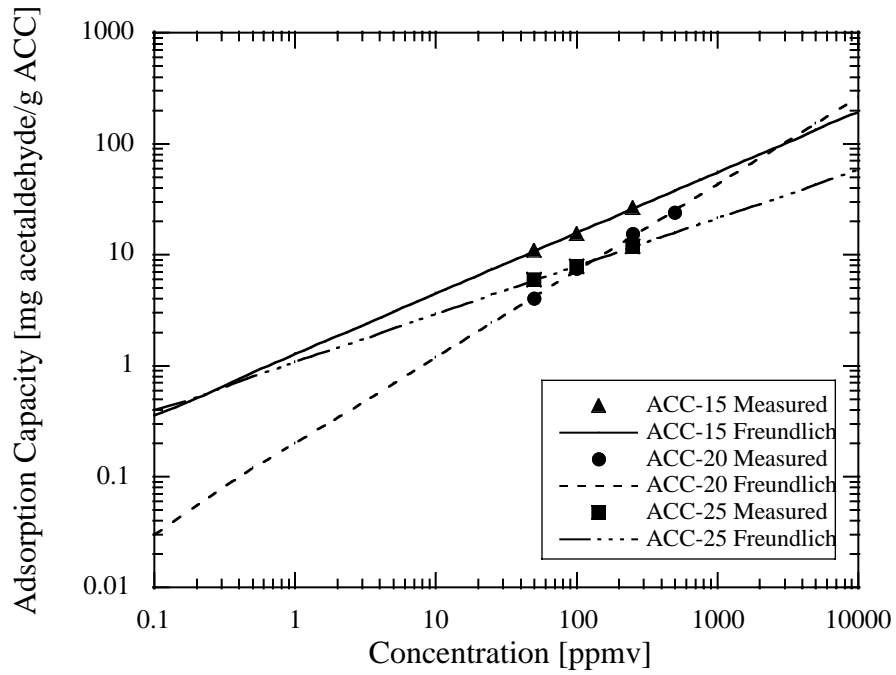


Figure 4.11. Experimental and Freundlich Modeled Adsorption Isotherms for Acetaldehyde and ACC.

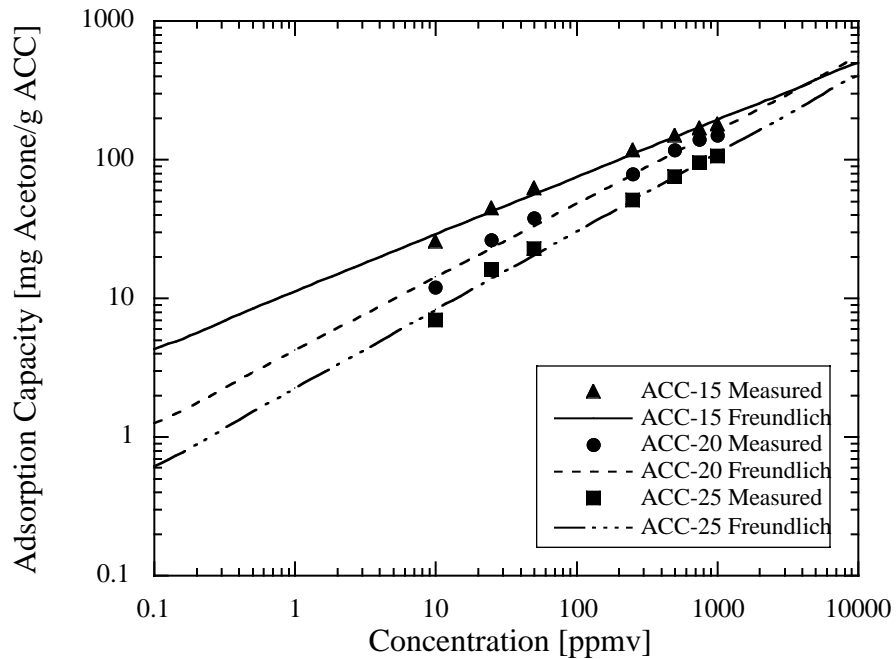


Figure 4.12. Experimental and Freundlich Modeled Adsorption Isotherms for Acetone and ACC.

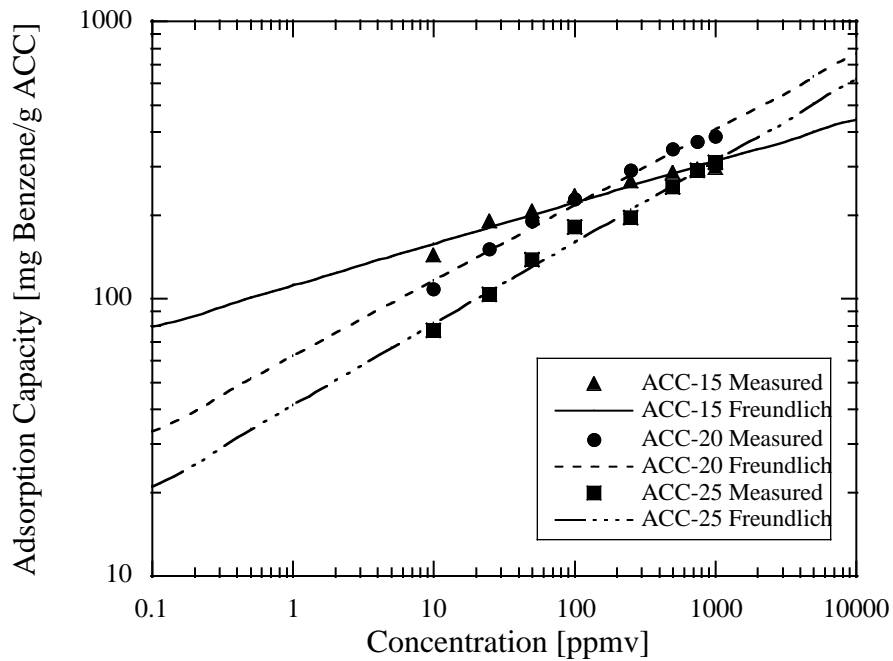


Figure 4.13. Experimental and Freundlich Modeled Adsorption Isotherms for Benzene and ACC.

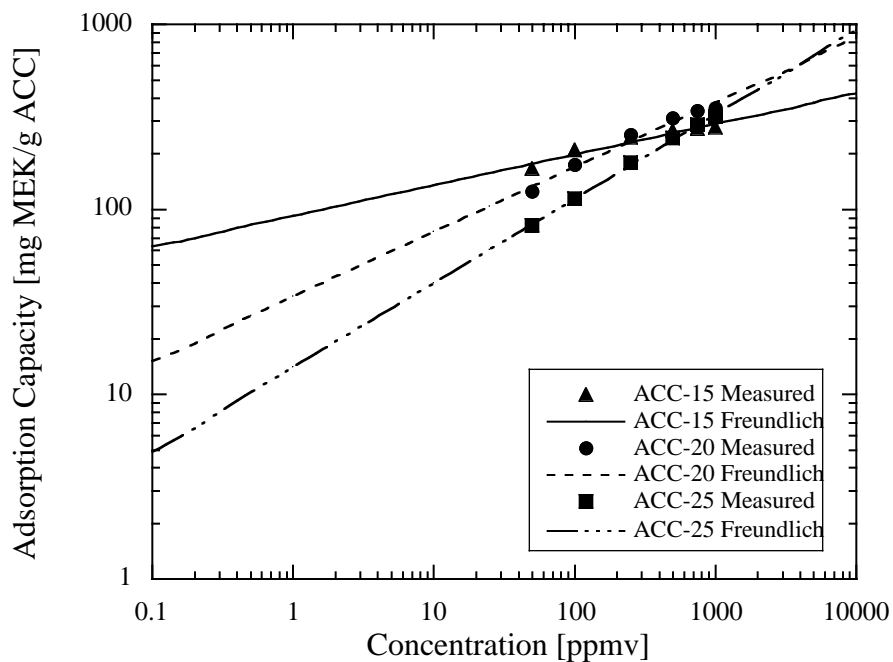


Figure 4.14. Experimental and Freundlich Modeled Adsorption Isotherms for MEK and ACC.

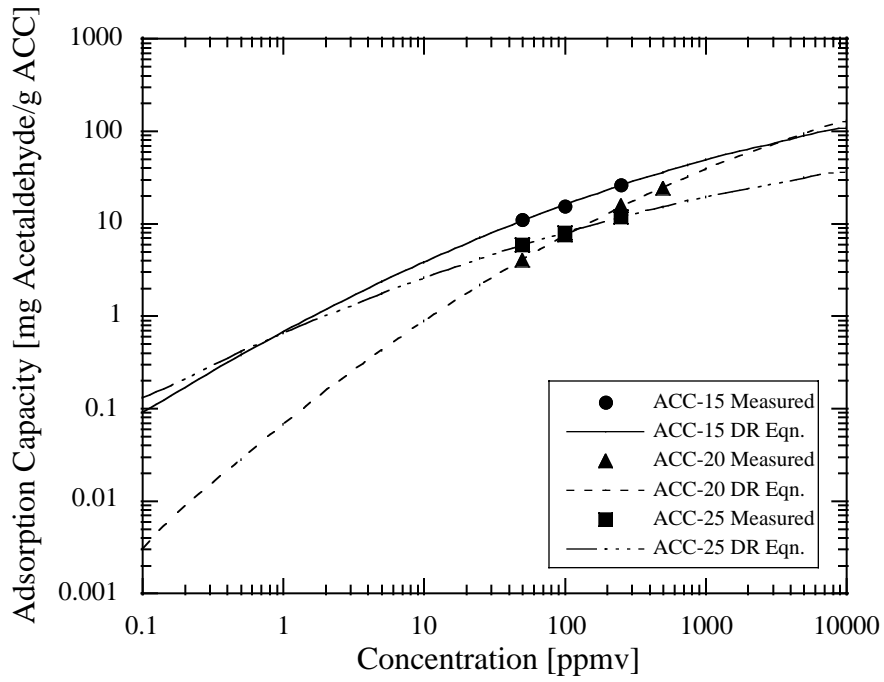


Figure 4.15. Experimental and DR Modeled Adsorption Isotherms for Acetaldehyde and ACC.

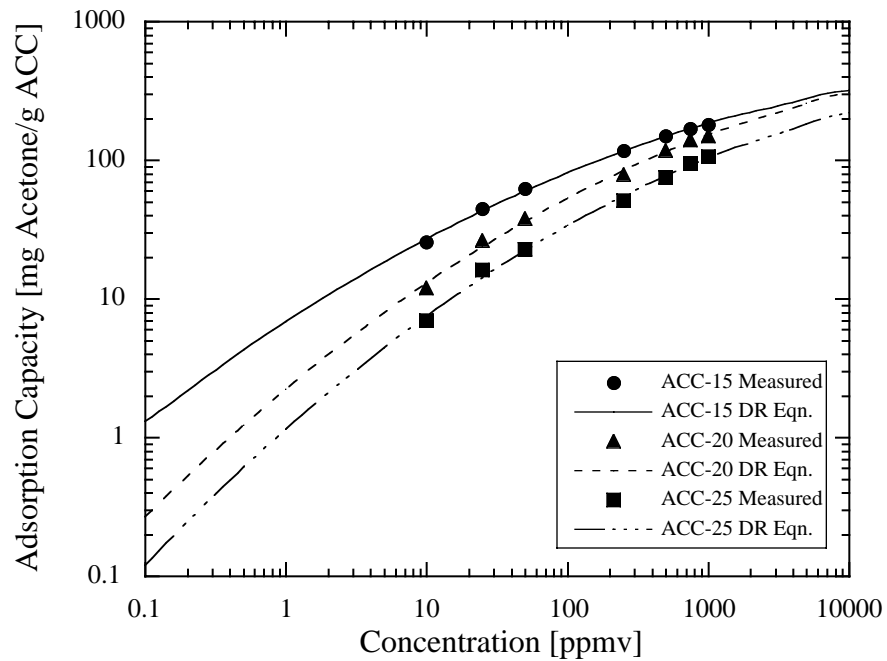


Figure 4.16. Experimental and DR Modeled Adsorption Isotherms for Acetone and ACC.

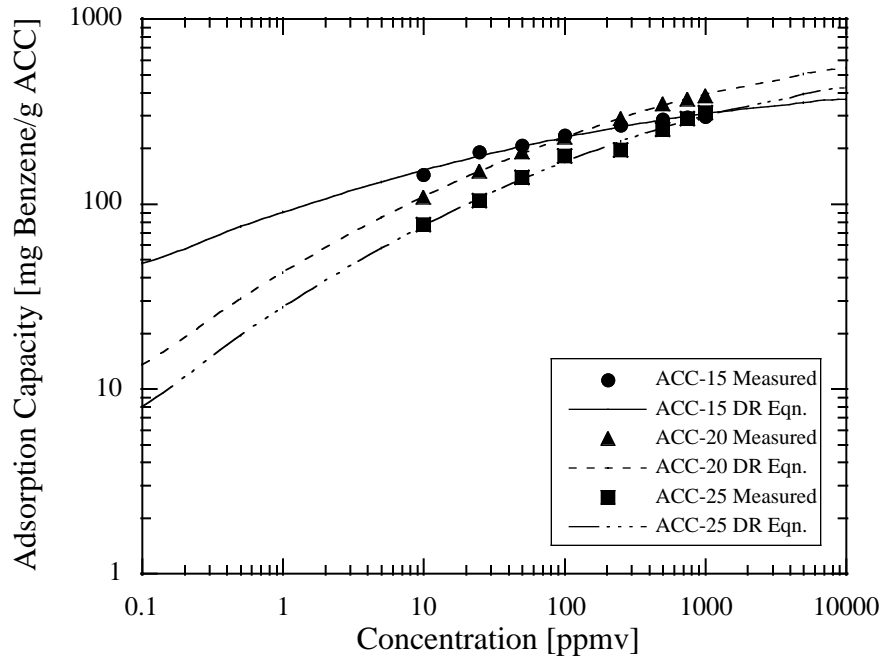


Figure 4.17. Experimental and DR Modeled Adsorption Isotherms for Benzene and ACC.

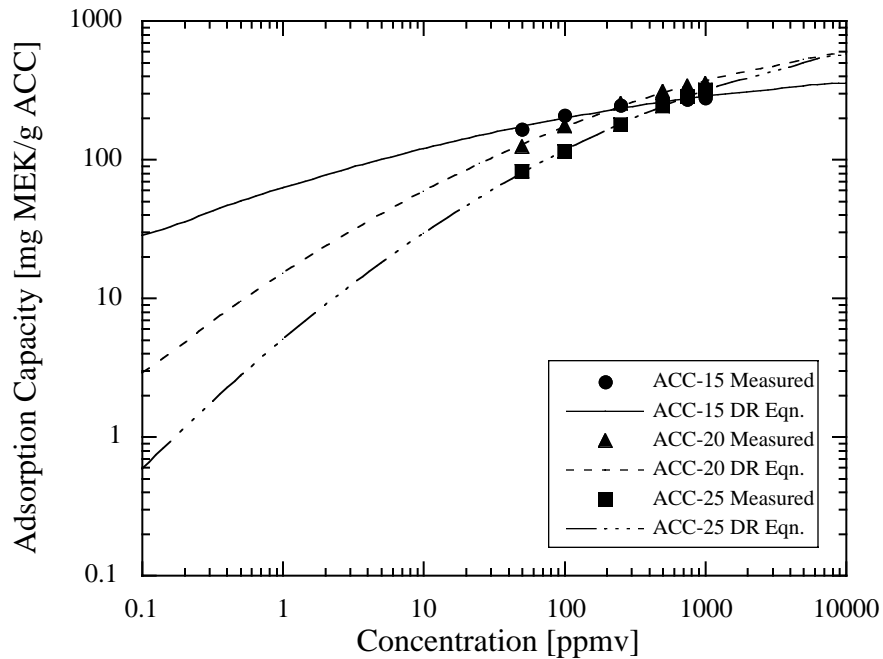


Figure 4.18. Experimental and DR Modeled Adsorption Isotherms for MEK and ACC.

Table 4.2. Freundlich Parameters for VOC Adsorbates and ACC.

	ACC-15	ACC-20	ACC-25
Acetaldehyde			
k	1.27	0.198	1.08
1/n	0.546	0.781	0.432
Correlation Coefficient (R)	0.999	0.997	1.00
Acetone			
k	2.42	4.24	2.26
1/n	0.413	0.529	0.565
Correlation Coefficient (R)	0.995	0.994	0.995
Benzene			
k	112	62.3	41.4
1/n	0.149	0.272	0.294
Correlation Coefficient (R)	0.978	0.995	0.992
MEK			
k	92.6	33.9	14.1
1/n	0.165	0.350	0.455
Correlation Coefficient (R)	0.966	0.989	1.00

Chapter 4: Single Component Adsorption Measurements and Modeling

benzene, and MEK on ACC are presented in Table 4.3. The DR equation gave good fits to the experimental

Table 4.3. DR Parameters for VOC Adsorbates and ACC.

	ACC-15	ACC-20	ACC-25
Acetaldehyde			
W_o [mg/g]	219.4	361.6	63.6
V_o [cm ³ /g] [†]	0.274	0.462	0.0812
E_o [kJ/mol]	14.5	11.9	16.3
x_o [nm]	0.827	1.01	0.735
$x_o\beta^{\ddagger}$ [nm]	0.538	0.656	0.478
Correlation Coefficient (R)	0.997	0.999	0.999
Acetone			
W_o [mg/g]	432.9	453.1	332.9
V_o [cm ³ /g]	0.548	0.574	0.421
E_o [kJ/mol]	15.4	13.6	13.1
x_o [nm]	0.782	0.885	0.914
$x_o\beta^{\ddagger}$ [nm]	0.610	0.690	0.713
Correlation Coefficient (R)	0.999	0.998	0.998
Benzene			
W_o [mg/g]	394.7	613.2	486.6
V_o [cm ³ /g]	0.450	0.699	0.555
E_o [kJ/mol]	23.9	17.8	17.2
x_o [nm]	0.502	0.674	0.699
$x_o\beta^{\ddagger}$ [nm]	0.502	0.674	0.699
Correlation Coefficient (R)	0.991	1.00	0.994
MEK			
W_o [mg/g]	389.3	700.8	719.2
V_o [cm ³ /g]	0.483	0.870	0.893
E_o [kJ/mol]	21.4	14.8	13.0
x_o [nm]	0.560	0.812	0.923
$x_o\beta^{\ddagger}$ [nm]	0.538	0.780	0.886
Correlation Coefficient (R)	0.980	0.996	1.00

[†]. Calculated from W_o and the adsorbate liquid density.

[‡]. Benzene was used as the reference adsorbate for the calculation of β (see Table 2.3).

data for all of the VOC adsorbates examined in this study. Use of the DR equation is recommended for more

accurate estimates of the adsorption capacities of the VOC adsorbates at concentrations other than those measured, because the DR equation is capable of fitting an entire type I adsorption isotherm, where the Freundlich equation is only accurate over limited concentration ranges. Differences in $x_0\beta$ may be due to narrow range of data fit, polarity of adsorbate, but are probably not due to molecular sieving effects.

4.5.3 Change of Affinity Coefficient in DR Equation for Adsorption Isotherm Prediction

The DR equation (equation 2.13) can be used to predict the adsorption of organic compounds using a suitable reference vapor. This is done by modifying the affinity coefficient, β , in equation 2.13. The affinity coefficients were calculated using the parachor method described by Dubinin (1960) and Quayle (1953) and are presented in Table 2.3. It can be seen in Figures 4.19-4.21 that using nitrogen at 77 K as a reference

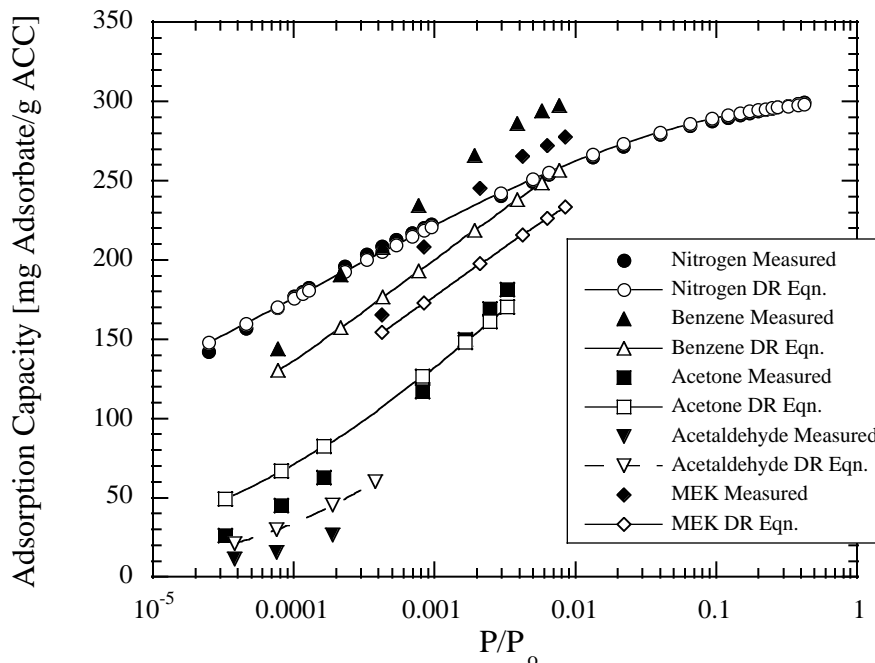


Figure 4.19. Predicted and Observed Adsorption Isotherms for ACC-15 Using N_2 at 77K as a Reference Vapor in the DR Equation.

vapor in the DR equation provides a reasonable estimate of the adsorption capacity of benzene, acetone, acetaldehyde, and MEK onto ACC. Better results should be obtained if a similar adsorbate is used as a reference in the DR equation, e.g. using benzene to predict the adsorption of a similar aromatic compound. This method of using a reference vapor to predict the adsorption can minimize the amount of experiments needed to characterize the adsorption properties of an adsorbent. Experimental adsorption isotherms could be determined for classes or organic compounds (e.g., aromatics and ketones), and then similar compounds

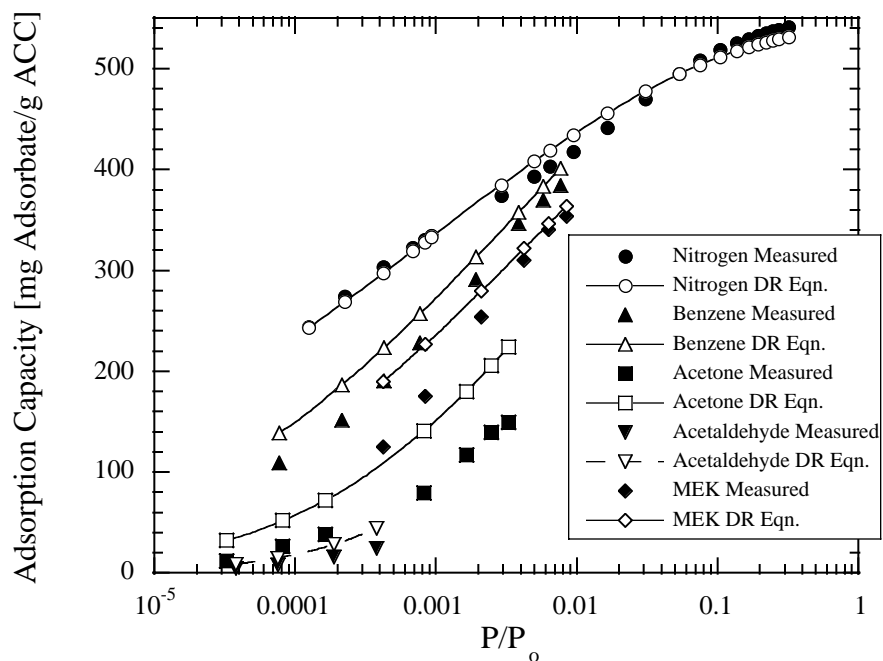


Figure 4.20. Predicted and Observed Adsorption Isotherms for ACC-20 Using N₂ at 77K as a Reference Vapor in the DR Equation.

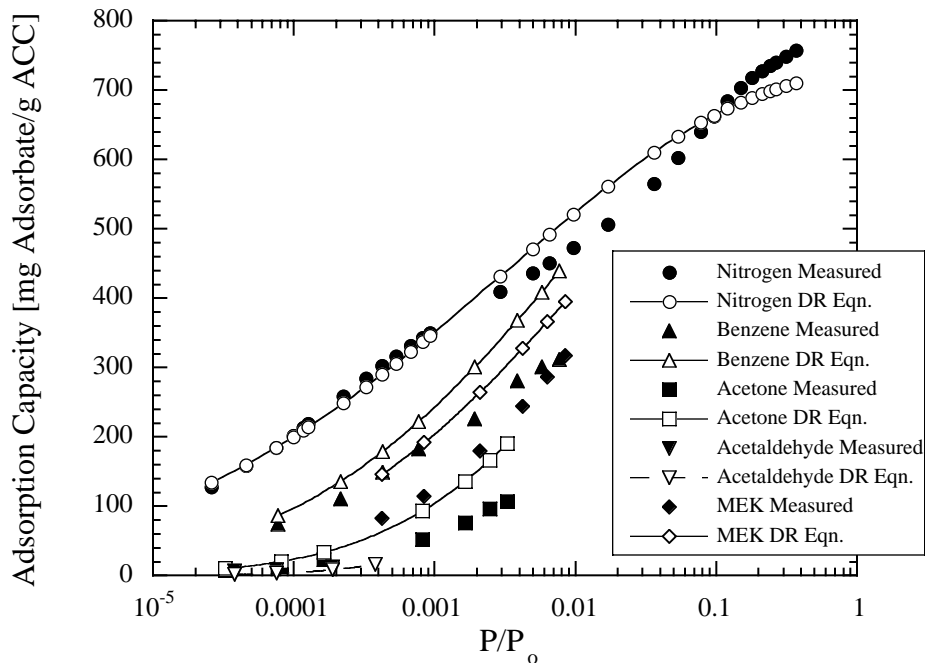


Figure 4.21. Predicted and Observed Adsorption Isotherms for ACC-25 Using N₂ at 77K as a Reference Vapor in the DR Equation.

could be used to model those compounds of interest for which experimental data are not available. If a similar reference vapor is not available for the compound of interest, either nitrogen at 77 K or benzene at 298 K are good general reference adsorbates.

The DR equation was used to predict the adsorption of other compounds of interest to indoor air quality, but not measured for ACC in this study over the 0.1 to 1000 ppmv concentration range. The adsorbates were grouped into two groups: nonpolar (and weakly polar) and strongly polar, based on a recommendation by Reucroft et al. (1971). Benzene was used as the reference adsorbate for nonpolar and weakly polar adsorbates (Figure 4.22), while acetone was used as the reference adsorbate for the strongly polar

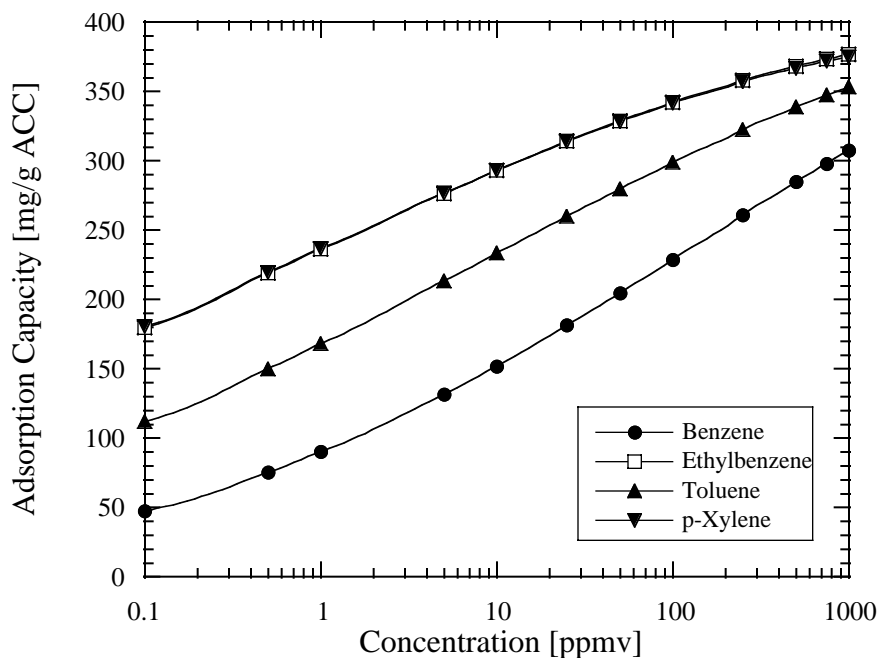


Figure 4.22. Modeled Adsorption Isotherms for VOCs Using Benzene as a Reference Adsorbate in the DR Equation and ACC-15. Benzene Adsorption Capacity was Experimentally Measured.

compounds (Figure 4.23). β values used are presented in Table 2.3.

When using a reference adsorbate to predict the adsorption of another adsorbate, the DR parameters must be either in units of cm^3/g or mmol/g , so the DR parameters presented in Table 4.3 were converted to a volume basis [cm^3/g] using the liquid densities of the adsorbates. These volume based W_0 's were then used to predict the adsorption capacities of the various adsorbates, and then the DR predicted volumes adsorbed were transformed back to a mass basis using liquid densities of the adsorbates.

Note that Figure 4.22 is plotted on a log-linear scale and that Figure 4.23 is plotted on a log-log scale, due to the low adsorption capacity of acetaldehyde. In Figure 4.23, the experimental results are plotted with those predicted with the DR equation. When comparing these predictions with those using nitrogen as the

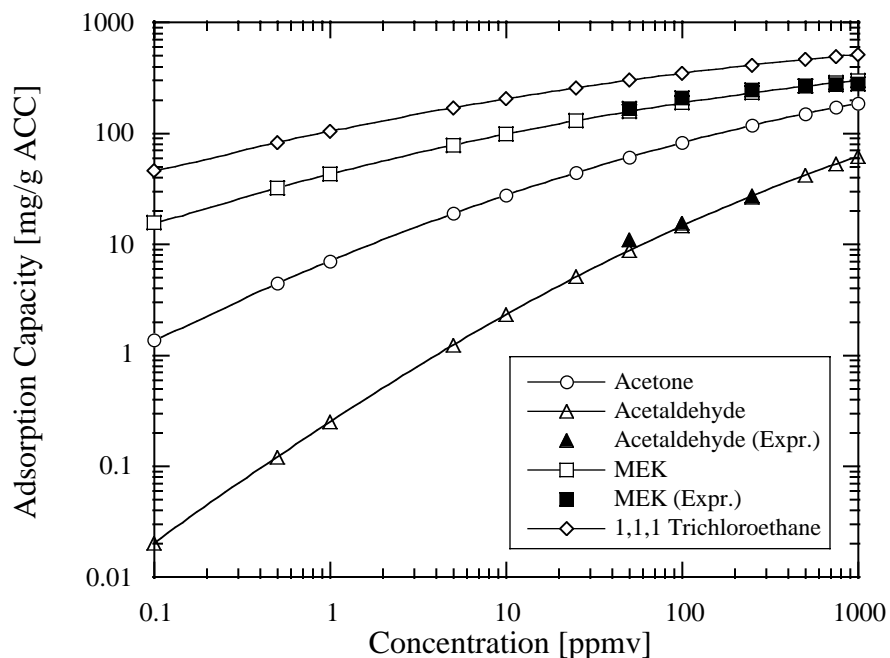


Figure 4.23. Modeled Adsorption Isotherms for VOCs Using Acetone as a Reference Adsorbate in the DR Equation and ACC-15. Experimental Plots for Acetaldehyde and MEK are Shown for Comparison to Modeled Curves. The Acetone Isotherm was Experimentally Determined.

reference adsorbate (Figure 4.19), it is clear that acetone was a better reference vapor for the highly polar compounds examined. The average errors when using acetone as the reference adsorbate was about 9% for acetaldehyde and about 5% for MEK.

4.6 Summary

Adsorption isotherms were measured for acetaldehyde, acetone, benzene, MEK, and water vapor and three ACC samples. For the 10 to 1000 ppmv concentration range examined, benzene exhibited the highest adsorption capacity on ACC, followed by MEK, acetone, and acetaldehyde. Water vapor adsorption was not significant on ACC until relative humidities above about 50% ($P/P_o > 0.5$), when capillary condensation of $H_2O_{(g)}$ occurred within ACC pores.

Equilibrium adsorption experiments were not performed for VOCs in the sub-ppmv concentration range, due to the long times (weeks to months) to reach equilibrium, and the high cost of compressed gases. The Freundlich and DR equations were used to model the adsorption capacities into the sub-ppmv range for the four adsorbates and three ACC samples examined in this research. The sub-ppmv concentration range is a more realistic concentration range for VOCs present in indoor air environments.

It has been suggested that when using the DR equation to predict adsorption capacities of organic compounds using a reference adsorbate, reference adsorbates of similar polarity should be used. This

Chapter 4: Single Component Adsorption Measurements and Modeling

hypothesis was examined by using benzene as a reference adsorbate for non-polar (and slightly polar) compounds (ethylbenzene, toluene, and p-xylene) and acetone as a reference for polar compounds (acetaldehyde, MEK, and 1,1,1-trichloroethane). The improvement in prediction of adsorption capacity was not determined for the non-polar compounds, but using acetone as a polar reference adsorbate, showed average errors of 9% for predicted adsorption of acetaldehyde and 5% for predicted adsorption of MEK.

4.7 References

- Cal, Mark P., Larson, Susan M., and Rood, Mark J., "Experimental and Modeled Results Describing the Adsorption of Acetone and Benzene onto Activated Carbon Fibers," *Environmental Progress*, **13**(1): 26-30, 1994.
- Dietz, V.R., "The Rates of Adsorption and Desorption of Water Vapor from Air Flows Through Activated Carbons," *Carbon*, **29**: 569-572, 1991.
- Dubinin, M.M., "Water Vapor Adsorption and the Microporous Structures of Carbonaceous Adsorbents," *Carbon*, **18**: 355-364, 1980.
- Mahle, J.J., and Friday, D.K., *Carbon*, **27**(6):835-843, 1989.
- Matheson Gas, personal communication, 1993.
- Reucroft, P.J., Simpson, W.H., and Jonas, L.A., "Sorption Properties of Activated Carbon," *Journal of Physical Chemistry*, 75(23):3526-3531, 1971.
- Venugopal, B., Kumar, R., and Kuloor, N.R., "Oxidation of Acetaldehyde to Acetic Acid in a Sparger Reactor," *I&EC Process Design and Development*, 6(1): 139-146, 1967.

Chapter 5

Adsorption on Chemically Modified ACC

5.1 Introduction

In an effort to maximize VOC adsorption, particularly in the case of compounds which are not readily adsorbed on ACC, e.g., acetaldehyde, and to minimize the adsorption of water vapor, several chemical treatments were performed on virgin ACC-20 (Figure 5.1). A sulfuric/nitric acid treatment produced a highly

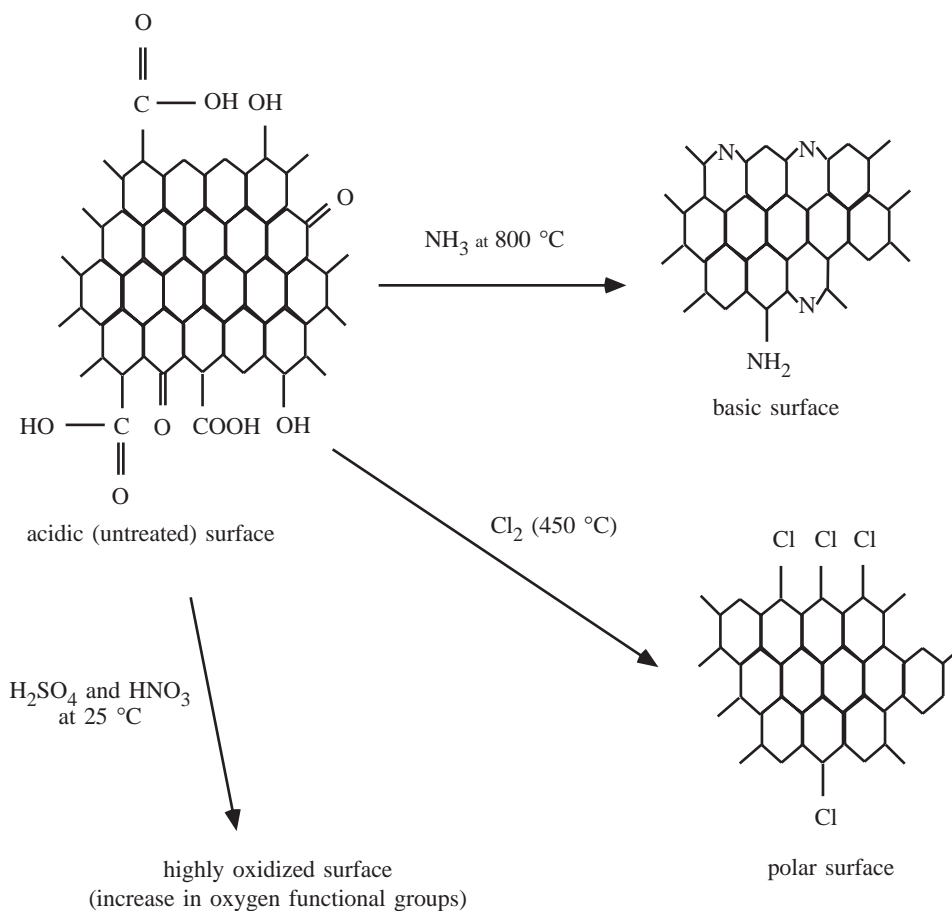


Figure 5.1. Chemical Treatment of ACC (Larson, et al., 1993).

oxidized surface; chemical treatment with NH_3 produced a basic surface and increased the nitrogen content of the ACC; and finally, Cl_2 was used to produce a polar surface. Adsorption isotherms were measured for

Chapter 5: Adsorption on Chemically Modified ACC

acetaldehyde, acetone, benzene, and water vapor to observe the effect on adsorption capacity for chemically treated ACC-20.

The starting material, ACC-20, was obtained from American Kynol Inc. (New York, NY). The chemical treatments of the ACC-20 along with the subsequent chemical and physical analysis were performed by E.D. Dimotakis of the Department of Material Science and Engineering at the University of Illinois at Urbana-Champaign. The pore volumes and the BET surface areas were measured with nitrogen at 77 K (Table 5.1). The micropore volumes were determined using a t-plot analysis (Gregg and Sing, 1982 and Dimotakis, Cal, et al., 1994a). The elemental analysis was performed at the Microanalysis Lab at the University of Illinois at Urbana-Champaign using inductive coupled plasma spectroscopy. The oxygen content was determined by mass difference, assuming that the ACC consisted of carbon, hydrogen, nitrogen, and oxygen. All of the ACC samples could be completely regenerated at temperatures slightly exceeding 100°C for 30 min with no apparent loss of chemical functional groups or change in adsorption capacity.

Table 5.1. Physical Characteristics and Elemental Composition of ACCs (Dimotakis, Cal, et al., 1994a).

ACC-20 Chemical Treatment	BET Surface Area [m ² /g]	Total Pore Volume [cm ³ /g]	Micropore Volume [cm ³ /g]	C [wt%]	H [wt%]	N [wt%]	O [wt%]	Cl [wt%]
3.9% O/untreated	1550	0.74	0.61	95.40 95.97 [†]	0.68	0.05	3.92 4.03 [†]	0
4.1% N (nitridated)	1738	0.84	0.59	91.96 94.34 [†]	0.27	4.50 4.06 [†]	3.23 1.60 [†]	0
7.8% Cl (chlorinated)	1523	0.73	0.54	87.71	0.06	0.27	4.15	7.8
16% Cl (chlorinated)	1374	0.66	0.51	77.93 88.94 [†]	0.01	0.06	6.00 3.27 [†]	16 7.8 [†]
21% O (oxidized)	1409	0.66	0.55	76.26 85.53 [†]	1.41	1.49	20.84 13.84 [†]	0
32% O (oxidized)	1105	0.47	0.35	64.76 76.60 [†]	1.55	0.72	32.32 23.39 [†]	0

[†]. % Elemental as determined by XPS (see section 5.3). Difference in Cl values between the two methods may be due to uncertainty in the calibration standard used (Dimotakis, 1994).

5.2 Preparation of Chemically Modified ACC

5.2.1 Modification of ACC-20 with Ammonia

About 1.0 g (± 0.1 g) of ACC-20 was placed in a 5 cm ID quartz tube in a temperature controlled tubular furnace. The tube was purged with N₂ for 5 min at 25°C, and the temperature was increased to 180°C for 15 min. Then at the desired reaction temperature (450-600°C), ammonia (NH₃) was introduced for the desired reaction time (6 to 12 hr). After completion, the gas was replaced with N₂ and the sample cooled to room temperature. The product was weighed and placed in closed vials for further characterization.

NH₃ treatment of the ACC samples at 450-600°C (12 hr) yielded an increase in the N content from 0 to 1% by mass. At 800°C (6 hr) a 4.1% N content was achieved, and etching of the ACC pores occurred, increasing the sample surface area to 1700 m²/g (at 4.1% N).

Nitridding the ACC-20 samples results in N 1s peaks at 399 eV and 400-403 eV (broad). The 399 eV peaks can be assigned to amine and pyridine type groups, and the 400-403 eV can be assigned to pyrolic nitrogen or amides or amino groups (literature values of about 400.2 eV) and ammonium derivatives (401.2 eV) (Briggs and Seah, 1983). Nitridding causes a minor decrease of the phenolic hydroxyl/ether peak. A slight increase of the shake-up peak at 291.1 eV relative to ACC-20 is also observed indicative of the fact that nitrogen can be introduced in the carbon skeleton as pyridine nitrogen.

5.2.2 Modification of ACC-20 with Chlorine

About 1.0 g (± 0.1 g) of ACC-20 was placed in a 5 cm ID quartz tube in a temperature controlled tubular furnace. The tube was purged with N₂ for 5 min and the temperature was increased to 180°C for 15 minutes and then at the desired reaction temperature Cl₂ was introduced for the necessary reaction period. After completion, the gas was replaced with N₂ and the sample cooled to room temperature ($25 \pm 1^\circ\text{C}$). The product was weighed and placed in closed vials for further characterization.

Chlorination of the samples was investigated at various temperatures for different times. A 16% Cl content was achieved at 450°C within 12 hr presumably by ring substitution. The BET surface area showed a slight decrease with increasing degree of chlorination. Samples with 7.8% Cl content showed very little change in BET surface area but the samples with 12.3% Cl had a BET surface area of 1440 m²/g and the sample with 16% Cl had a surface area of 1374 m²/g.

Chlorination at 450°C [ACC20-(16% Cl)] results in appearance of a Cl 2p peak at 201 eV of the XPS spectrum. Also chlorination causes an increase of the shake-up band at 291.1 eV (possibly associated with changes in charge transfer upon chlorination), as well as of the carboxylic and phenolic hydroxyl/ether

bands relative to ACC-20. At higher temperatures (800°C) a decrease in the number of hydroxyl/ether peaks was observed (Puri and Bansal, 1967).

5.2.3 Oxidation of ACC-20

A 1/1 (volume/volume) mixture of H₂SO₄/HNO₃ was used to oxidize the pore surface to an oxygen content of about 21% after 10 min at room temperature (25 ± 1°C). Longer treatments (≥ 4 days) resulted in a further increase in oxygen content to about 32%. The N₂ BET surface area decreased with increasing degree of oxidation, probably due to the additional oxygen functional groups blocking access to the smaller pores; e.g. ACC20-(21% O) had a BET surface area of 1400 m²/g, and ACC20-(32% O) had a BET surface area of 1150 m²/g (Table 5.1). Oxidation results in an increase in the carboxylic peak (289 eV) in the XPS spectrum. Oxidation also produces some shifting in the form of the bounded oxygen, as it is oxidized from one form to the other.

5.3 X-Ray Photoelectron Spectroscopy (XPS) Measurements

XPS was used to determine the elemental content (O, N, Cl and C) of the surface of the treated and untreated ACC samples (Briggs and Seah, 1983). The work was carried out at the Materials Research Laboratory of the University of Illinois at Urbana-Champaign, using a PHI 5400 (Perkin-Elmer, Physical Electronics Inc.) instrument. Mg-Kα radiation and a power of 400 Watts at 15 kV were used. The samples were dried at 150°C for 30-45 min prior to analysis since the technique requires ultrahigh vacuum (10⁻⁸ to 10⁻¹⁰ torr). To analyze for the surface groups the carbon region of the XPS spectrum was deconvoluted to individual peaks (Table 5.2).

XPS techniques were used to characterize the chemical changes on the surface of the fiber down to about 30 Å to 100 Å which is the maximum depth that the emitted photoelectrons can escape and be detected (Briggs and Seah, 1983). XPS can identify the N, Cl or O groups present based on their binding energy values. It was assumed that the chemical nature of the surface is similar to that of the core of the sample. Table 5.2 describes the percent of total carbon area of each group as a function of the binding energy (variations within 0.7 eV are observed for the treated samples): phenol or ether (285 eV), carbonyl (287 eV), carboxylic (288.8 eV) and unsaturated bond transitions (291.1 eV, also known as shake-up peaks) (Foster, 1993).

5.4 VOC Adsorption on Chemically Modified ACC

Adsorption capacities were examined for acetaldehyde, acetone, and benzene with untreated and chemically modified ACC-20. Results are presented in the following sections. Experimental procedures used to determine the adsorption capacities for the chemically modified ACC are described in Chapter 4. In all

Table 5.2. XPS Deconvolution of the Carbon 1s Peak Area for Chemically Modified ACC-20 (Dimotakis, Cal, et al., 1994a).

Binding Energy [eV]	Percentage of Total Area of Carbon Peak					
	3.9% O (untreated)	21% O	32% O	12.3% Cl	16% Cl	4.1% N
285 (C-C, C-H)	50.94	55.9	46.86	57.28	42.08	48.43
286 (phenol, hydroxyl, C-OH)	27.87	14.92	24.68	21.00	31.12	24.20
287 (carbonyl, C=O)	9.29	13.03	7.64	8.12	8.23	8.14
289 (carboxylic, C=OOH)	5.58	9.99	14.59	7.16	8.56	7.90
291 (shake-up band, $\Pi \rightarrow \Pi^*$)	6.32	6.15	6.23	6.43	10.00	11.35

cases the VOC adsorbates were completely desorbed from the ACC by heating to about 120°C for 30 min, permitting complete recovery of the adsorption capacity.

5.4.1 Acetaldehyde Adsorption

Acetaldehyde typically has a low adsorption capacity on activated carbons, including ACC. Therefore, any chemical treatment that could substantially enhance the adsorption of acetaldehyde (and similar compounds, such as formaldehyde) could be potentially useful. Comparison of the adsorption capacities (at 25°C and 1 atm total pressure) for a series of chemically modified ACC-20 samples that were untreated, oxidized, nitrified and chlorinated as described by Table 5.1 are presented in Figure 5.2.

The largest gas-phase acetaldehyde concentration in air examined was 500 ppmv, while 1000 ppmv was the highest concentration of acetone and benzene studied. It was observed that acetaldehyde undergoes conversion to acetic acid at higher concentrations, making the adsorption capacity measurements invalid (Venugopal et al., 1967; Matheson Gas, 1993). The highly oxidized sample, ACC20-(32% O), exhibits a much higher adsorption capacity for acetaldehyde in the 50 to 500 ppmv concentration range when compared to untreated ACC-20. At 50 ppmv ACC20-(32% O) adsorbs 400% more acetaldehyde than untreated ACC-20 and at 500 ppmv it adsorbs 130% more acetaldehyde. The less oxidized sample, ACC20-(21% O), also shows enhanced acetaldehyde adsorption similar to that of ACC20-(32% O).

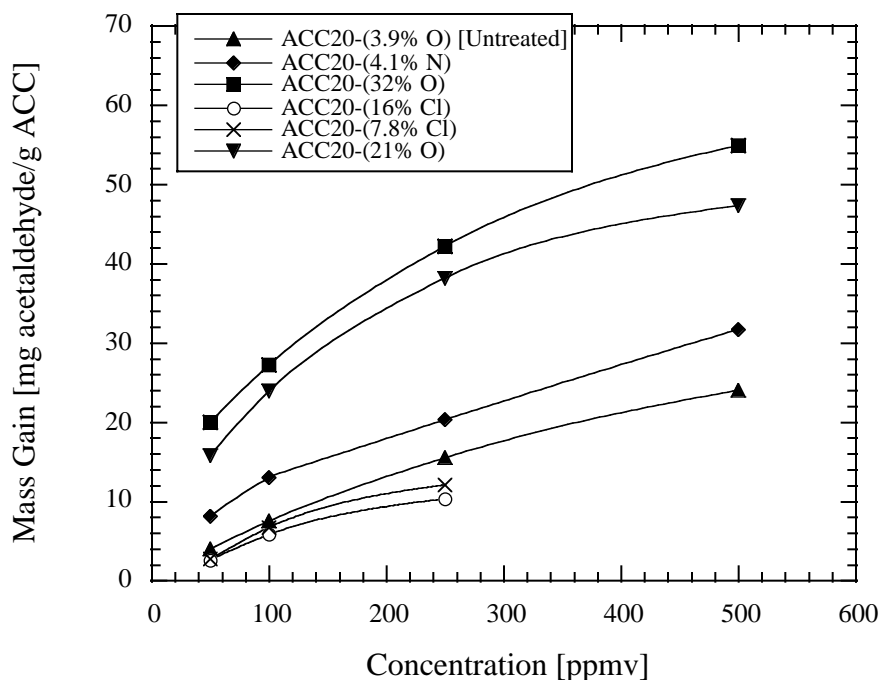


Figure 5.2. Adsorption of Acetaldehyde on Chemically Modified ACC.

The increase in acetaldehyde adsorption capacity on oxidized ACC is theorized to be due to an increase in dipole interactions and hydrogen bonding that occurs between the acetaldehyde molecules and the additional carboxylic groups present on the oxidized ACC-20 (Table 5.1). This effect appears to most pronounced at lower adsorbate concentrations, and diminishes at higher adsorbate concentrations, when the larger adsorbent pores begin to fill. It has been reported in the literature that surface oxygen groups can affect adsorption (Zawadski, 1981; Boehm, 1966; Szymanski and Rychlicki, 1991).

Nitridated ACC20-(4% N) shows improved acetaldehyde adsorption capacity over untreated ACC-20 of 51% at 50 ppmv and 9% at 500 ppmv. This increase in adsorption capacity may be due to interaction with the basic surface or may be due to the change in pore structure of the ACC. Finally, in the case of the chlorinated ACC20-(7.8% Cl) a slight decrease in the adsorption capacity is observed compared to the untreated ACC. The decrease in adsorption capacity appears to be related to the ACC surface chemistry instead of physical properties because the pore volume is similar to that of ACC20-(21% O) (Table 5.1).

5.4.2 Acetone Adsorption

The adsorption isotherms for acetone adsorption (at 25°C and 1 atm total pressure) on untreated and chemically modified ACC-20 are shown in Figure 5.3. Over the concentration range examined (25-1000 ppmv acetone in air), the highly oxidized sample, ACC20-(32% O), exhibited the highest adsorption capacity for acetone. At 1000 ppmv, the adsorption capacity for acetone on ACC20-(32% O) is 53% larger

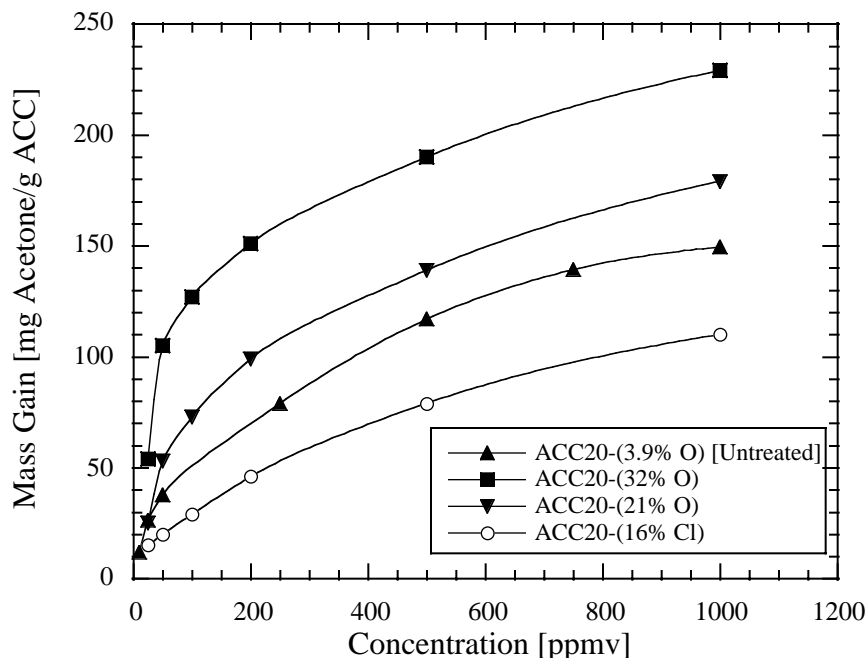


Figure 5.3. Adsorption of Acetone on Chemically Modified ACC.

than the adsorption capacity for untreated ACC [ACC20-(3.9% O)]. At 25 ppmv, the difference in adsorption capacities is even more dramatic, 54 mg/g for ACC20-(32% O) versus 26 mg/g for ACC20-(3.9% O), or a 108% improvement in adsorption capacity. As with acetaldehyde adsorption, since the total pore volume of ACC20-(32% O) is actually less than the pore volume of ACC20-(3.9% O) ($0.47 \text{ cm}^3/\text{g}$ versus $0.74 \text{ cm}^3/\text{g}$, respectively), the increased adsorption capacity for acetone is theorized to be due to an increase in dipole interactions and hydrogen bonding that occurs between the acetone molecules and the additional carboxylic groups present on the oxidized ACC-20.

The chlorinated ACC20-(16% Cl) sample shows a decrease in acetone adsorption throughout the concentration range examined (Figure 5.3). Chlorination of the fiber results in a decrease in surface area compared to the original ACC20-(3.9%) ($1374 \text{ m}^2/\text{g}$ vs. $1550 \text{ m}^2/\text{g}$), and does not appear to be effective in promoting the adsorption of acetone, as does oxidation. This comparison is even more pronounced with ACC20-(21% O) which has very similar surface area ($1409 \text{ m}^2/\text{g}$) to ACC20-(16% Cl) or ACC20-(32% O) with a surface area of only $1105 \text{ m}^2/\text{g}$.

5.4.3 Benzene Adsorption

Adsorption isotherms for benzene and the series of chemically modified ACC are presented in Figure 5.4. Since benzene is nonpolar and essentially immiscible in H_2O , a hydrophilic surface should result in decreased adsorption (Puri et al., 1973). Oxidation of the ACC resulted in a 34% decrease in adsorption

capacity for 1000 ppmv benzene in air, which is the same as the observed decrease in surface area (Figure 5.4 and Table 5.1). Therefore, oxidation had little or no effect on benzene adsorption, but rather the

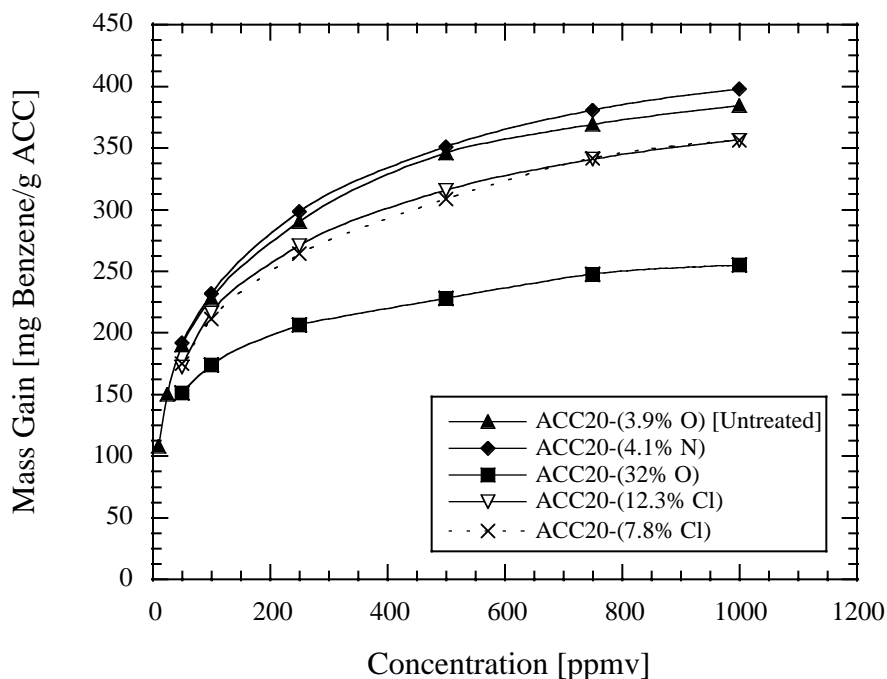


Figure 5.4. Adsorption of Benzene on Chemically Modified ACC.

difference in adsorption capacity is due to changes in surface area and/or pore volume between ACC20-(3.9% O) and ACC20-(32% O). The nitrided (basic) surface shows a slight increase in benzene adsorption capacity, while the chlorinated ACC20-(7.8% Cl) showed a slight decrease in adsorption capacity as compared to ACC20-(3.9% O). This decrease in adsorption capacity may be attributable to the decrease in micropore volume observed on the chlorinated ACC samples or may also be attributed to experimental error in the measurements (Table 5.1).

5.4.4 Dubinin-Radushkevich (DR) Parameters for VOC Adsorption

DR parameters for the chemically modified ACC samples and the VOC adsorbates (acetaldehyde, acetone, and benzene) are presented in Table 5.3. The DR parameters are not available for every adsorbate-adsorbent combination due to the availability of the chemically modified ACC, but every type of chemical treatment was evaluated for every VOC adsorbate.

The differences in W_0 values presented in Table 5.3 and Table 5.1 may be attributed to the different methods and different adsorbates used to obtain the micropore volumes. In Table 5.3, the DR equation was used to obtain the micropore volume and in Table 5.1 the t-plot method was used. Additionally, the DR

micropore volume was determined using the concentration range of 10-1000 ppmv. The 1000 ppmv upper value is lower than Dubinin suggests for determining the micropore volume (see Chapters 2 and 4).

Table 5.3 also presents the adsorption energy (E_o) and the slit-pore half-width (x_o) using the DR equation. x_o values are presented in their unnormalized and normalized forms. Since the relation for x_o was derived using benzene as the adsorbate, x_o values need to be normalized by multiplying by the affinity coefficient, β . Error may be introduced when determining the normalized x_o value due to uncertainties in β , but the normalized x_o values for the untreated (3.9% O) ACC-20 appear to agree well. The adsorption capacity enhancement observed for acetaldehyde adsorption on oxidized ACC-20 is demonstrated in Table 5.3 as an increase in adsorption energy (E_o) and a decrease in pore-size half-width (x_o).

Table 5.3. DR Parameters for VOC Adsorption on Chemically Modified ACC-20.

	3.9% O (untreated)	21% O	32% O	7.8% Cl	12.3% Cl	16% Cl	4.1% N
Acetaldehyde							
W_o [mg/g]	362	259	253	487	-- [†]	307	223
W_o [cm ³ /g]	0.462	0.331	0.323	0.622	--	0.392	0.285
E_o [kJ/mol]	11.9	15.2	15.8	11.1	--	11.6	13.9
x_o [nm]	1.01	0.79	0.76	1.08	--	1.03	0.86
$x_o\beta$ [nm]	0.65	0.51	0.49	0.70	--	0.67	0.56
Acetone							
W_o [mg/g]	453	567	520	--	--	345	--
W_o [cm ³ /g]	0.573	0.718	0.658	--	--	0.437	--
E_o [kJ/mol]	13.6	13.6	16.2	--	--	12.9	--
x_o [nm]	0.88	0.88	0.74	--	--	0.93	--
$x_o\beta$ [nm]	0.69	0.69	0.58	--	--	0.72	--
Benzene							
W_o [mg/g]	615	--	352	553	562	--	633
W_o [cm ³ /g]	0.701	--	0.401	0.631	0.641	--	0.722
E_o [kJ/mol]	17.8	--	21.1	18.0	17.9	--	17.7
x_o [nm]	0.68	--	0.57	0.67	0.67	--	0.68
$x_o\beta$ [nm]	0.68	--	0.57	0.67	0.67	--	0.67

[†]. data not available.

5.5 Water Vapor Adsorption on Chemically Modified ACC

Adsorption of $\text{H}_2\text{O}_{(\text{g})}$ on chemically modified ACC-20 was examined in addition to the adsorption of VOCs. Since $\text{H}_2\text{O}_{(\text{g})}$ is ubiquitous in ambient environments, it would be useful to chemically modify an ACC to inhibit $\text{H}_2\text{O}_{(\text{g})}$ adsorption while promoting VOC adsorption. As with the examination of VOC adsorption on chemically modified ACC, three chemical treatments were examined: oxidized, nitrated and chlorinated.

As with water vapor adsorption isotherms previously presented for untreated ACC-15, ACC-20, and ACC-25, hysteresis exists between the adsorption and desorption curves for the chemically modified ACC-20. The different chemical treatments altered the extent of the hysteresis, and in the case of the oxidized ACC-20, altered the shape of the adsorption isotherm.

The adsorption-desorption isotherms for water vapor with microporous and non-porous carbons have been studied by several researchers (Barton and Koresh, 1982; Barton and Evans, 1991; Carrott, 1992; Dubinin, 1980; and Hall and Williams, 1986). It is believed that two factors influence water vapor adsorption: (1) the number of oxygen containing sites (surface oxides) present on the carbon, and (2) the pore size distribution of the carbon. The presence of oxygen containing sites are believed to promote water vapor adsorption, but they may also limit water vapor adsorption by changing the pore size distribution and the total pore volume of the carbon.

Water vapor adsorption on active carbon is believed to occur in two steps: (1) adsorption on oxygen containing (hydrophilic) sites where hydrogen-bonding can enhance adsorption, and (2) pore filling due to capillary condensation (Dubinin, 1980). Capillary condensation typically occurs at higher P/P_0 values ($P/P_0 > 0.5$), and results in a sharp increase adsorption of water vapor, as evidenced on water vapor adsorption isotherms. Additionally, water vapor molecules adsorbed on surface oxide sites can act as secondary adsorption centers for further adsorption (Barton et al., 1973). Water vapor adsorption of active carbon is classified as Brunauer type V (Gregg and Sing, 1982).

Theories to describe hysteresis in microporous adsorbents have been reviewed by Everett (1967). The most widely accepted theory is the “ink bottle” theory. During the desorption process it is assumed that small pores constrict the openings to larger pores such that adsorbed water in those larger pores is not released until the relative pressure corresponds to that of the smaller pore radius. At present there is no model which describes both the adsorption and desorption of water vapor on active carbons.

5.5.1 Water Vapor Adsorption on Oxidized and Nitrated ACC

The adsorption of water vapor on ACC20-(32% O) differs significantly from the usually observed type V isotherm, and more closely resembles a type II isotherm (Figure 5.5). ACC20-(32% O) is expected to have many more oxygenated or hydrophilic sites than any of the other ACC due to its high oxygen content. The

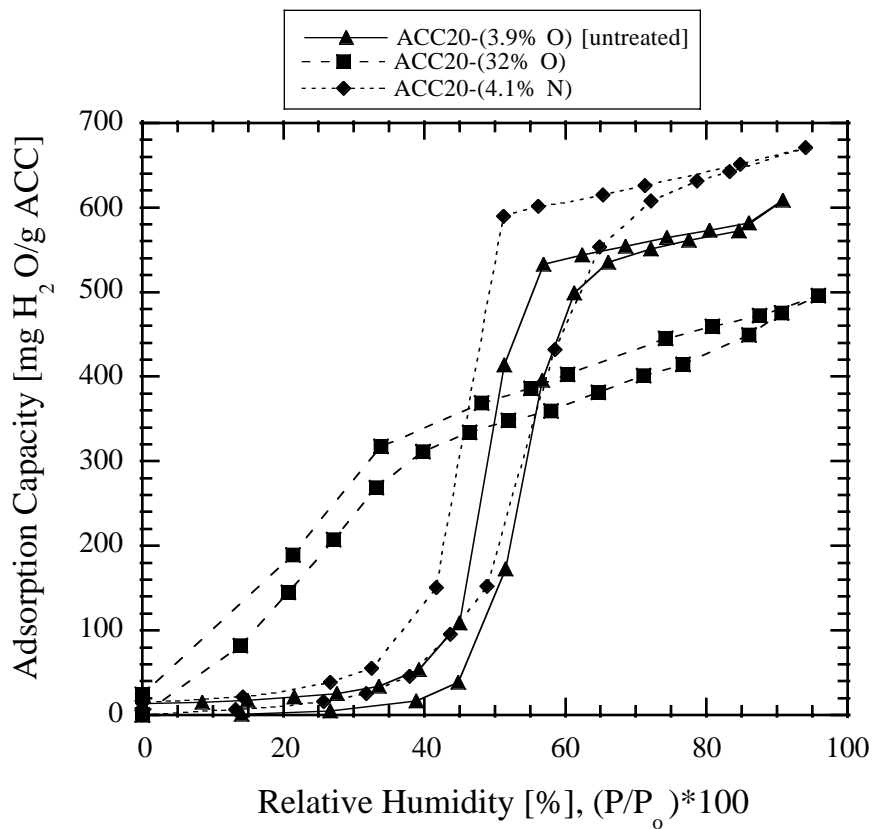


Figure 5.5. Adsorption and Desorption of Water Vapor on Oxidized and Nitrated ACC-20.

XPS data in Table 5.2 shows a higher number of carboxylic bonds than the untreated ACC-20, confirming that some of the hydroxyl and carbonyl bonds were oxidized to carboxylic bonds. The XPS data also shows that more carbon-oxygen (hydrophilic) bonds were formed during oxidation compared to untreated ACC-20. The increase in carboxylic groups may be responsible for the enhanced water vapor adsorption at low relative humidities. From Table 5.2 and the adsorption isotherm data, it appears that carboxylic groups have the most influence on water vapor adsorption at low RH. The difference between the adsorption and desorption curves (hysteresis) is not as pronounced here, as it is for the untreated ACC. This may be due to the increase in hydrogen-bonding between water and the oxidized carbon, allowing removal of water molecules in a more continuous manner.

5.5.2 Water Vapor Adsorption on Nitrated ACC

Adsorption-desorption isotherms for nitrated ACC20-(4.1% N) are presented in Figure 5.5. ACC20-(4.1% N) exhibits an increase in water vapor adsorption capacity (200 to 600%, depending upon the RH) in the lower RH range (RH < 50%). This may be due to the increase in carboxylic sites compared to untreated

ACC20-(3.9% O), as represented in the XPS data in Table 5.2. It has also been suggested that nitrogen can also constitute polar sites for $H_2O_{(g)}$ adsorption (Bradley and Rand, 1993; Tomlinson, et al., 1993), thereby increasing $H_2O_{(g)}$ adsorption at low RH. ACC20-(4.1% N) exhibits about a 10% higher water vapor adsorption capacity than ACC20-(3.9% O) at high RHs. This is due to the increased total pore volume of ACC20-(4.1% N) observed in Table 5.1. The widening in the adsorption hysteresis curve in for ACC20-(4.1% N) in Figure 5.5 is most likely due to a change in pore size distribution.

5.5.3 Adsorption of Water Vapor on Chlorinated ACC

Adsorption isotherms for water vapor and ACC are presented in Figure 5.6. Table 5.1 shows a decrease

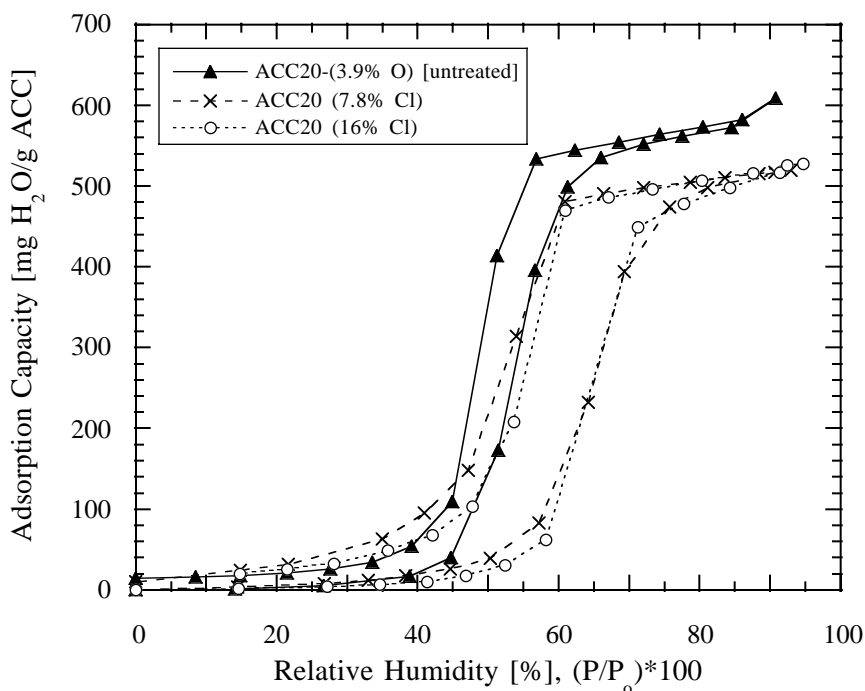


Figure 5.6. Adsorption and Desorption of Water Vapor on Chlorinated ACC-20.

in BET surface area, a decrease in carbon content (in wt%), and a slight increase in oxygen content with increasing chlorination. The decrease in surface area may be due to chlorine atoms limiting or closing off access to the smaller micropores present on the ACC. Water vapor adsorption was decreased at RHs < 60% and where capillary condensation occurred (the step rise in the adsorption curve) was shifted to higher RHs for the chlorinated ACCs. The amount of water vapor adsorbed at saturation was decreased due to a decrease in pore volume (Table 5.1). While chlorination increases the amount of polar sites present on the ACC due to the addition of chlorine atoms, these sites do not appear to be favorable for water adsorption, as are carboxylic sites. Chlorination appears to increase the hydrophobicity of ACC.

5.6 Summary

ACC-20 was chemically modified, producing oxidized, chlorinated, and nitrated samples. Adsorption capacities for VOCs in the 10 to 1000 ppmv concentration and water vapor from 0 to 95% RH were measured. Oxidized ACC-20 showed an enhanced physical adsorption for acetaldehyde, acetone, and water vapor, probably due to increased dipole-dipole interactions and hydrogen bonding. Oxidation of ACC-20 changed the shape of the water vapor adsorption isotherm, so that it no longer resembles a Brunauer type V. Benzene showed a decreased adsorption capacity (about 20 to 30% less, depending upon concentration) on oxidized ACC-20, which may be due to an increase in hydrophilicity of ACC-20, or a change in pore size distribution.

Chlorination had little effect on VOC adsorption capacity, except in the case of acetone, where a decrease in adsorption capacity occurred (20 to 40% decrease, depending upon concentration). This may be due to pore blocking by chlorine molecules, or a decrease in hydrogen bonding between the ACC functional groups and acetone. Nitridation of ACC showed little effect on organic adsorption capacity, but increased the saturation adsorption capacity for water vapor by 10% on ACC-20 and increased the breadth of its hysteresis loop. These changes were the result of changes in the pore size distribution of ACC-20. DR parameters were determined for VOC adsorption on ACC-20.

5.7 References

- Barton, Stuart S., Evans, Michael, J.B., and Harrison, Brian H., "Surface Studies on Carbon: Water Adsorption on Polyvinylidene Chloride Carbon," *J. Colloid and Interface Science*, **45**(3): 542-548, 1973.
- Barton, Stuart S., and Koresh, Jacob E., "Adsorption Interaction of Water with Microporous Adsorbents, Part I. Water Vapor Adsorption on Activated Carbon Cloth," *Chem. Soc. Faraday Trans. I*, **79**: 1147-1155, 1983.
- Barton, Stuart S. and Evans, Michael, J.B., "The Adsorption of Water Vapor by Porous Carbon," *Carbon*, **29**(8): 1099-1105, 1991.
- Boehm, H.P., *Adv. Catal.*, **16**:179, 1966.
- Bradley, R.H., and Rand, B., "The Adsorption of Vapours by Activated and Heat-Treated Microporous Carbons. Part 2. Assessment of Surface Polarity Using Water Adsorption," *Carbon*, **31**(2): 269-272, 1993.
- Briggs, D., and Seah, M.P., *Practical Surface Area Analysis by Auger and X-ray Photoelectron Spectroscopy*, John Wiley and Sons, New York, 1983.
- Carrott, P.J.M., "Adsorption of Water Vapor by Non-Porous Carbons," *Carbon*, **30**(2): 201-205, 1992.
- Dimotakis, E.D., Department of Material Science, University of Illinois at Urbana-Champaign, personal communication, 1994.

Chapter 5: Adsorption on Chemically Modified ACC

- Dimotakis, E.D., Cal, M.P., Economy, J., Rood, M.J., Larson, S.M., "Chemically Treated Activated Carbon Cloths (ACCs) for Removal of VOCs from Gas Streams: Evidence for Enhanced Physical Adsorption," submitted for publication to *Environmental Science and Technology*, 1994a.
- Dimotakis, E.D., Cal, M.P., Economy, J., Rood, M.J., Larson, S.M., "Water Vapor Adsorption on Chemically Treated Activated Carbon Cloths," submitted for publication, 1994b.
- Dubinin, M.M., "Water Vapor Adsorption and the Microporous Structures of Carbonaceous Adsorbents," *Carbon*, **18**: 355-364, 1980.
- Everett, D.H., "Adsorption Hysteresis," in *The Solid Gas Interface*, ed. by E. Alison Flood, Marcel Dekker, New York, p. 1015, 1967.
- Foster, K.L., "The Role of Micropore Size and Chemical Nature of the Pore Surface on the Adsorption Properties of Activated Carbon Fibers," Ph.D. Thesis, University of Illinois at Urbana-Champaign, Department of Material Science and Engineering, 1993.
- Gregg, J. and Sing, K.S.W., *Adsorption, Surface Area and Porosity*, 2nd ed., Academic Press, London, 1982.
- Hall, P.G., and Williams, R.T., "Sorption of Nitrogen, Water Vapor, and Benzene by Charcoal Cloth," *J. Colloid and Interface Science*, **113**(2): 301-307, 1986.
- Larson, Susan M., Rood, Mark J., Cal, Mark P., Graf, Oliver W., Omar, Ali, Foster, Kenneth L., and Economy, James, "Adsorption of Indoor Organic Gases onto Activated Carbon Fibers," Second Year Progress to the Center for Indoor Air Research, 1993.
- Matheson Gas, personal communication, 1993.
- Puri, B.R., Bansal, R.C., *Carbon*, **5**:189, 1967.
- Puri, B.R., Kaistha, B.C., Vardan, Y., and Mahajan, O.P., *Carbon*, **11**: 329-336, 1973.
- Syzmanski, G. and Rychlicki, G., "Importance of Oxygen Surface Groups in Catalytic Dehydration and Dehydrogenation of Butan-2-ol Promoted by Carbon Catalysts," *Carbon*, **29**(4/5): 489-498, 1991.
- Tomlinson, J.B., Freeman, J.J., and Theocharis, C.R., "The Preparation and Adsorptive Properties of Ammonia-Activated Viscose Rayon Chars," *Carbon*, **31**(1): 13-20, 1993.
- Venugopal, B., Kumar, R., and Kuloor, N.R., "Oxidation of Acetaldehyde to Acetic Acid in a Sparger Reactor," *I&EC Process Design and Development*, 6(1): 139-146, 1967.
- Zawadski, J., "IR Spectroscopy Investigations of Acidic Character of Carbonaceous Films Oxidized with HNO₃ Solution," *Carbon*, **19**:19-25, 1981.

Chapter 6

Multicomponent Adsorption Measurements and Modeling

6.1 Introduction

Since indoor air environments are multicomponent systems consisting of many VOCs and water vapor, this section examines the effects of that humid air has on the adsorption capacity of soluble (acetone) and insoluble (benzene) VOCs. The effects of humid air on VOC adsorption are modeled with the Manes model. Adsorption capacities of acetone and benzene in a multicomponent system are measured and modeled using ideal adsorbed solution theory (IAST).

6.2 Experimental Methods

Two multicomponent adsorption systems were examined, and each system used a similar experimental procedure. Both systems consisted of a custom gas generation system (see Section 4.2.1), a Cahn gravimetric balance to measure the total mass adsorbed (see Sections 4.2.1 and 4.2.2), multi-ported hang-down tube on the gravimetric balance for gas sampling, and a gas chromatograph/mass spectrophotometer (GC/MS) (Hewlett-Packard GC Model 5890 Series II, MSD Model 5971) (Figure 6.1).

For the measurement of adsorption capacities of VOCs in humid air streams, a Gortex membrane-based humidifier was placed in the gas generation system. The humidifier consisted of a stainless steel tube with a Gortex membrane annulus. Water flowed over the outside of the membrane and the gas stream flowed on the inside of the membrane. The humidity of the gas stream was determined by the gas flow rate and the temperature of the water flowing over the membrane. A peristaltic pump was used to control the water flow rate at about 50 cm³/min. Water temperature over the membrane was varied from 4°C to 35°C to achieve relative humidities (RHs) from 35% to 90%. RH was measured with a dew point hygrometer (General Eastern). Due to the relatively large mass of the stainless steel humidifier, water at the desired temperature was passed through the humidifier for approximately one hour before the start of an experiment to establish a steady state temperature within the humidifier. One hour was sufficient to produce steady, reproducible RH values. Gas flow rate through the humidifier was 150 or 250 cm³/min, depending upon the experiment.

Acetone is soluble in water, and therefore some acetone is scrubbed out the gas stream as it passes through the humidifier. At a total gas flow rate of 150 cm³/min and an inlet acetone concentration to the

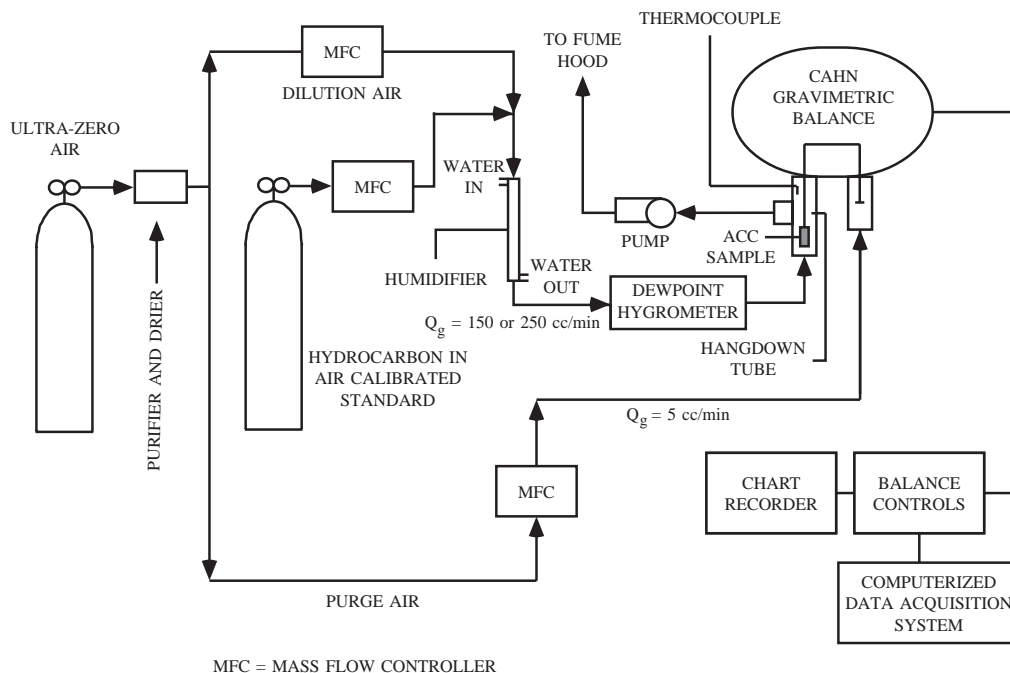


Figure 6.1. Experimental Apparatus for Measurement of VOC Adsorption in Humid Air Streams.

humidifier of 1000 ppmv, the concentration of acetone exiting the humidifier was 350 ppmv. Likewise at 250 cm^3/min and 1000 ppmv of acetone entering the humidifier, 500 ppmv exited the humidifier. Benzene is insoluble in water, so the concentration entering and exiting the humidifier was the same.

Concentration of the VOC for the humidified-air/VOC experiments was measured both upstream and downstream of an ACC sample that was placed on the gravimetric balance. The hang-down tube on the gravimetric balance has nine ports along its side with tube fittings and GC septa (9.5 mm teflon coated) (Figure 6.2). A gas-tight syringe (250 μL) was used to measure the gas-phase organic concentrations. The upstream concentration was measured 15 cm below the ACC sample in the gravimetric balance, and the downstream concentration was measured 20 cm above the ACC sample. Sampling too close downstream of the ACC sample results in an artificially low gas-phase organic concentration, due to VOC concentration gradients immediately downstream of the ACC sample. Three samples were taken and discarded, to clean the syringe, before the fourth sample was taken and injected into the GC/MS.

The GC/MS was calibrated and tuned before the start of each experiment. A three point calibration was used for each organic compound. The calibration points were 1000, 500, and 0 ppmv. Ten samples were taken with 500 and 1000 ppmv calibrated gas samples and related to the peak area output of the GC/MS. The

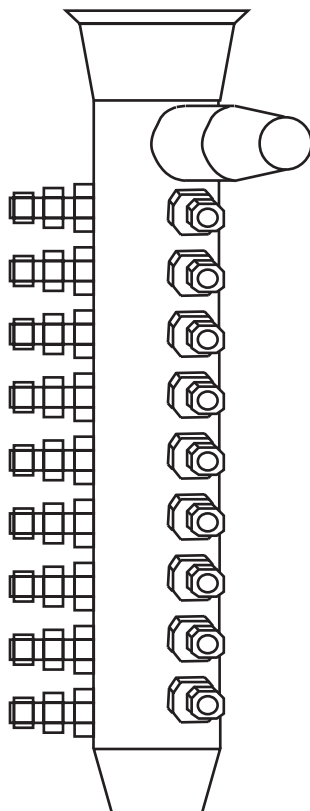


Figure 6.2. Multi-ported Gravimetric Balance Hang-down Tube.

standard deviation of the samples was within 3% of the mean. Linear regression was used to relate GC/MS peak area output to gas-phase organic concentration.

During an experiment, the downstream gas-phase concentration was measured as often as the sampling procedure would allow. This meant that samples were generally taken every 2 to 3 min. The retention time for acetone on the GC column (HP-1 cross-linked methyl silicone gum) was 0.7 min at 37°C and the retention time for benzene was 1.29 min at 37°C. The total mass gain of the ACC sample was recorded using an IBM PC computer and *Labtech Notebook* (see Section 4.2.2).

The same basic procedure was followed for multicomponent organic adsorption from dry gas streams, except that the humidifier was not used. Instead the desired concentrations of the organic species were obtained by adjusting the flow rates of each species while keeping the total gas flow rate constant at 250 cm³/min.

The humid-air/VOC systems examined were 350 ppmv acetone, 500 ppmv acetone, 500 ppmv benzene, and 1000 ppmv benzene at about 40, 60, and 90% RH using ACC-20. An acetone-benzene-ACC-20 system was examined at total organic concentration of 1000 ppmv (0.76 mm Hg) and 0.25, 0.5, and 0.75 mole/volume fractions in dry air. The same ACC-20 sample with a mass of 0.036 g was used for all of the

multicomponent adsorption experiments and was regenerated before each experiment. There was no detectable change in the mass of the ACC sample after each thermal regeneration.

6.3 Multicomponent Data Analysis

The amount of VOC adsorbed was determined with the total adsorption capacity data (gravimetric data) and the influent and effluent gas-phase VOC concentrations. The amount of water vapor adsorbed was determined by material balance. VOC adsorption capacity is determined by integrating the influent and effluent VOC concentrations [mg/cm^3] over the experimental run time and then taking their difference and multiplying by the total gas flow rate [cm^3/min] and dividing by the ACC sample mass [g] (equation 6.1).

$$\text{VOC adsorption capacity} = \frac{\left(\left[\int_{t_1}^{t_2} (\text{influent}) dt \right] - \left[\int_{t_1}^{t_2} (\text{effluent}) dt \right] \right) (\text{total gas flow rate})}{\text{ACC sample mass}} \quad (6.1)$$

Several test runs were performed using only acetone or benzene in dry air to test the above method of determining adsorption capacity. Figure 6.3 shows the adsorption capacity of benzene on ACC-20 as a function of time. Temporal dependent influent and effluent concentrations for the same experiment as a

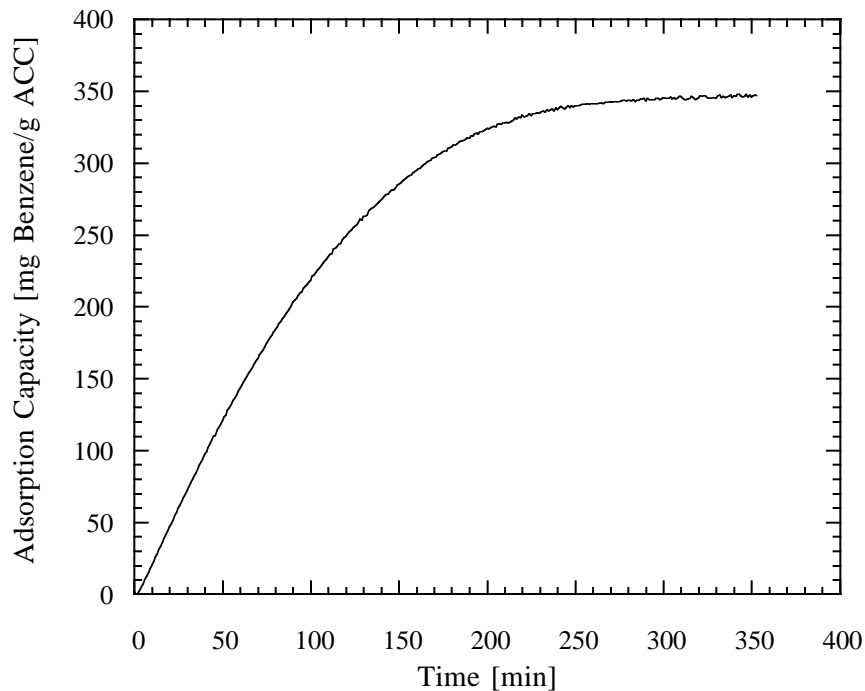


Figure 6.3. Adsorption of 500 ppmv Benzene onto ACC-20 as a Function of Time.

function of time are presented in Figure 6.4. The influent concentration was determined during calibration of the GC/MS and an average value was taken. That is why a straight line appears for the influent concentration in Figure 6.4 and not a series of data points. The measured mean value was 500 ± 15 ppmv.

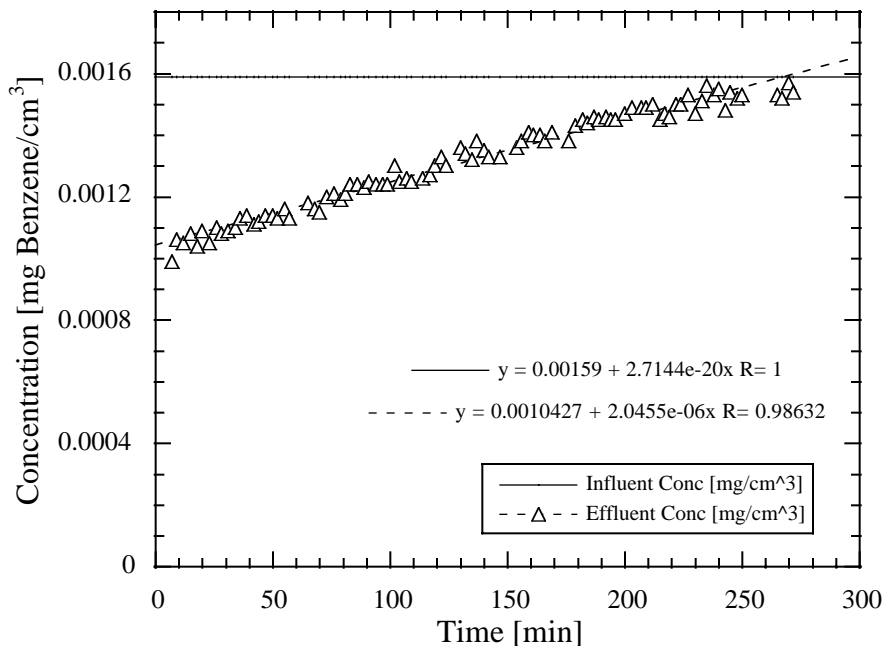


Figure 6.4. Influent and Effluent Benzene Concentrations as a Function of Time.

Integrating from 10 to 260 min, using a gas flow rate of $250 \text{ cm}^3/\text{min}$, and an ACC sample mass of 0.036 g in equation 6.1 yields a benzene adsorption capacity of 389 mg/g. Comparing this to the gravimetric adsorption capacity measurement of 346 mg/g (Figure 6.3) results in 14% difference. For the acetone and benzene test runs, the integration method was within 20% of the gravimetric method. About 3 to 5% of this difference can be attributed to uncertainties in the analytical measurement techniques. The resulting difference may be due to inhomogeneous mixing in the gravimetric balance sampling tube.

6.4 Multicomponent Adsorption Experimental Results

Adsorption of 500 ppmv benzene on ACC-20 at several RHs was examined. Figure 6.5 presents the kinetic results of 500 ppmv benzene and RH values ranging from 0% to 86%. The rapid decreases in adsorption capacity present in Figure 6.5 are the result of passing dry air over the ACC sample with the same benzene concentration (500 ppmv). The water adsorbed on the ACC was very quickly desorbed, giving a good estimate of the amount of water adsorbed on the ACC. Very little benzene was desorbed during the short time period of the water desorption, because benzene is much more strongly adsorbed than water.

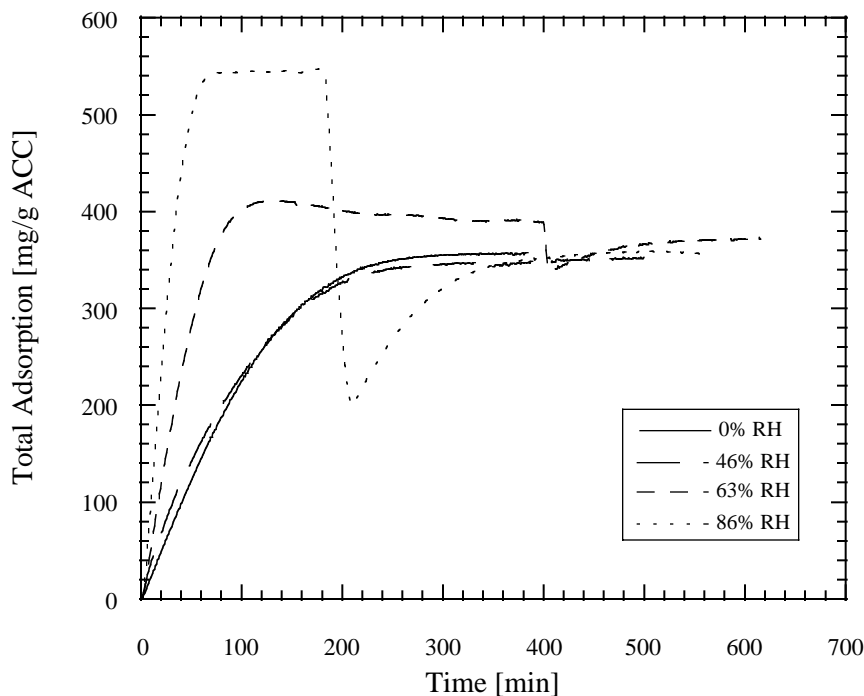


Figure 6.5. Adsorption of 500 ppm Benzene on ACC-20 at Several Relative Humidities.

The total mass adsorbed and the adsorption capacities for benzene and water vapor are presented in Figure 6.6 for 500 ppmv benzene and five RH values and in Figure 6.7 for 1000 ppmv benzene and four RH values. Figure 6.6 shows that the presence of water vapor in the gas stream does not have much of an effect on the adsorption of 500 ppmv benzene until about 65% RH, when a rapid decrease results in benzene adsorption capacity with increasing RH. This RH is also about where capillary condensation of water vapor occurs within the ACC pores (Dubinin, 1980). Water vapor condenses within the ACC pores, making them unavailable for benzene adsorption. As can be seen in Figure 6.7, increasing the benzene concentration can have a significant effect on the amount of water vapor adsorbed. At 86% RH and 500 ppmv, 284 mg water/g ACC is adsorbed, while at 86% RH and 1000 ppmv, only 165 mg/g water is adsorbed. The lower the benzene concentration, the more profound the effect of water vapor is on its adsorption capacity on ACC.

Adsorption of 500 ppmv acetone on ACC-20 at several RHs is presented in Figure 6.8. The rapid decreases in adsorption mass present in Figure 6.8 are the result of passing dry air over the ACC sample at an acetone concentration of 500 ppmv. The water adsorbed on the ACC sample was very quickly desorbed, giving a good estimate of the amount of water adsorbed on the ACC. Very little acetone was desorbed during the short time period of the water desorption, because acetone is much more strongly adsorbed than water.

The total mass adsorbed and the adsorption capacities for acetone and water vapor are presented in Figure 6.9 for 500 ppmv acetone and four RHs. The presence of water vapor in the gas-stream with acetone

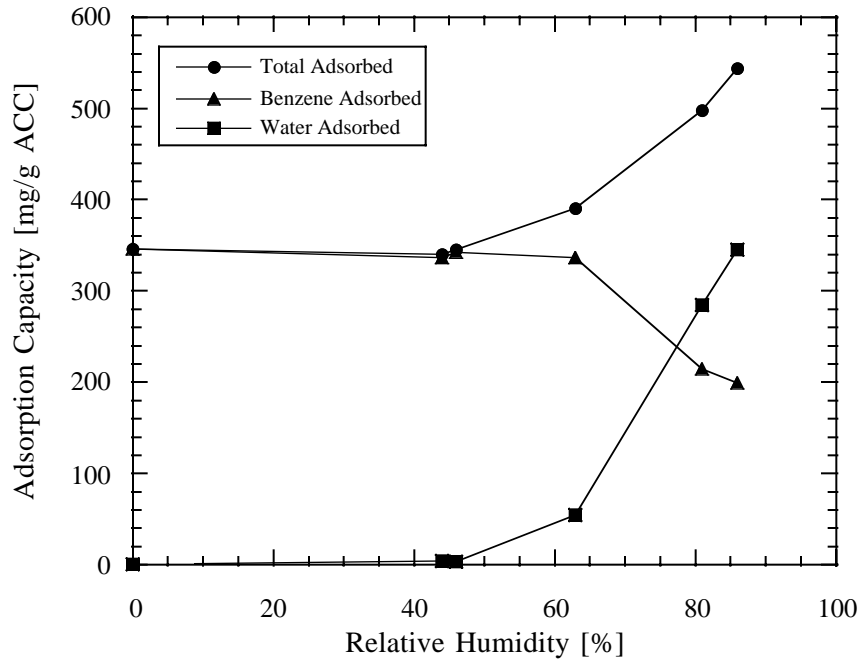


Figure 6.6. Adsorption Capacity Dependence on Relative Humidity of 500 ppmv Benzene on ACC-20.

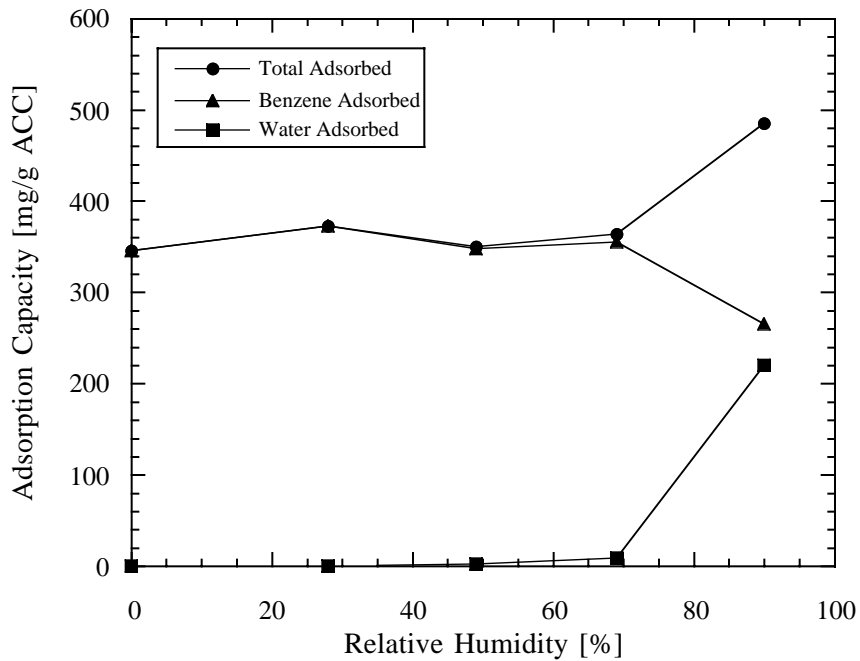


Figure 6.7. Adsorption Capacity Dependence on Relative Humidity of 1000 ppmv Benzene on ACC-20.

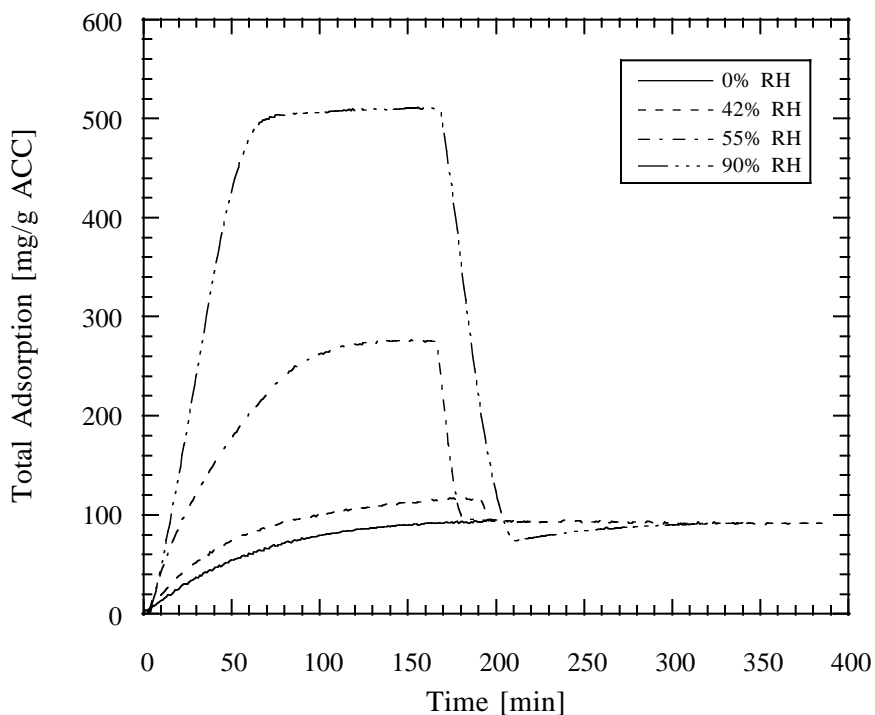


Figure 6.8. Adsorption of 500 ppmv Acetone on ACC-20 at Several Relative Humidities.

had little effect ($< 20\%$ decrease) on the adsorption capacity of acetone even at RHs of 90%. This is most likely because acetone is infinitely soluble in water, whereas benzene is insoluble and hydrophobic.

Examining Figure 6.5 along with Figure 6.6 and Figure 6.8 along with Figure 6.9, one can see that adding water vapor to an VOC-containing gas stream actually increases the rate of VOC adsorption by 3 to 4 times at high RH ($\sim 90\%$).

The adsorption of 1000 total ppmv (0.76 mm Hg) acetone and benzene was examined at 0, 0.25, 0.5, 0.75, and 1.00 mole/volume fractions of acetone and benzene. Due to the limited data set available, the experimental results are presented along with the modeled results in Section 6.6 (Figure 6.14).

6.5 Modeling Adsorption of VOCs from Humid Air Streams

The method of Manes (Section 2.6, equation 2.49) was used to model the adsorption of acetone and benzene at RH values. The method of solution for the Manes model is somewhat tedious, as it requires a graphical approach. It would be possible to solve the solution numerically, if one had an adsorption isotherm equation that would fit the entire water vapor isotherm. One could then set up a system of nonlinear equations to solve for the equal volumetric adsorption capacities of the water vapor and the organic and obtain the corresponding normalized adsorption potentials (A/V).

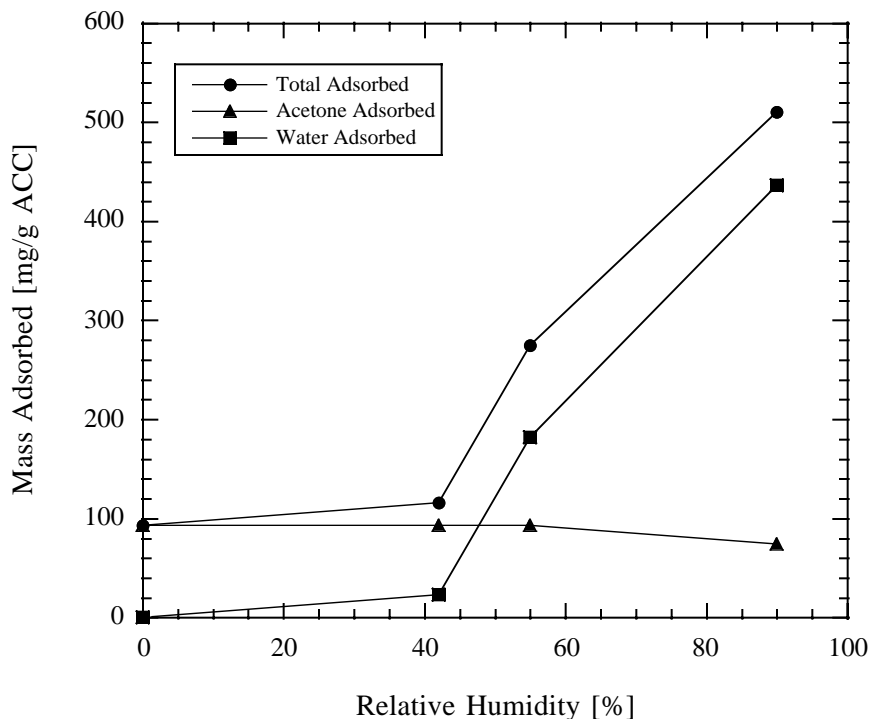


Figure 6.9. Adsorption Capacity dependence on Relative Humidity of 500 ppmv Acetone on ACC-20.

The graphical approach used to solve for the parameters in the Manes model requires plotting A/V versus volume adsorbed for organic and water vapor both on the same plot. This is illustrated with acetone and water vapor in Figure 6.10. An acetone A/V was chosen on the plot (dashed line) and the A/V for water vapor corresponding to the same volume adsorbed was determined using interpolated data from the pure component adsorption isotherm. The A/V 's for the acetone and water vapor corresponding to the same volume adsorbed were used along with equation 2.49 to calculate the diminished adsorption potential. The same procedure was used for benzene and water vapor.

Results from using the Manes model with experimental data for acetone and benzene are presented in Figures 6.11 and 6.12. As expected, the Manes method worked much better modeling the adsorption of benzene in humid air. As discussed in Section 2.6, the Manes method applies only to immiscible organics, such as benzene. All of the experimental acetone data were grouped around the 65% RH modeled curve in Figure 6.12, indicating the Manes model provided a poor prediction for acetone adsorption from humid air. This is as expected, since acetone is infinitely soluble in water.

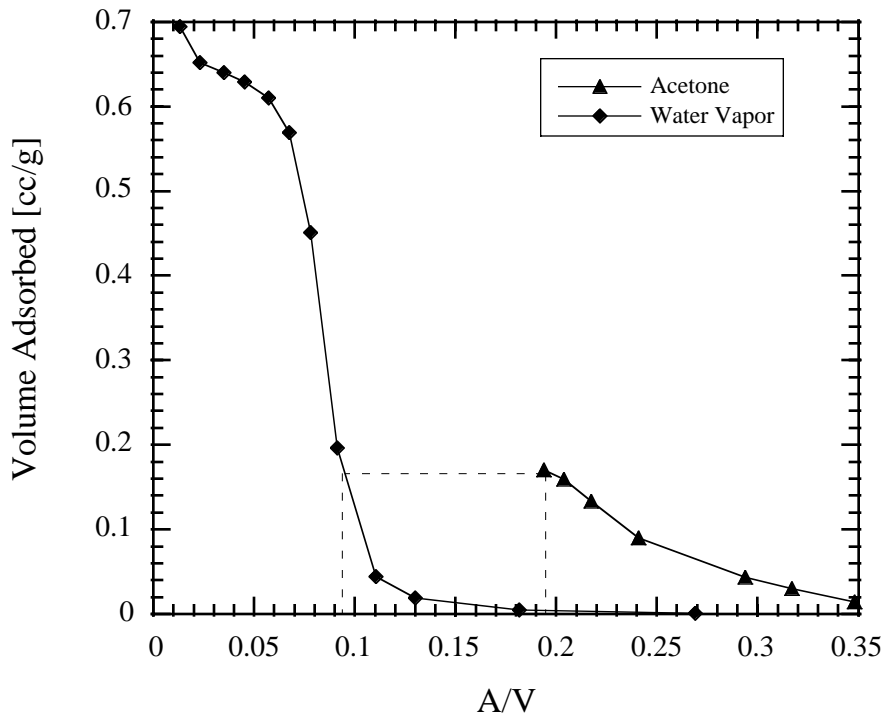


Figure 6.10. Adsorption Potential for Acetone and Water Vapor.

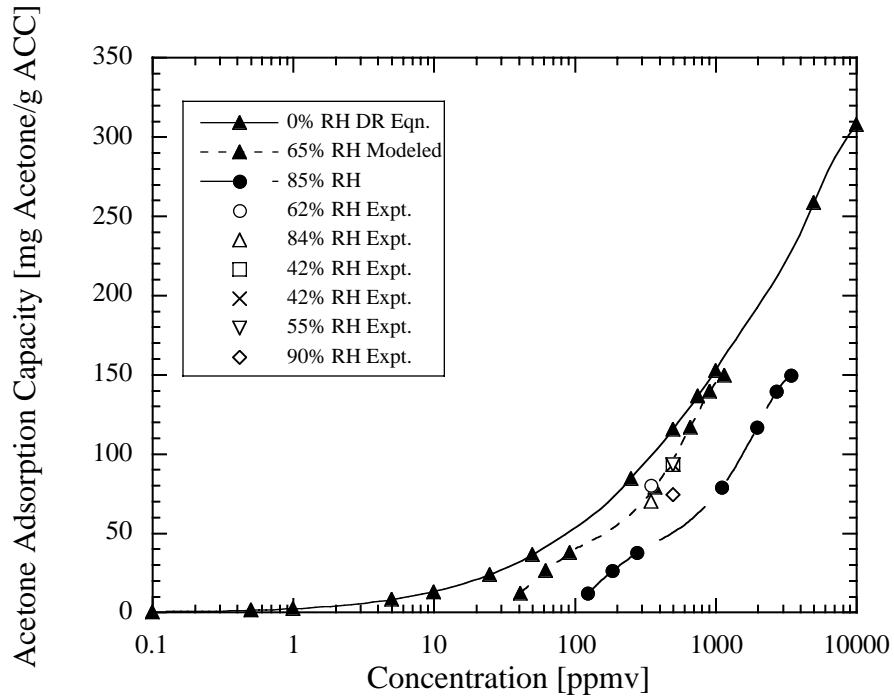


Figure 6.12. Measured and Modeled Results for Acetone Adsorption on ACC-20 at Various Relative Humidities.

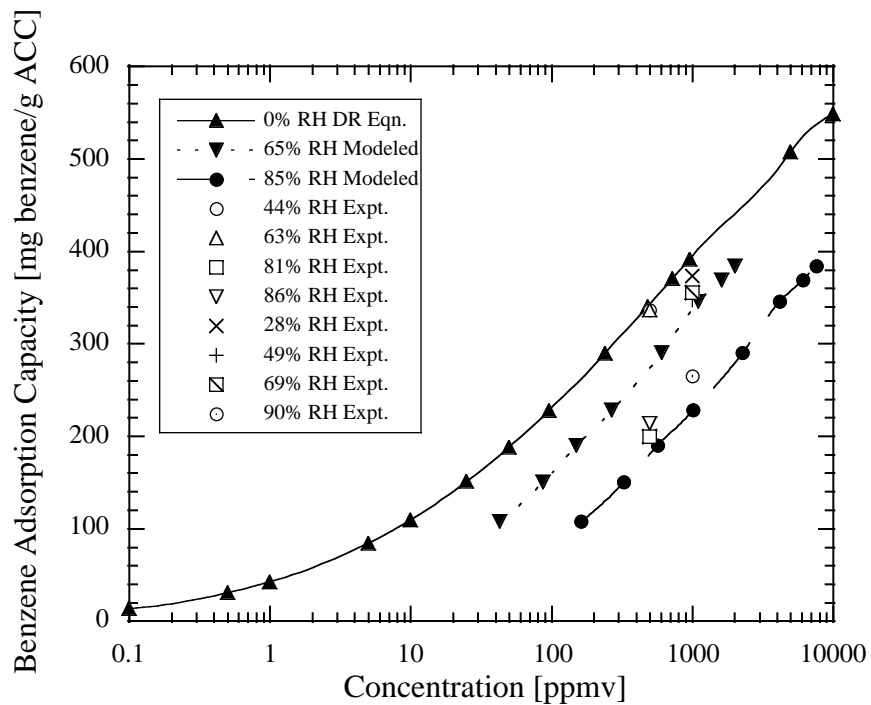


Figure 6.11. Measured and Modeled Results for Benzene Adsorption on ACC-20 at Various Relative Humidities.

6.6 Modeling Multicomponent VOC Adsorption

Ideal adsorbed solution theory (IAST) (Myers and Prausnitz, 1965) was used to model the adsorption of acetone and benzene on ACC-20. Combining equations 2.38, 2.39, 2.41, 2.42, 2.43, and 2.47 of IAST results in a set of seven nonlinear equations and 9 unknown variables (P , x_1 , x_2 , y_1 , y_2 , P_1^o , P_2^o , Ψ_1^o , Ψ_2^o). The number of equations and unknowns can be reduced by specifying P , y_1 , y_2 , and utilizing the relationships $x_2 = 1 - x_1$ and $\Psi_1^o = \Psi_2^o$, resulting in four equations and four unknowns (x_1 , Ψ , P_1^o , P_2^o). The DR parameters used in equation 2.47 are presented in Table 6.1. A program utilizing Newton's method for solving systems

Table 6.1. DR Parameters Used in IAST Modeling.

	Benzene	Acetone
n_m [mmol/g]	7.85	7.80
E_o [kJ/mol]	17.8	13.6
β	1.00	1.00
P_o [mm Hg]	96	229

of nonlinear equations was written in *HiQ*®[†] and was used to perform the IAST calculations.

IAST relies on calculating all adsorbate properties at the same spreading pressure, because at equilibrium all adsorbate components of the mixture have the same spreading pressure. Figure 6.13 illustrates the reduced spreading pressure, Ψ , for acetone and benzene as a function of adsorbate partial pressure. One can see from Figure 6.13 that for acetone and benzene to have the same spreading pressure, the gas-phase adsorbate concentration must be much greater for acetone.

The results of the IAST calculations along with experimental data for acetone-benzene mixtures are presented in Figure 6.14. The experimental data represents a total gas-phase organic concentration of 1000 ppmv (0.76 mm Hg). Experimental gas-phase mole fractions of acetone and benzene examined were: 0, 0.25, 0.50, 0.75, and 1.00. IAST did well predicting the total amount of organic adsorbed, but it over-predicted benzene adsorption and under-predicted acetone adsorption. One should note, that as discussed earlier, the experimental data in Figure 6.14 is probably within 20% of its true value.

Adsorbed-phase activity coefficients were calculated using equation 2.38 and are presented in Table 6.2. For the acetone-benzene mixture at a total pressure of 0.76 mm Hg, benzene exhibited activity coefficients greater than one, while acetone exhibited activity coefficients less than one. The values of the activities coefficients shows that the acetone-benzene mixture is highly non-ideal. For the 0.25 benzene-0.75 acetone gas-phase mole fraction mixture, IAST over estimated the adsorbed-phase mole fraction of benzene by 52%

[†]. *HiQ*®, Version 2.1 for the Power Macintosh, National Instruments, Austin, TX, 1994.

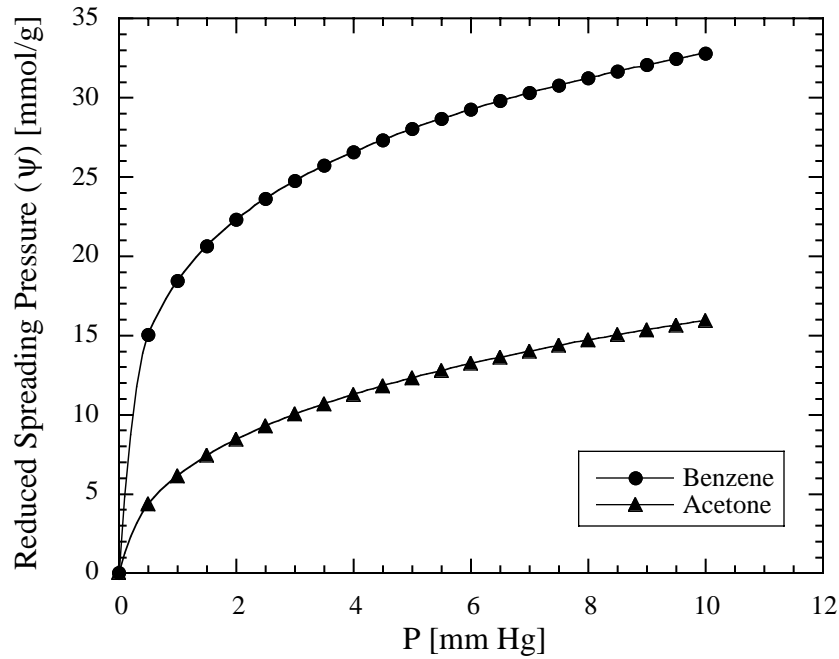


Figure 6.13. Reduced Spreading Pressure for Acetone and Benzene as a Function of Adsorbate Partial Pressure.

Table 6.2. Calculated Activity Coefficients for Acetone-Benzene Mixture at a Total Pressure of 0.76 mm Hg.

Adsorbate	y_{acetone}	y_{benzene}	Calculated x_i	Measured x_i	P_i^o	γ_i	Percent Deviation from Ideality
Benzene	1.0	0.00	0.00	0.00	0.00	--	--
	0.75	0.25	0.866	0.569	0.219	1.52	52
	0.50	0.50	0.946	0.808	0.402	1.17	17
	0.25	0.75	0.980	0.879	0.581	1.12	12
	0.00	1.00	1.00	1.00	0.760	1.00	0
Acetone	0.00	1.00	0.00	0.00	0.00	--	--
	0.25	0.75	0.0197	0.121	9.66	0.163	513
	0.50	0.50	0.0540	0.192	7.07	0.280	257
	0.75	0.25	0.134	0.431	4.26	0.310	222
	1.00	0.00	1.00	1.00	0.76	1.00	0

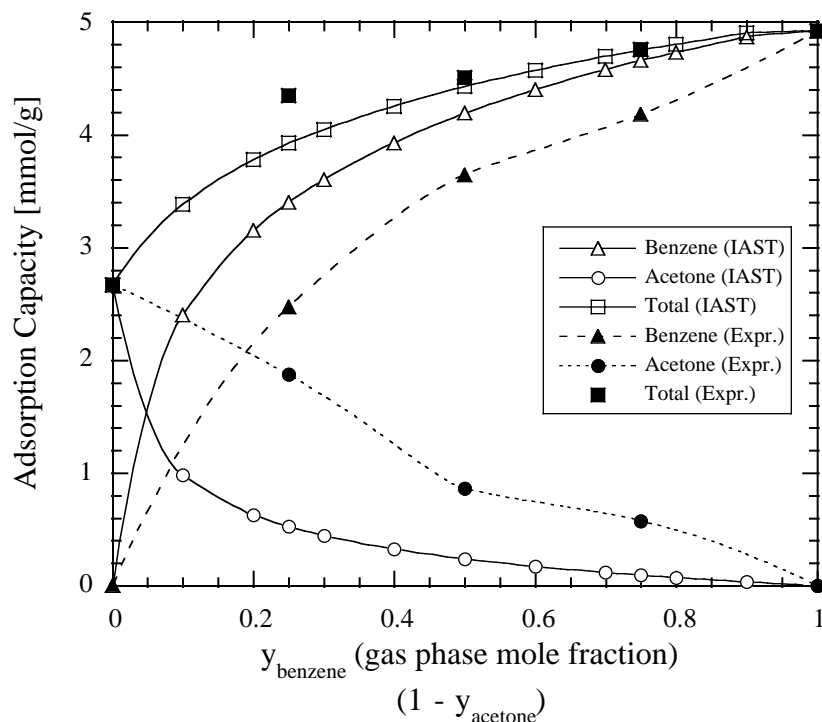


Figure 6.14. Measured and Modeled Adsorption of Acetone and Benzene on ACC-20 at 1000 ppmv (0.76 mm Hg) Total Concentration.

and underestimated the acetone adsorbed-phase mole fraction by 222%, and for a 0.75 benzene-0.25 acetone mixture, IAST overestimated the benzene adsorbed-phase mole-fraction by 12% and underestimated the acetone adsorbed-phase mole fraction by 513% (Table 6.2).

As can be seen in Table 6.2, differences in the IAST predicted values and the experimental data are due to non-idealities of the adsorbed-phase mixture and must be compensated for by introducing activity coefficients into adsorbed solution theory (AST) and using a relationship, such as, the Wilson equation to calculate the activity coefficients of the mixture components (Reid, et al., 1987). Currently, there are no methods for predicting adsorbed-phase activity coefficients without experimental mixture data. To obtain the parameters needed in an activity coefficient relation, an extensive and accurate data set is needed (15 or more data points at a range of adsorbate partial pressures and gas-phase mole fractions), because the relationships typically involve three or more parameters for each component in a set of nonlinear equations. Due to the limited data set available for acetone and benzene, it was not possible to make modifications to AST utilizing activity coefficients in an attempt to better its predictions.

6.7 Summary

Indoor air environments are multicomponent systems composed of many VOCs and water vapor. An attempt was made in this section to characterize the effects of humid air on the adsorption capacity of soluble (acetone) and insoluble (benzene) compounds on ACC-20. Acetone showed little decrease in its adsorption capacity on ACC, up to about 90% RH, while water vapor had an effect on benzene adsorption starting around 65% RH, and became more pronounced as RH increased. As benzene concentration was increased, the diminishing of benzene adsorption capacity due to increased RH lessened. IAST did well predicting the total amount adsorbed of a 1000 ppmv acetone-benzene mixture, but over-predicted the individual amount of benzene adsorbed and under-predicted the amount of acetone adsorbed. The errors between the IAST modeled results and the experimental data are due to adsorbed-phase non-idealities.

6.8 References

- Dubin, M.M., "Water vapor adsorption and the microporous structures of carbonaceous adsorbents," *Carbon*, **18**, 355-364 (1980).
- Manes, M., "Estimation of the effects of humidity on the adsorption onto activated carbon of the vapors of water-immiscible organic liquids," *Fundamentals of Adsorption Proceedings of the Engineering Foundation Conference*, A. L. Myers and G. Belfort, Eds., Bavaria, West Germany, 335-344, 1983.
- Myers, A. L. and Prausnitz, J. M., "Thermodynamics of mixed-gas adsorption," *AIChE Journal*, **11**(1):121-127, 1965.
- Reid, R.C., Prausnitz, J.M., and Poling, B.E., *The Properties of Gases and Liquids, 4th edition*, McGraw-Hill, New York, 1987, 741 pp.

Chapter 7

Summary and Conclusions

Granular activated carbon (GAC) and powdered activated carbon (PAC) have long been used to effectively treat drinking water, waste water, and industrial gas streams. Undesired contaminants are removed by adsorption onto activated carbon. While activated carbon has been used extensively in industrial applications, little research has been performed to evaluate using activated carbon to remove low concentrations of volatile organic compounds (VOCs) from indoor air environments. In this research, activated carbon cloth (ACC) is examined for its equilibrium adsorption capacity for VOCs of relevance to indoor air quality.

Three types of ACC samples were characterized in terms of its pore size distribution using the Horvath-Kawazoe and Dubinin-Stoeckli models. Both models showed a narrow pore size distribution present almost entirely in the micropore range. The breadth of the pore size distribution and the mean pore size increased with increased activation and increasing BET surface area of the ACC sample.

Adsorption isotherms were measured for acetaldehyde, acetone, benzene, MEK, and water vapor and three ACC samples. For the 10 to 1000 ppmv concentration range examined, benzene exhibited the highest adsorption capacity on ACC, followed by MEK, acetone, and acetaldehyde. Water vapor adsorption was not significant on ACC until relative humidities above about 50% ($P/P_0 > 0.5$), when capillary condensation of $H_2O_{(g)}$ occurred within ACC pores.

Equilibrium adsorption experiments were not performed for VOCs in the sub-ppmv concentration range, due to the long times (estimated at weeks to months) to reach equilibrium, and the high cost of compressed gases. The Freundlich and DR equations were used to model the adsorption capacities into the sub-ppmv range for the four adsorbates and three ACC samples examined in this research. The sub-ppmv concentration range is a more realistic concentration range for VOCs present in indoor air environments.

It has been suggested that when using the DR equation to predict adsorption capacities of organic compounds using a reference adsorbate, reference adsorbates of similar polarity should be used. This hypothesis was examined by using benzene as a reference adsorbate for non-polar (and slightly polar) compounds (ethylbenzene, toluene, and p-xylene) and acetone as a reference for polar compounds (acetaldehyde, MEK, and 1,1,1-trichloroethane). The improvement in prediction of adsorption capacity was not measured for the non-polar compounds, but using acetone as a reference adsorbate for polar compounds, predictions showed average errors of 9% for acetaldehyde and 5% for MEK.

ACC-20 was chemically modified, producing oxidized, chlorinated, and nitrated samples. Adsorption capacities for VOCs in the 10 to 1000 ppmv concentration and water vapor from 0 to 95% RH were measured. Oxidized ACC-20 showed an enhanced physical adsorption for acetaldehyde, acetone, and water vapor, probably due to increased dipole-dipole interactions and hydrogen bonding. Oxidation of ACC-20 changed the shape of the water vapor adsorption isotherm, so that it no longer resembles a Brunauer type V. Benzene showed a decreased adsorption capacity on oxidized ACC-20, which may be due to an increase in hydrophilicity of ACC-20, or a change in pore size distribution.

Chlorination had little effect on VOC adsorption capacity, except in the case of acetone, where a decrease in adsorption capacity occurred. This may be due to pore blocking by chlorine molecules, or a decrease in hydrogen bonding between the ACC functional groups and acetone. Nitridation of ACC showed little effect on organic adsorption capacity, but increased the saturation adsorption capacity for water vapor on ACC-20 and increased the breadth of its hysteresis loop. These changes were the result of changes in the pore size distribution of ACC-20. DR parameters were determined for VOC adsorption on ACC-20.

Indoor air environments are multicomponent systems composed of many VOCs and water vapor. An attempt was made to characterize the effects of humid air on the adsorption capacity of soluble (acetone) and insoluble (benzene) compounds on ACC-20. Acetone showed little decrease in its adsorption capacity on ACC, up to about 90% RH, while water vapor had an effect on benzene adsorption starting around 65% RH, and becoming more pronounced as RH increased. As benzene concentration was increased, the diminishing of benzene adsorption capacity due to increased RH lessened. IAST did well predicting the total amount adsorbed of a 1000 ppmv acetone-benzene mixture, but over-predicted the individual amount of benzene adsorbed and under-predicted the amount of acetone adsorbed. The errors between the IAST modeled results and the experimental data are due to adsorbed-phase non-idealities.

These results are important for the design of adsorption systems utilizing ACC. This includes improving and maintaining indoor air quality, and well as other applications, such as, industrial filtration systems, and organic sampling devices.